METHOD FOR COMPLIANCE CONTROLLED ADHESIVE SWITCHING AND MAGNETICALLY CONTROLLED SWITCHABLE ADHESIVES

A Thesis
Submitted to the Graduate Faculty
of the
North Dakota State University
of Agriculture and Applied Science

By

Jared Michael Risan

In Partial Fulfillment
for the Degree of
MASTER OF SCIENCE

Major Department:
Mechanical Engineering

November 2013

Fargo, North Dakota

North Dakota State University
Graduate School

Title

Method for Compliance Controlled Adhesive Switching and Magnetically Controlled Switchable Adhesives

By

Jared Michael Risan

The Supervisory Committee certifies that this ***disquisition*** complies with North Dakota State University's regulations and meets the accepted standards for the degree of

MASTER OF SCIENCE

SUPERVISORY COMMITTEE:

Dr. Fardad Azarmi
Co-Chair

Dr. Andrew Croll
Co-Chair

Dr. Vicki Gelling

Dr. Chad Ulven

Approved:

12/9/2013
Date

Dr. Alan Kallmeyer
Department Chair

ABSTRACT

Adhesives are used in a variety of ways and are so common that they are easily overlooked. Adhesive hooks, tapes, glues, and switchable climbing mechanisms used by insects and lizards are clear examples of how adhesives are beneficial to society and nature. The development of novel switchable adhesives is a research area that is largely incomplete. In fact, very few switchable adhesives exist on the market today; hence their development would tremendously impact the adhesive industry. This thesis studies a mechanism for stiffness controlled switchable adhesion by utilizing a magnetically switchable device. The influence of nanopowder reinforcement on the compliance of polymeric-metallic composite switchable adhesives is investigated. Highly compliant composites are switched by magnetic and mechanical clamping leading to changes in compliance and adhesion. Material characterization is done with lap-shear testing while effects of reinforcement and clamping methods are studied. Ultimately, magnetic switching is consistent with a simple mechanical model.

ACKNOWLEDGMENTS

I would like to thank Dr. Fardad Azarmi of Mechanical Engineering and Dr. Andrew Croll of Materials and Nanotechnology for agreeing to be my academic advisors in such a short period of time. Both advisors worked closely with me, attending countless meetings and supplying significant academic guidance, so that my first exposure to original research could be a positive experience. Their helpful input to this research project as well as their impact on my education at North Dakota State University has been tremendously valuable. I would also like to thank Dr. Chad Ulven of Mechanical Engineering and Dr. Vicki Gelling of Coatings and Polymeric Materials for agreeing to be on my Master's Thesis Supervisory Committee.

Additionally, I would like to thank the Materials Characterization Analysis Laboratory at the Center for Nanoscale Science and Engineering for all the helpful skills I learned over the years while employed for Eric Jarabek. Exposure to research as an undergraduate student while working in the lab impacted my life in more ways than one and motivated me to pursue a Master's Degree in Mechanical Engineering. Other people who I would like to thank and who deserve credit for helping me are: Shannon Viestenz for assisting me in the machine shop making jigs and other experimental gadgets, Tanya Erickson for being so knowledgeable in the administrative handling of my ME Master's Degree requirements, Scott Payne for performing Scanning Electron Microscopy, and Chris Leither for drawing the AutoCAD schematics.

Finally I would like to thank my friends and family specifically: Mom, Dad, Jennifer, Jessica, Dan, Ellie, and Bennett. Thanks so much for influencing my life! 1 Corinthians 1:25 (NIV)

TABLE OF CONTENTS

LIST OF TABLES

LIST OF FIGURES

Figure Page

CHAPTER 1: INTRODUCTION

Adhesives have been used for centuries to hold two surfaces together by interfacial forces such as valence forces, interlocking forces, or both [**1**]. The first use of adhesives can be traced back to ancient cultures which used resins from trees, beeswax, and gum, among other natural adhesives, to bind materials together [**2**]. The importance of adhesives for daily applications did not get lost with the ancient cultures that first used them and is still an active area of research for academia and industry today. Adhesives are used in a variety of ways and are so common that they are often overlooked aspects of a system's mechanical design. The ubiquitous use of adhesive hooks, tapes and labels, as well as glues is a clear example of how adhesives are beneficial to society. Moreover, the drive to successfully mimic the switchable adhesive climbing mechanisms used by insects and lizards, such as the gecko, show that the study of adhesion is still yielding questions of fundamental scientific interest [**3**].

This thesis develops a novel platform for a switchable adhesive. Specifically, the use of a composite consisting of highly compliant polymeric rubber and magnetic nanopowder is examined for adhesion control. One reason the polymeric-metallic composite adhesive developed for this thesis is superior to other switchable adhesives is because of its ease during manufacture. Additionally the polymeric-metallic composite used in this thesis has a unique ability to switch a mechanical property, namely compliance, between a stretchable and less stretchable state while in the presence of a magnetic clamp. To our knowledge controlling compliance has yet to be used for switching adhesion and changes in compliance, by way of magnetic clamping, has proven to be a simple switch with unlimited repeatability. The purpose of this thesis is to show that adhesion can be switched by compliance alone.

The organization of this thesis is as follows: an overview of adhesion, the motivation for this research, fracture and contact mechanics, adhesive characterization, a literature review, research objectives, experimental setup, results and discussion, and summary and recommendations. The overview of adhesion contains brief discussions of surface energy and wettability, factors that influence adhesion, and classes of adhesives from which to provide a general framework in selecting a potentially compliant controlled switchable adhesive. The motivation for this research, evident in the switchable adhesive ability of climbing lizards, gives justification for the importance of the thesis. A basic knowledge of fracture and contact mechanics is required to carry out this work. Additionally, background information on adhesive characterization is absolutely necessary for interpreting and analyzing sample failure. Finally a literature review of contemporary research in the field of switchable adhesion is presented in an effort to evaluate how this original research expands what has already been reported in literature.

1.1. Overview of Adhesion

An adhesive bond consists of two components, an adhesive and an adherend, or substrate. Adhesives are advantageous compared to other joining methods like riveting, bolting, or welding because they have the ability to bond quickly, they have favorable weight-to-strength ratios, and they are relatively inexpensive [**2**]. Adhesives can bond many classes of materials such as plastics, metals, ceramics, composites, and wood. Adhesives can be found in the form of liquids, pastes, or solid films and they all on their own or through the application of pressure will come in contact with a substrate and will experience a net attractive interaction resulting in bond formation [**4**].

The theory of adhesion consists of mechanical, physical, and chemical interactions between two bonded surfaces. Mechanical adhesion occurs when the adhesive penetrates the surface and interlocking occurs. Porous substrates help increase mechanical interlocking and occasionally abrasives are used to pretreat a substrate to increase roughness. Physical adhesion occurs when a difference in electrostatic attraction exists between the two adherends. Chemical adhesion is broken into three subclasses: adsorption, chemisorption, and diffusion. During chemical adsorption, secondary bonding such as Van der Waals interactions, hydrogen bonding, and induced dipole bonding contributes to adhesive strength. During chemisorption primary chemical bonds (i.e. covalent bonds) are created to form the adhesive connection. Lastly, chemical diffusion describes the notion that polymer chains can cross over and entangle at the surface interface between a polymer adhesive and polymer substrate, or that long chains take time to diffuse into substrate roughness [**5**].

1.1.1. Wettability: Surface Energy and Surface Tension

Determining whether two surfaces will come into contact, or adhesively bond, depends on the surface energy. Surface energy is the energy associated with making new surfaces due to breaking of bonds of atoms saturated within the bulk of a material. Another way to describe surface energy is the deficit of bonding at the surface [**6**]. Commonly surface tension is incorrectly used when referencing surface energy. Surface tension is the resistive force of liquid molecules at the surface to separate under deformation. Surface energy is related to surface tension by Equation 1.

$$\tau = \gamma + A\frac{\partial \gamma}{\partial A} \qquad \text{(Equation 1)}$$

Where τ is the surface tension, γ is surface energy, and A is the surface area. For a perfect fluid, the surface energy and surface tension are exactly equal since average distances between molecules in a liquid do not change when deformed. However for elastic solids under deformation, the surface energy and surface tension are not the same since bond lengths and bond energies have changed due to stretching [**6**].

The degree in which one surface will coat the other surface is dependent on the surface energies and is termed as wettability. Generally, in order for an adhesive to wet a surface and spread, the surface energy of the substrate must be higher than the surface energy of the adhesive. However the interfacial energy, created by the boundary of the two materials in contact, contributes to dictating how easily a surface is wetted. Physically this is explained by the principle of minimum energy, a variant of the second law of thermodynamics. A high surface energy substrate can be coated with a lower surface energy adhesive resulting in a net lowering of energy within the system.

Characterization of surface energy can be conducted with a contact angle test. Contact angle tests relate surface energies of a liquid drop and solid surface with the interfacial energy. A contact angle test is depicted in Figure 1 where γ_1 and γ_2 are the surface energies of the two bodies, γ_{12} is the interfacial energy. During a test, a drop of liquid (e.g. adhesive glue, ink, etc.) is placed on a substrate and the contact angle θ is measured.

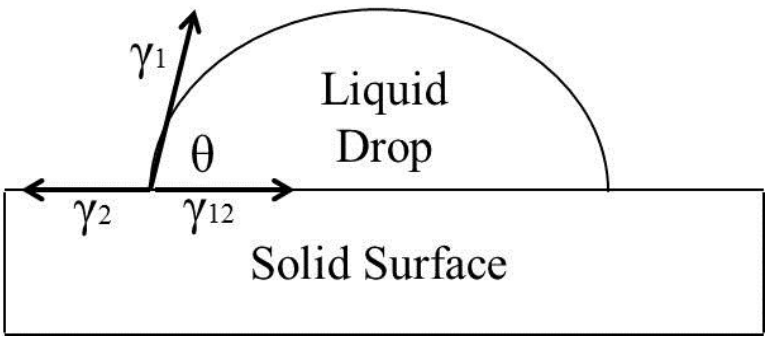

Figure 1: Contact angle of a liquid droplet wetted to a rigid solid surface

If θ is small then a liquid drop will spread and wet more of the surface. When θ is large or greater than 90° then the surfaces of the adhesive and substrate are incompatible and wetting is a challenge. The surface energy of the liquid must be lower than the surface energy of the substrate for good wettability [**7**]. Wetting is required to increase interactions between the adhesive and substrate, and good wetting is an especially important factor that influences overall adhesion.

1.1.1.1. Adhesion Defined

Familiarity of surface energy and wettability permits a formal definition of the work of adhesion to be stated. The work of adhesion is mathematically defined by Equation 2.

$$w = \gamma_1 + \gamma_2 - \gamma_{12} \qquad \text{(Equation 2)}$$

where the work of adhesion, *w*, is the energy required to create (or separate) unit areas due to the elimination of two bare surfaces and the creation of an interface [**8**]. The work of adhesion is a useful quantity because it distinguishes between contact and separation of two materials (for further information see the end of Section 1.4.3.2).

The work of adhesion is related to the contact angle, θ, which again is the result of a balance of equilibrium forces at the contact line between a liquid drop and solid surface (shown in Figure 1), by the Young-Dupree equation:

$$w = \gamma_1(1 + cos\theta) \qquad \text{(Equation 3)}$$

The Young-Dupree equation, relates contact angle, and hence the surface energy due to molecular bonds, to the work of adhesion, and therefore describes net attractive interactions on a molecular scale. As such, resulting mechanical, physical, and chemical adhesive interactions between two bonded surfaces have an origin at the molecular level. Thus, *adhesion* can be defined as the process of attraction between two particles or surfaces which brings them into contact. If the materials in contact are the same, then the attraction is labeled as *cohesive* [**8**].

1.1.2. Factors that Influence Adhesion

There are several factors and pretreatments that influence whether two surfaces will bond. Wetting, dictated by surface energies, is critical for adhesion. One important factor in improving adhesion is substrate cleaning as a pretreatment prior to applying an adhesive. Dipping the substrate in solvents is a common cleaning method used to remove dust, oil, grease, release agents, plasticizers, etc. from a substrate [**5**]. Contaminants can decrease the surface energy of a substrate causing wetting difficulties.

Other surface pretreatments can improve wettability by increasing the active groups on a substrate. Several pretreatment methods such as chemical etching, corona discharge, flame treatment, and plasma treatment, can promote adhesion. Chemical etching consists of a chemical reaction on the surface of a substrate that etches away unwanted phases and exposing the desired

materials and phases. Corona discharge is an electric spark that increases reactive sites by causing oxidation on the surface which changes the surface energy. Another pretreatment method is an oxidative flame treatment which is similar to corona discharge in that it improves bonding. Plasma treatment is an advanced method to alter the surface characteristics compared to the flame and corona treatments but it is a very expensive technique. Plasma is an oxidative treatment that increases the amount of energetic hydroxide and oxide pendant groups effectively increasing the surface energy.

In addition to altering the surface energy, changes in surface area can influence adhesion. Mechanical abrasion, although does not influence surface energy and therefore wettability, does change the amount of surface area. Mechanical abrasion induces roughness to a substrate which promotes adhesion through interlocking [**5**]. If a surface is too rough, primers are sometimes applied first to act as a base coat by filling in an excessively porous substrate. In addition, primers can act as a chemically active species to increase adhesion by surface energy modification.

1.1.3. Classes of Adhesives

There are several classes of adhesives such as: structural, water based, radiation cured, hot melt, or pressure sensitive. Some considerations for choosing adhesives are based on strength of the adhesive bond, cost, ease of application, and resistance to environmental effects [**4**]. Structural adhesives generally consist of two part thermoset systems which are typically used because they withstand high stress, high temperature, solvent attack, and are creep resistant. Two part systems, such as the epoxies, tend to become rigid after curing due to the loss of solvents or by crosslinking [**4**]. Some examples of structural adhesives are epoxies,

cyanoacrylics (e.g. superglues), and silicones. Water based adhesives can be colloidal materials that naturally occur or are created synthetically and combined with water. Examples include starch-based adhesives and rubber latex. Radiation cured adhesives can be acrylics or epoxies and are cured by UV radiation or electron beams. Finally, hot melt adhesives are thermoplastics that are heated until they melt and then are applied to surfaces. Once they are applied they are cooled down until they harden and interlock the two surfaces together [**4**]. Each of these classes, except for pressure sensitive adhesives, experiences some chemical or physical change (i.e. cure or melting) and can only be used once.

1.1.3.1. Pressure Sensitive Adhesives

While there are many classes of adhesives, pressure sensitive adhesive (PSA) systems fill a common niche because with slight application of pressure, an adhesive bond is formed. PSAs are viscoelastic meaning that they exhibit a combination of viscous or elastic behaviors depending on the chemical formulation. PSAs can be tailored to behave in either a more viscous or elastic manner, however they are not designed to have permanent material property changes as seen in the curing of an epoxy. The constant viscoelastic nature of PSAs allows the material to be permanently "tacky" [**2**]. A measure of rate of change of separation force with time is defines tack, or in other words, describes how quickly something will adhere by intimately wetting out another surface [**9**].

One of the limitations of tacky PSAs, such as tapes, is a reduction of adhesiveness during cycling due to contamination of dust and dirt particles which come into contact with the viscous dominated surface of the adhesive. Contaminates attached to the adhesive can effectively decrease contact area between a substrate and adhesive during bonding. Dry PSAs overcome the

limitations of tacky PSAs because the decrease in viscosity of a dry, highly elastic PSA prevents attachment of dust particles to adhesives resulting in better adhesion. This is because contaminates, like dust and dirt, are unable to be significantly wetted by an elastic PSA, unlike a traditional viscoelastic PSA where dust or dirt remains on the surface. Dust or dirt on dry elastic PSAs can be cleaned and removed permitting the adhesive to bond uninhibitedly over multiple loading cycles. Another reason an elastic PSAs is beneficial for repeated cycling is because tacky PSAs have degradation with use as can be observed by residues being left behind after the removal of the adhesive. The loss of residue implies that viscoelastic PSAs are rarely reusable over many repetitions. However, dry reversible switchable PSAs, or PSAs lacking tack, can be used again and again since they are cleanable and do not degrade on each use.

1.2. The Gecko: A Highly Efficient Switchable Adhesive System

Switchable adhesion is commonly observed in nature and successfully replicating the process synthetically is a contemporary research goal for designing smart adhesives. Geckos have the ability to quickly and effectively switch adhesion on and off for locomotion and climbing. Not only can geckos repeatedly switch adhesion, but they are also able to achieve high force capacities when adhered to inverted surfaces. In addition, geckos do not have a bias in adhering only to a specific surface. Strong attachment, ease of release, and the ability to cling to a variety of surfaces are qualities which geckos possess that have not been synthesized in bio-mimic adhesive designs to date.

Fibrillar features from the morphology of a gecko's footpad have been found to aid in achieving high force capacities. Figure 2 shows scanning electron microscope (SEM) images of fibrillar features from the tokay gecko's foot [**10**].

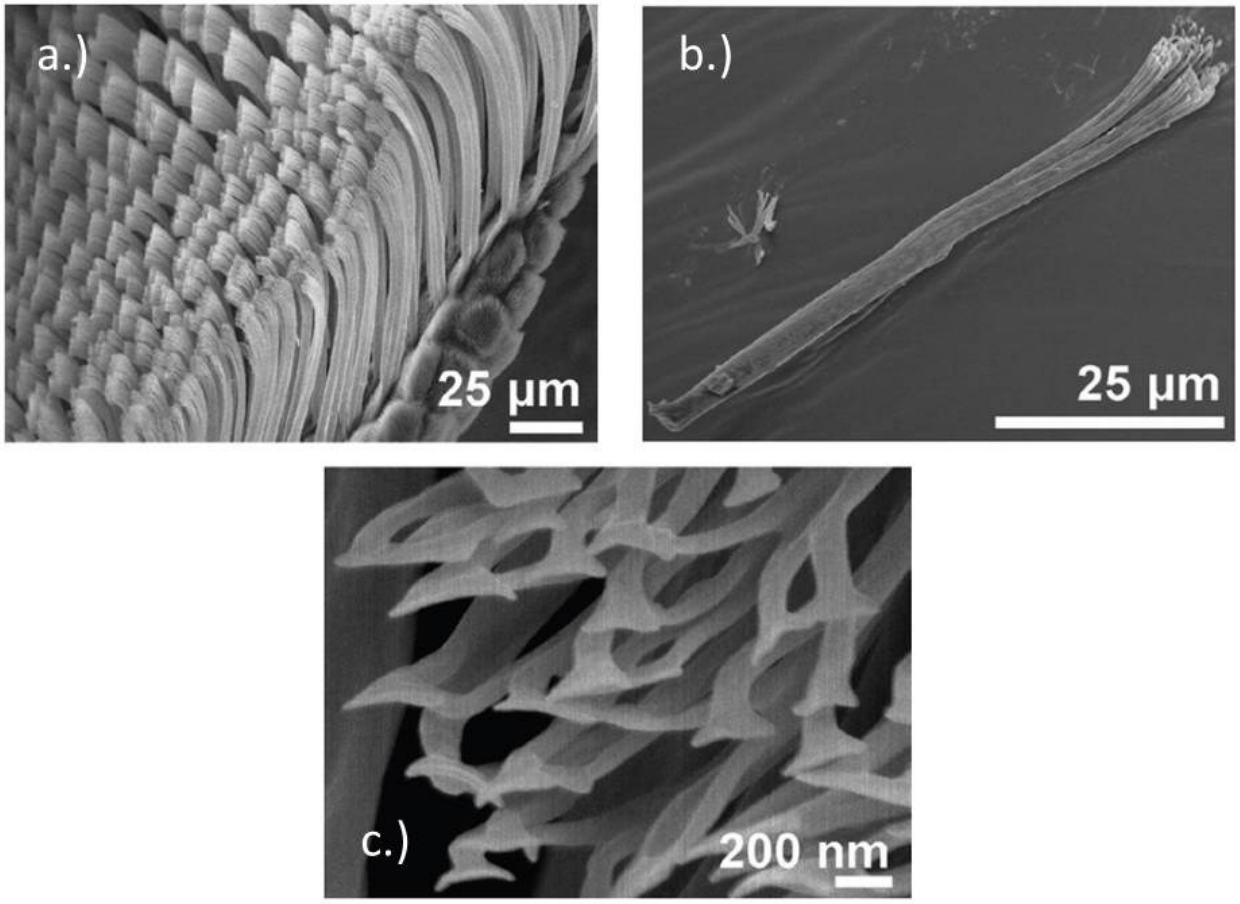

Figure 2: SEM images of the Tokay gecko's fibrillar features [10]

Figure 2 (a) shows rows of setae, (b) a single seta, and (c) terminal spatula tips of a single seta from the tokay gecko's footpad. Forests of setae contribute to the increase of true contact area achieved by micro- and nano-scale splitting of terminal spatulas. Splitting of fibrillar features, or an increase in system compliance, permits intimate contact between the footpad and rough surfaces in which the gecko traverses; (e.g. trees, rocks). More specifically, separation of setae creates substantial molecular to molecular contact so that Van der Waals attractive forces become significant. The increase of Van der Waals interactions due to setal splitting explains, in part, the high force capacities observed in geckos. Additionally, the use of nonspecific Van der Waals forces explains why a gecko can attach to multiple surfaces since the atoms between a

gecko's setae and substrate experience an attractive force when separated by only a few angstroms.

Low energy release is another feature geckos possess which is preferred for smart adhesive design. Much effort has been devoted to determining how geckos are able to switch off adhesion effectively. It has been observed that geckos hyperextend their toes to induce peeling as a mechanism for release. Synthetically, several methods have been studied as possible switching mechanisms [**11**]. (For more information on current research of synthetic switching mechanisms see Section 2.1.)

Geckos have the benefit of switching and attaining high force capacities so much current research is aimed at mimicking fibrillar features of a gecko's footpad by synthesizing complex polymeric structures [**12**] [**13**] [**14**] [**15**] [**16**]. The problems associated with synthetic bio-mimic adhesives are that they are complex to make since they consist of micro- and nano-scaled fibrillar pillars densely packed together. Fabrication of complex micro- and nano-scaled polymeric fibrillar features is achieved through specialized lithographic etching techniques. Silicon molds are used to cast rubber into the form of fibrillar adhesive pads by etching silicon wafers. As such, the creation of a bio-mimic adhesive pad must take place inside an expensive cleanroom laboratory.

In addition to difficulty in manufacturing fibrillar bio-mimic adhesives, the sole influences of fibrillar features are in question. As a bio-mimic fibrillar pad area increases in size, the contribution of setal splitting decreases due to the length scale associated with the setae. Micro- and nano- scaled setae only help increase contact at the micron or sub-micron length scale. A hierarchy of fibers must be maintained at every length scale for a large bio-mimic adhesive pad to benefit from fibrillar features. Ultimately bio-mimics fail to achieve high force

capacities at large length scales implying that the exclusive contribution of fibrillar features is not the only design parameter of importance in understanding the climbing ability of geckos [**10**].

1.2.1. Bio-inspiration: A Motivation for Research

Replication of a synthetic adhesive device that has attributes including: strong attachment, ease of release, unlimited switching, and complete lack of specific surfaces on which to adhere is clearly bio-inspired by the gecko. However, when designing a reversible adhesive device, simply assuming that mimicking a gecko's morphology absolutely guarantees these qualities is a design misstep. For example, ancient Greeks widely examined bird feathers in an attempt to understand flight. Numerous design sketches, during the time of the Italian renaissance, have demonstrated unsuccessful human attempts at feather only flight. Using this analogy, merely mimicking gecko morphology instead of understanding fundamental adhesive principles is an incorrect approach in creating a bio-inspired adhesive. Therefore to design a gecko like adhesive, an arbitrary shaped material must be assumed. In addition, a gecko can adhere to various substrates implying that to design a switchable adhesive, a specific material surface chemistry cannot be relied upon [**10**].

Using an energy balance approach and considering any material of an arbitrary shape, force capacity has been shown to scale as:

$$F = \sqrt{G_c}\sqrt{\frac{A}{C}} \qquad \text{(Equation 4)}$$

where F is the maximum sustainable adhesive force, G_c is the critical energy release rate (for further information on G_c see Section 1.3.3), A is the contact area, and C is the compliance [**10**].

It is evident by Equation 4 that to control attachment, only three influential parameters, G_c, A, and C, can be adjusted to optimize a bio-inspired switchable adhesive. On a macroscopic scale, the contact area, A, of a switchable adhesive is constant making it an ineffective control parameter for switching. Likewise, the critical energy release rate, G_c is a property set by the materials comprising the interface, and since it is material specific, it is not a useful design parameter in developing a switchable adhesive that can adhere to countless surfaces. On the other hand, manipulating compliance, or a material's stiffness, is a mechanical switch not limited by the surface chemistry involved.

Soft materials often have higher force capacities than rigid elastic materials because the compliance is high in the normal direction which allows them to conform to a surface and therefore increase the contact area. However, according to Equation 4, a low compliance in the parallel direction will result in a higher critical force [**10**]. Figure 3 is a reference to the influential compliance directions.

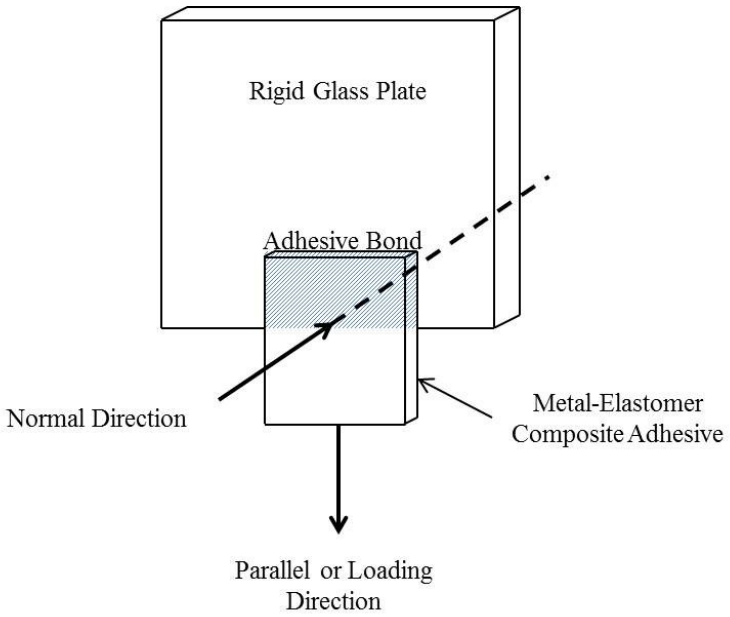

Figure 3: Directions of a lap-shear test

1.3. Fracture Mechanics and the Failure of Adhesives

Fracture mechanics is a field of materials science that studies the rupture of a solid body into two or more parts [**17**]. Traditionally fracture mechanics is typically only considered when discussing fracture of a solid body; however the extension of the field of fracture mechanics can also be used to describe the rupture of two adhesive bodies that have come into contact. Fracture mechanics can be described from a multidisciplinary perspective therefore different terminology, nomenclature and even historical developments in the two methodologies exist. Ultimately though, to design a switchable adhesive a basic understanding fracture mechanics is absolutely necessary [**10**].

1.3.1. A Theoretical Criterion of Rupture

As previously mentioned, the separation of an adhesive and substrate is similar to solid body fracture since both describe how much force is required to cause rupture. The theory of rupture in solids was first developed by Griffith is based on a thermodynamic energy balance where the potential energy always wants to be at a minimum for an elastic solid body under surface forces or deformations [**17**] [**18**]. When a material undergoes deformation, internal elastic strain energy is built up at a stress riser (e.g. void, scratch on a surface). A crack is created when the internal elastic strain energy is continuously decreased by releasing energy into a surrounding volume of material which is a relaxation of the internal stress (e.g. internal energy is released when a bent stick snaps in half). The decrease in energy is countered by an increase in surface energy due to the formation of two new surfaces [**18**]. A crack will propagate if the elastic strain energy is larger than the surface energy [**18**]. As the crack grows, the elastic strain energy and the surface energy continually fluctuate until equilibrium is reached. Equilibrium is

reached when the first derivative of the total potential energy (per unit thickness) with respect to crack length is zero [**18**].

1.3.2. Crack Propagation with Plasticity

Significant modifications by Irwin on the rupture of solid bodies have expanded the field of fracture mechanics [**19**]. Commonly stress is very high at a crack tip, due to a point singularity, which most likely means that the yield stress is surpassed [**17**]. In reality a material undergoes plastic deformation once the yield stress is reached before it will rupture. Figure 4 depicts this concept:

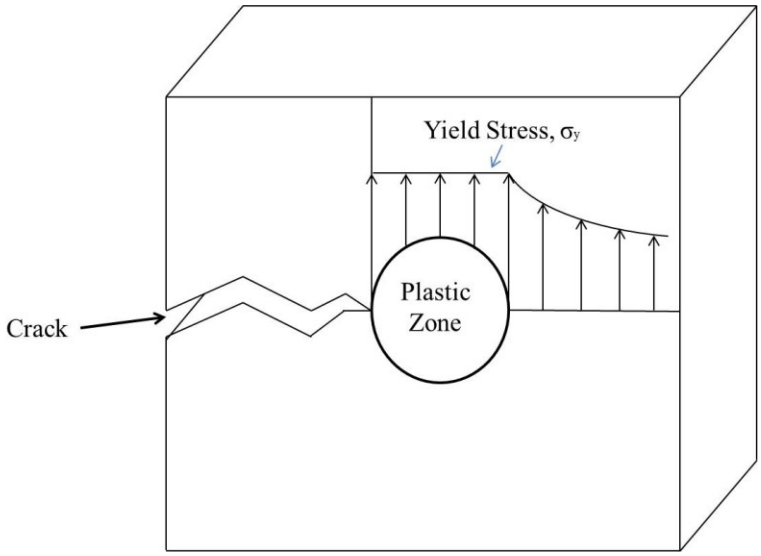

Figure 4: Stress and plastic zone size at a crack tip

Yielding experienced at the crack tip and the deformation of the plastic zone to follow takes *time*. In brittle materials at low temperatures and fast crack speeds, the plastic work done at the crack tip due to yielding is negligible. In ductile materials though, the plastic work blunts the crack tip effectively improving fracture toughness by slowing down the crack speed of a propagating crack. The rate of crack propagation, or change of energy with crack length, is

significant and is defined by a parameter called the strain energy release rate, *G* which is both an adhesion energy and a fracture toughness parameter (for further discussion on *G* see the following Section as well as Section 1.3.3) [**19**].

1.3.2.1. G - Fracture Toughness Parameter

Fracture mechanics allow a quantitative measurement of the resistance of a material to crack propagation when information is known about applied stress, crack length, and fracture toughness [**17**]. Fracture toughness describes how well a material will resist rupture, or in other words, how "tough" it is to fracture or pull apart. There are several ways to define the resistance to crack growth such as Crack Opening Displacement, *J*-Integral, and *R* Curve, but *G*, the energy release rate is the only fracture toughness parameter discussed in detail. *G* is a material property that expresses the response of a crack, relative to its velocity, to the crack extension force [**17**].

The crack extension force is commonly related to other fracture toughness parameters. The relationship of *G* to the stress intensity factor is well known [**20**].

$$\mathrm{G} = \frac{K^2}{E}\ plane\ stress \qquad \text{(Equation 5)}$$

And

$$\mathrm{G} = \frac{K^2}{E}(1 - v^2)\ plane\ strain \qquad \text{(Equation 6)}$$

where *K* is the stress intensity factor, *E* is the modulus, and *v* is Poisson's Ratio. Equation 5 and Equation 6 relate *G* to the stress intensity factor *K,* but *G* can also be expressed in terms of the other fracture toughness parameters by:

$$\mathrm{J} = \mathrm{G} = \frac{K^2}{E'} = \lambda\sigma_y\delta \qquad \text{(Equation 7)}$$

where J and $\lambda\sigma_y\delta$ are the fracture toughness parameters for J-Integral and crack opening displacement respectively [**17**].

1.3.3. Critical Energy Release Rate, G_c

Historically, research on solid body fracture predated fracture in adhesives. Therefore, understanding solid body fracture is a useful prerequisite for discussing the energy release rate as an adhesive energy. As fracture mechanics has not traditionally aligned itself with adhesion, differences appear between Griffith's definition of rupture in solid bodies compared to a comprehensive view of fracture in a more generalized sense. Griffith stated that for brittle fracture, the fracture toughness is exactly equal to the surface energy. Griffith's view of fracture, since limited to brittle materials only, fails to account for energetic losses associated in the fracture of an adhesive; energetic losses change the surface energy. Therefore from an energetic standpoint, adhesive fracture is viewed differently than a traditional engineering approach to fracture toughness in solid metals, yet both are governed by fracture mechanics.

The strain energy release rate can be expressed in either unit: force per crack length (N/m) or surface energy (J/m^2). Explicitly stated, the strain energy release rate is the force per crack length and it is equivalent to the adhesion energy. Fracture occurs when the stress corresponds to a *critical* value, G_c, and the *critical* energy release rate is a property set by the materials comprising of the interface. Considering G_c in terms of Newtons per meter can be best illustrated as the force to cause crack extension. This definition of G_c is more consistent with engineering nomenclature and, when considering fracture of solid bodies, is better categorized as a fracture toughness parameter [**17**]. On the other hand, considering G_c, the critical energy release rate, in terms of Joules per meter squared can be best described as the rate of conversion of elastic strain energy into thermal energy during crack extension [**19**]. It is more

straightforward to refer to the critical energy release rate as a term related to surface energy, or the adhesive energy binding two materials together, when using the second definition of G_c. Clearly the critical energy release rate can be classified as a fracture toughness parameter or as an adhesive energy; however in designing switchable adhesives, the surface energy definition is more appropriate since it accounts for energetic losses associated with non-brittle fracture. (For further information on energetic losses associated with surface energy see Section 1.4.3.3)

It is important to understand the adhesion energy, G_c, is not optimized for any particular surface in the gecko. A gecko is not bound by what materials it can adhere to; instead it clings to different surfaces. Rather, a gecko has the ability to increase its true contact area of attachment by setal splitting. Therefore, focusing on mechanics must be considered as a key point in advancing switchable adhesive designs beyond purely chemical attempts at switching.

1.3.4. Fracture of Viscoelastic Bodies

Mathematically, fracture mechanics defines G as:

$$G = \frac{\partial U_E}{\partial A} + \frac{\partial U_P}{\partial A} \qquad \text{(Equation 8)}$$

where U_E and U_P are the elastic and potential energies and A is the contact area of the two elastic bodies, the adhesive and the substrate. The stored energy at the interface U_s can be written as:

$$dU_s = -(\gamma_1 + \gamma_2 - \gamma_{12})dA = -w\,dA \qquad \text{(Equation 9)}$$

where γ_1 and γ_2 are the surface energies of the two bodies, γ_{12} is the interfacial energy, and w is the thermodynamic work of adhesion between the adhesive and substrate (see Figure 1 as a reference) [**21**]. The sum of total energy becomes:

$$dU_T = dU_E + dU_P + dU_S = (G - w)dA \leq 0 \qquad \text{(Equation 10)}$$

For a differential change in energy, Equation 10 shows that if the energy release rate *G* is greater than the thermodynamic work of adhesion *w*, then a differential reduction in contact area will occur and a crack will propagate resulting in the fracture of the two surfaces. Conversely if *G* is less than *w*, then a differential increase in the contact area will happen and the crack will recede [**21**]. Table 1 summarizes this:

Table 1: Summary of fracture mechanics

Mathematical Expression	Result	Physical Interpretation
G < w	Crack Recedes	Joining of Two Surfaces
G > w	Crack Propagates	Fracture of Two Surfaces
G = w	Equilibrium	No Change

1.4. Contact Mechanics

Contact mechanic theories are used to describe the shape of two objects in contact while being deformed under an applied force. Fracture mechanics deals with separation of bodies and depends on how the energy is stored within the deformation. Solid body fracture does not depend on contact mechanics because the elastic strain energy can be determined in a simpler way (e.g. examining a strained cube). However, for separation of two objects, fracture mechanics depends on the geometry, and therefore contact mechanics, to provide fundamental models associated with the rupture of two bodies. While fracture mechanics describes rupture in a general sense, contact mechanics is necessary to understand rupture of *two* unique bodies. Furthermore, contact mechanics add a method to determine where a crack is and how to determine compliance. Therefore an introduction to contact mechanics of elastic solids, JKR-

theory of adhesion, and further details on the measurement of G_c, the critical energy release rate are tremendously useful.

1.4.1. Hertz: Non-Adhesive Contact of Elastic Solids

The motivation which lead to the development of the field of contact mechanics came from understanding deformation mechanisms of steel train wheels in contact with steel railroad tracks [**22**]. For example, a rigid sphere and a flat surface with different moduli, Hertz stated that:

$$a^3 = \frac{3\,PR}{4\,E^*} \qquad \text{(Equation 11)}$$

where a is the radius of contact, P is the load, R is the radius of the sphere, and E^* is the reduced modulus. An illustration of the parameters used in Equation 11 is shown in Figure 5.

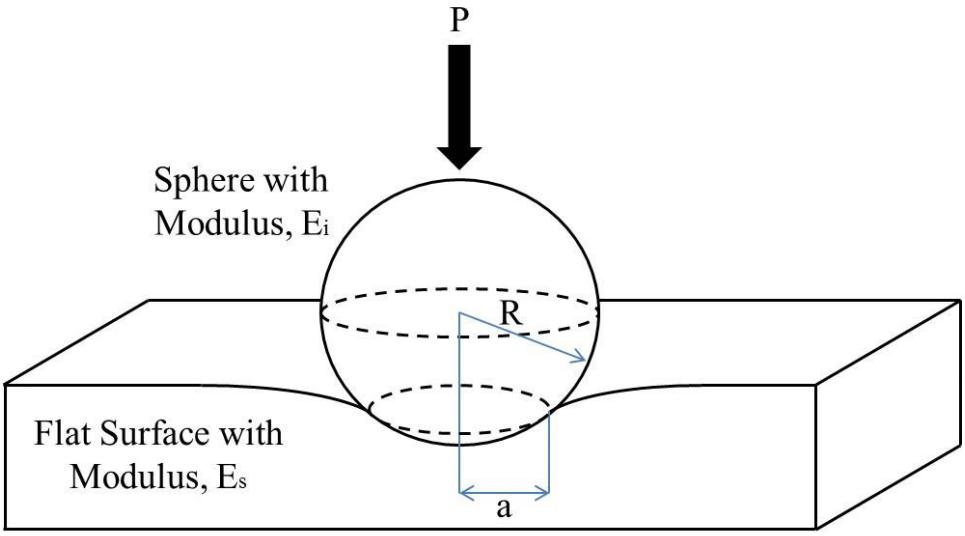

Figure 5: Schematic of contact between a rigid sphere and flat specimen

The reduced modulus, E^*, which combines the modulus of the flat surface and the modulus of the sphere, is different than the modulus of elasticity but is related by:

$$\frac{1}{E^*} = \frac{(1 + {v_s}^2)}{E_s} + \frac{(1 + {v_i}^2)}{E_i} \qquad \text{(Equation 12)}$$

where v_s is the Poisson's ratio of the flat surface, E_s is the modulus of elasticity of the flat surface, v_i is the Poisson's ratio of the sphere, and E_i is the modulus of elasticity of the sphere [**23**].

1.4.2. JKR Theory of Adhesion

Hertz's approach is limited to describing non-adhesive interactions when two elastic bodies are mechanically deformed under contact with an applied load. If the force required to deform a material is large, such as the case for metals and ceramics, then adhesive interactions are reduced to nanometer length scales. This is because the elastic energy stored is large compared to the adhesive energy rendering adhesion insignificant [**24**]. However, when the forces are small and deformation is large, such as the case for a soft elastic solid, then adhesion is significant [**25**]. Such a modification to the Hertz theory is included in the JKR (Johnson-Kendall-Roberts) contact theory [**25**].

JKR theory states that the surface energy and strength of adhesion between elastic bodies are related when the forces are small relative to large deformations. This is often the case associated with contact between soft materials. The strength of adhesion must be overcome by work required to separate the two surfaces. This work goes into creating new surfaces; or the increase in surface energy. Frequently surface energy is thought of in terms of a liquid drop on a substrate that finds equilibrium by spreading out due to a minimization of potential energy, but elastic solid body equilibrium largely depends on how the elastic forces are distributed [**25**]. Figure 6 shows the distribution of forces between two spheres in contact, where Figure 6 (a) is

the contact radius of elastic spheres: a_0 Hertz/a_1 JKR adhesion theory while being deformation under a load. Image (b) illustrates the distribution of stress where is compressive at the center and tensile at edge for contact mechanics (dashed line A) and JKR adhesion theory (line B) [**25**]

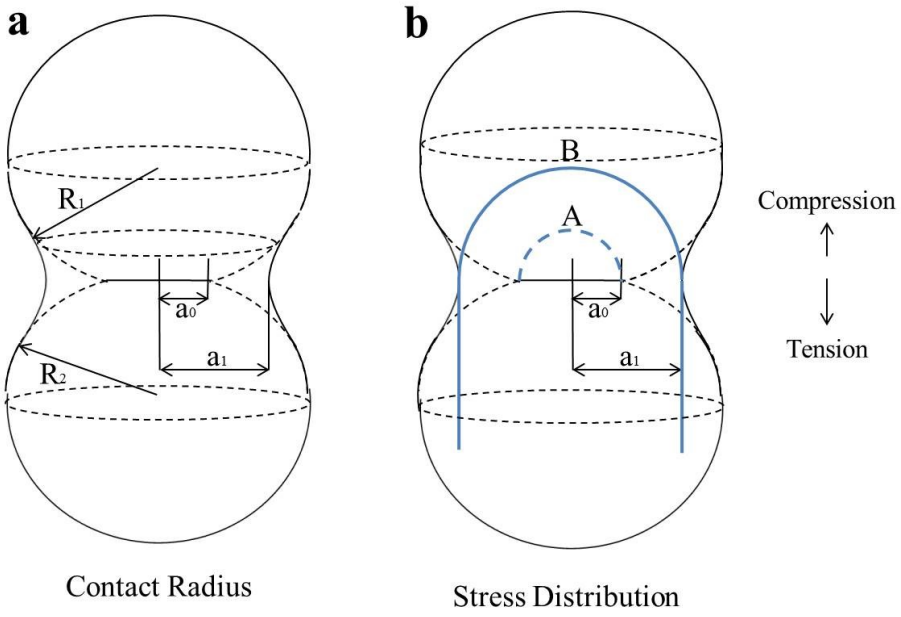

Figure 6: Elastic spheres in contact with and without surface forces

A typical JKR experiment would use a soft elastic polymeric hemisphere and place it in contact with a smooth, optically transparent glass slide. The contact patch can be monitored by placing a microscope under the glass slide and measuring displacement as the force required to increase contact between the hemisphere and glass slide is controlled. At low loads the contact patch is found to be larger than predicted by Hertz. The increased contact area at low loads corresponds to an adhesive tensile interaction at the edge of the deformed sphere. A modified contact mechanics equation was formulated by JKR to describe the adhesive effect. Equation 13 summarizes JKR theory:

$$a^3 = \frac{3R}{4E^*}\left(P + 3\pi G_c R + \sqrt{6\pi G_c R P + (3\pi G_c R)^2}\right) \qquad \text{(Equation 13)}$$

where the variables are the same Equation 11 and G_c is the critical energy release rate [**25**]. G_c is a surface energy, and when zero, reduces Equation 13 to the non-adhesive Hertz solution found by Equation 11.

1.4.3. G_c and the Adhesion of Soft Solids

JKR theory is used to describe adhesion and depends on G_c. Figure 7 gives a scaling relationship for material classes and illustrates when adhesive interactions become important for corresponding values of G_c/E, with $G_c = 0.1$ J/m^2. Figure 7 shows that the critical energy release rate is quite small for metals and ceramics but adhesion starts to become significant for elastomers. The concept of the critical energy release rate being the adhesion energy is easily understood, but G_c is not constant throughout a test because it depends on the rate in which the contact area is changing (i.e. crack velocity). However G_c, the critical energy release rate can be determined using the JKR theory despite it being a nontrivial property to measure [**24**].

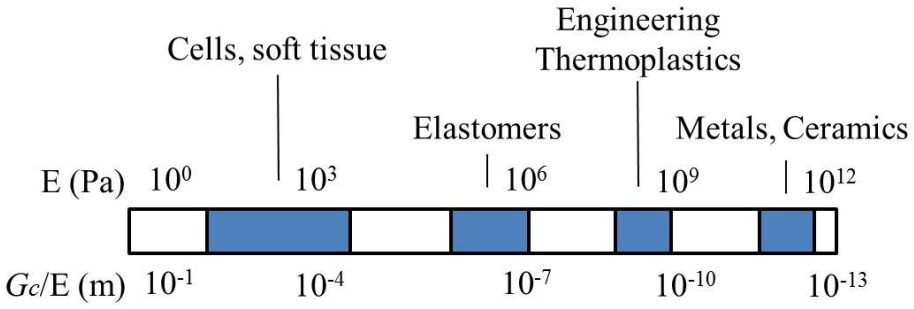

Figure 7: Characteristics of elastic moduli for different material classes

1.4.3.1. A Measurement of G_c

The determination of G_c requires input of a calculated value for the combined modulus before using Equation 13 even though both properties are measured at the same time during an experiment. To solve for G_c, the same experimental method as JKR is employed. A

hemispherical polymer tip is brought into contact with an optically transparent glass slide where the load, displacement, and contact radius is recorded. To find the modulus Equation 14 is used:

$$\delta_{\mathrm{JKR}} = \frac{a^2}{3R} + \frac{P}{2E^* a} \qquad \text{(Equation 14)}$$

Knowing the radius of the hemispherical polymer tip allows for a direct calculation of the combined modulus E^* [**24**]. It is interesting to note that the modulus is independent of the adhesion G_c. Once the modulus has been determined G_c can be calculated using:

$$\mathrm{G_c} = \frac{(P' - P)^2}{8\pi E^* a^3} f_{G_c}(a, h) \qquad \text{(Equation 15)}$$

where $f_{G_c}(a, h)$ is a finite-size correction factor for G_c dependent on a specific geometry and P' is the load multiplied by its own distinct geometric correction factor [**24**].

1.4.3.2. Crack Velocity Dependence of G_c

Unlike the modulus, the energy release rate is not constant throughout a test but depends on the rate at which the contact radius is increasing or decreasing. Figure 8 is a schematic that plots the energy release rate as a function of the contact radius which clearly differentiates between the advancing (increasing contact radius) and receding (decreasing contact radius) portions of an experiment [**24**]. Somewhere in between the advancing portion and receding portion of a test is the thermodynamic work of adhesion w. The thermodynamic work of adhesion describes the increase in free energy due to two separate surfaces becoming one surface [**24**]. As a test advances, w sets an upper bound for G_c. When a test recedes, w is a lower bound for G_c. At equilibrium the critical energy release rate G_c equals the thermodynamic work of adhesion w.

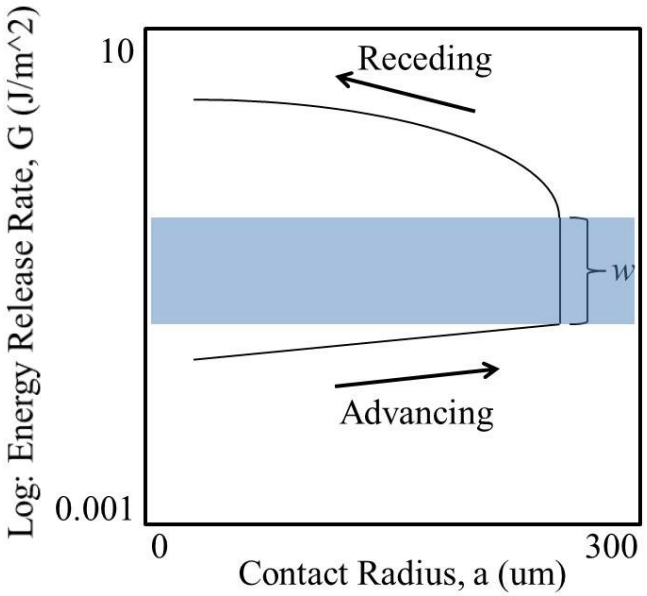

Figure 8: A schematic of energy release rate vs. contact radius

During separation of a JKR hemispherical probe and substrate, the decrease contact radius can be viewed as crack propagation. The relationship between contact radius and crack velocity, v, is:

$$v = -\frac{da}{dt} \qquad \text{(Equation 16)}$$

The negative sign in Equation 16 is attributed to the advancement of a crack corresponding to a receding contact patch. As such, it can be seen that the critical energy release rate depends on the velocity of crack propagation making G_c a rate dependent property [**24**].

1.4.3.3. Relationship between G_c and Contact Angle

To review, a contact angle, θ, is created when the adhesive energy of a liquid drop, solid surface energy, and interfacial energy are in equilibrium. The relationship for advancing contact of a liquid drop on a substrate is:

$$G_a = \gamma_1(1 + cos\theta_a) \qquad \text{(Equation 17)}$$

The relationship for receding contact of a liquid drop on a substrate is:

$$G_r = \gamma_1(1 + cos\theta_r) \qquad \text{(Equation 18)}$$

Figure 9 depicts the relationships of G_c and the contact angle to a dynamic drop in non-equilibrium conditions. A brief glance at Equation 3 checks that at equilibrium (i.e. no advancing nor receding), the critical energy release rate, G_c, equals the thermodynamic work of adhesion, w, which is the same conclusion portrayed in Figure 8.

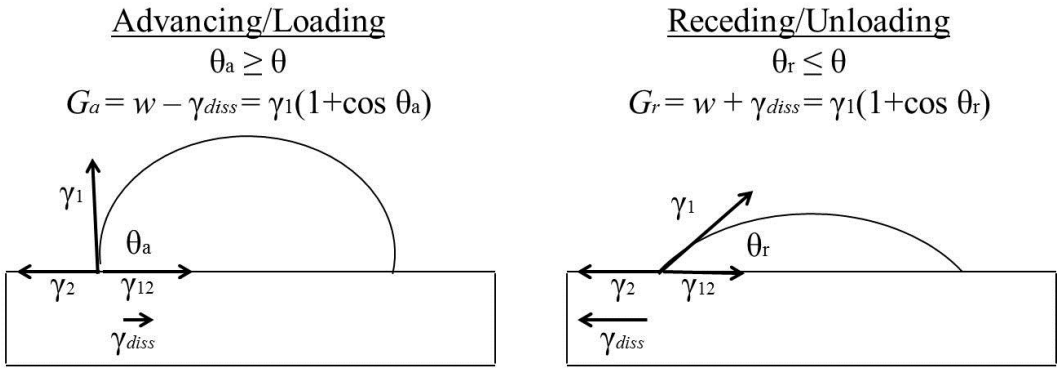

Figure 9: Relationship between G_c and contact angle

When contact angles are not in equilibrium, energy is being dissipated in an area very close to the contact line. The dissipated energy per unit area, γ_{diss}, can be thought of a force per length that opposes movement of the contact line. The dissipated energy increases G_c when contact is receding and conversely decreases G_c when contact is advancing. The relationships are given by:

$$G_r = w + \gamma_{diss}, \qquad G_a = w - \gamma_{diss} \qquad \text{(Equation 19)}$$

It is important to observe that energetic losses change the adhesive energy, giving more credence to the viewpoint of G_c being associated as a surface energy as opposed to a fracture toughness parameter in the adherence of soft solids [**24**].

1.5. Adhesive Characterization

To develop a releasable adhesive system, adhesive characterization must be performed. While there are several ways to characterize adhesion (e.g. the JKR test described above), peel is a commonly used adhesive measurement [**2**]. Peel is justified as a method of characterization, specifically for thin elastic adhesive films, due to the ability of the test to directly measure material properties. Peel characterization has been legitimized by several ASTM standards such as: ASTM D-1002, D-0903, and D-1781 [**26**] [**27**] [**28**]. As a counter example, alternative adhesive measurements like the so-called "napkin ring test," fail to fully work out the independent variables that contribute to adhesion. A failure force measurement of adhesion can still be made using a napkin ring test but one cannot easily relate the failure force to material properties (e.g. E, G_c, film thickness, etc.). As such, the napkin ring adhesive test has since been decertified as a proper ASTM testing standard [**29**] Therefore since the mechanics of peel are well known, and there is simplicity in testing, a peel test is a suitable method for adhesive characterization [**30**]. The remainder of this section covers compliance of an elastic film, thin-film peeling, and fracture mechanics of a lap-shear adhesive joint.

1.5.1. Compliance of an Elastic Film

According to Equation 4, compliance is important in understanding the force capacity of an elastic adhesive film. This section is entirely devoted to describe normal compliance of an elastic film. Rationale for not choosing, say, compliance of a cantilever under shear deformation

is because normal compliance is most applicable for understanding lap-shear testing, a subset of peel, the type of adhesive failure characterized in this thesis (See Figure 47: Clamping model illustration for further clarification). In short, a basic introduction to compliance is needed so that explicit expressions for thin-film peeling, the mode of characterization for this research, can be made.

Compliance of an elastic film can be determined using the theory of elasticity. Figure 10 illustrates the geometry of an elastic film being deformed, *x*, under a normal force, *F*.

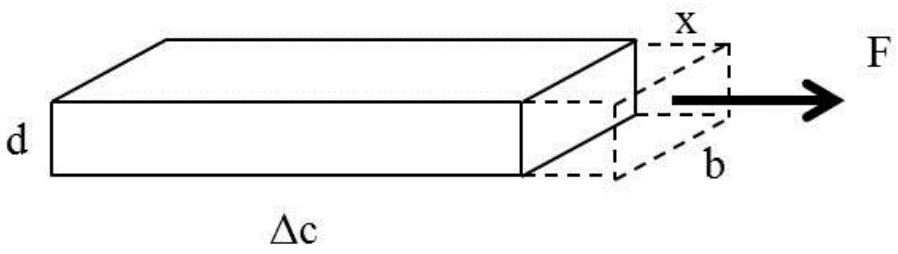

Figure 10: Mechanics of an elastic film

According to Hooke's Law, the stress is related to the strain in the film by the modulus, *E* [**17**]. Equation 20 writes the relation:

$$\frac{F}{bd} = E\frac{x}{\Delta c} \qquad \text{(Equation 20)}$$

Compliance is defined as extension per force and can be visualized in a physical sense as a material's flexibility [**17**]. Using the definition of compliance and rearranging Equation 20, the compliance of a thin elastic film becomes:

$$\frac{x}{F} = compliance = C = \frac{\Delta c}{bdE} \qquad \text{(Equation 21)}$$

Where x is the displacement, F is the normal force, C is the compliance, d is the thickness, b is the width, Δc is the length, and E is the elastic modulus of the film.

1.5.2. Thin-Film Peeling

Peeling an adhesive layer from a rigid substrate while carefully monitoring the displacements and forces present, leads to a simple adhesive measurement known as a peel test [**2**]. Figure 11 is an illustration of such a test.

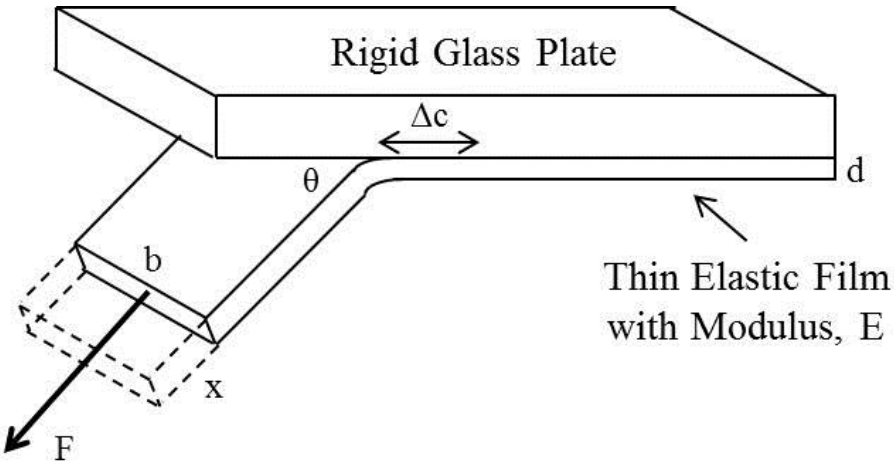

Figure 11: Peeling of an elastic film from a rigid substrate

Peeling an elastic film from a substrate involves the balance of three energies: the surface energy U_S, the potential energy U_P, and the elastic energy U_E [**30**]. The surface energy term is due to the formation of new surfaces during fracture of the adhesive and substrate. It is simply defined by the surface area multiplied by the surface energy, γ. Equation 22 restates this:

$$U_s = -(b\Delta c)\gamma \qquad \text{(Equation 22)}$$

The potential energy term deals with the work done while peeling and depends on a specific angle θ of peel. In order to determine the potential energy, or work applied to the film, the extension, x, is needed. Figure 12 shows the extension in the film, x, as well as the advancement of the crack, Δc, after a force, F, has been applied [**30**].

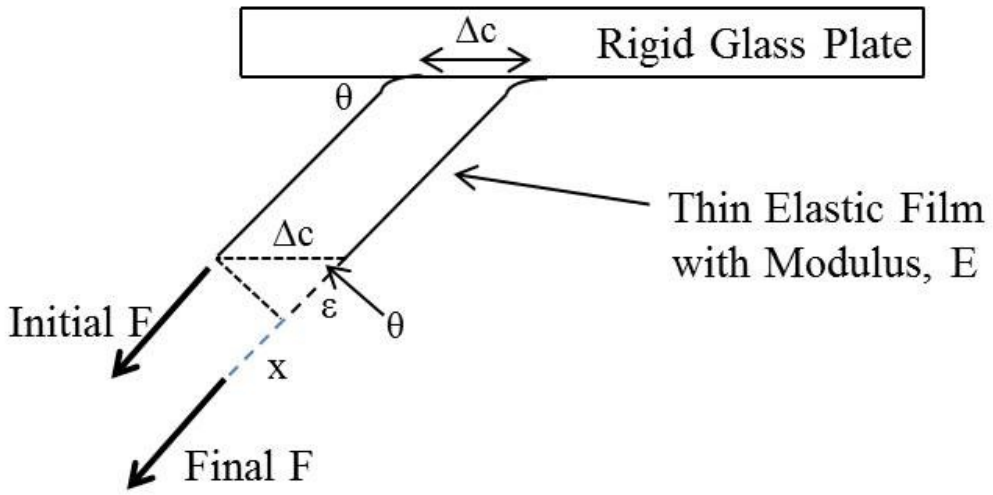

Figure 12: Potential energy term

During peel, the length of the extended film does not change and only the part of the film still adhered to the substrate experiences strain. Equation 23 expresses this:

$$\Delta c = x + \varepsilon = x + (\Delta c)\cos\theta \qquad \text{(Equation 23)}$$

Now the extension, x can now be solved for and multiplied times the force required to extend the crack Δc. The product is the potential energy and is given by Equation 24:

$$U_P = Fx = F[\Delta c(1 - \cos\theta)] \qquad \text{(Equation 24)}$$

Finally, the elastic energy term is the elastic strain stored in only stretching the released part of the film during the advancement of the crack. This is the same as the stored energy in a spring so by assuming a Hookean response it is written as:

$$U_E = \frac{1}{2}kx^2 = \frac{1}{2}\frac{1}{C}(FC)^2 \qquad \text{(Equation 25)}$$

Substituting in compliance from Equation 21 into Equation 25 gives the elastic energy as:

$$U_E = \frac{F^2 \Delta c}{2bdE} \qquad \text{(Equation 26)}$$

Equation 27 gives the result of the balance of the surface energy, potential energy, and elastic energy.

$$\left(\frac{F}{b}\right)^2 \frac{1}{2dE} + \left(\frac{F}{b}\right)(1 - \cos\theta) - \gamma = 0 \qquad \text{(Equation 27)}$$

It can be seen that Equation 27 is quadratic in the peel strength (*F/b*). When the peel angle is 90° the elastic energy term accounts for approximately 1% of the other two terms and can be neglected. At this point, it is harmless to approximate the surface energy γ as the adhesive energy G_c since energetic losses associated with surface energy is included in the definition of G_c. At this specific angle there is a direct relationship between the peel strength (*F/b*) and G_c such that a measurement of G_c can be made for a particular crack speed. As the peel angle approaches zero, lap-shear conditions occur and the relationship for peel strength becomes [**30**]:

$$\left(\frac{F}{b}\right) = \sqrt{2dEG_c} \qquad \text{(Equation 28)}$$

It should be noted that by substituting Equation 21 into Equation 28, Equation 28 can be rewritten into the form of Equation 4. It was necessary to delay a derivation of Equation 4 until a general introduction to adhesion, discussions of fracture mechanics, contact mechanics, Hookean material assumptions, etc. had been introduced before a deeper understanding behind the driving equation for this research could be thoroughly explained [**10**] [**30**].

1.5.3. Stability of Crack Growth for a Lap-Shear Adhesive Bond

A remark on the stability of crack propagation for lap-shear adhesive bond can be made by examining the second derivative of the total energy with respect to the contact area. For stable or controlled rupture of the crack:

$$\frac{\partial^2 U_T}{\partial A^2} = \frac{\partial G}{\partial A} > 0 \qquad \text{(Equation 29)}$$

In the case for rupture of an adhesive lap shear bond it is assumed that the interface will separate in an uncontrolled manner meaning that once a crack begins to propagate, it happens in a sudden, rapid, and continuous fracture [**10**].

$$\frac{\partial^2 U_T}{\partial A^2} = \frac{\partial G_c}{\partial A} < 0 \qquad \text{(Equation 30)}$$

CHAPTER 2: LITERATURE REVIEW

Knowledge on a specific topic can be gained by reviewing literature within a particular area of research. Once a working knowledge has been gained, only then can innovations and improvements to current problems associated with standard practices be addressed. Performing a literature review helps estimate how original research improves upon or expands what is already known of a certain subject. Therefore, in order to design an innovative reversible adhesive system, it is important to understand what has already been studied and what is currently being researched.

The following chapter is a review of the contemporary research topic of switchable adhesion. A few selected publications have been chosen to portray common switching mechanisms currently being researched by other universities. Examples of the types of switching mechanisms presently investigated are: thermal, light, pH, solvent, magnetic, electric, mechanical, etc. This chapter also covers past research conducted at the University of Massachusetts which directly inspired this work.

2.1. Switching Mechanisms

Initially there have been two independent strategies in designing reversible adhesives, either controlling chemical functionality or topography [**11**]. Controlling the chemistry of adhesion has been a traditional means to switch adhesion. Two examples of chemical switches are: curing of superglue when exposed to moisture as well as a material undergoing a phase change (e.g. melting) to become much tackier. Topographical switching simply implies changes to contact area between an adhesive and substrate. As an example, an adhesive pad containing

compliant micro-scaled posts can be tilted sideways under external stimuli to change surface topography. The changes to surface topography on such a system obviously affect the total contact area of the adhesive.

Current research has suggested that many materials exhibit hierarchical organization on different length scales. For instance, a gecko has toes on a macro-scale, each toe contains thousands of micro-scale setae, and on a nano-scale each seta contains multiple spatula tips that promote Van der Waals interactions when in close proximity to other atoms (see Figure 2). The hierarchy of structure seen at the macro-level down to the micro- and nano-level implies that the contribution of both, chemistry and topography, might be of significance [**11**].

As a word of caution though, there is great difficulty in synthetically maintaining a hierarchy of structure at every length scale. As an adhesive pad increases in size, the contribution of small scale hierarchy decreases due to the mismatch in length scales: large pad and small topographical structure on the pad. Micro-and nano-scaled topography only help increase contact at the micron or sub-micron length scale. For large adhesive pads to benefit from small scale topography, a hierarchy must be maintained at every length scale.

Not only are there concerns regarding topography, but apprehensions exist for chemical switching too. Chemical switches are not ideal since considerable amounts of time are needed for chemical switches to happen. In other words, chemical switching is slow and often non-repeatable. Chemical switching relies heavily upon surface specificity (e.g. "surface A" *only* sticks to "surface B"). It is obviously much more preferred to have an adhesive that does not have limitations to the chemistry involved and is not designed around a specific value of G_c.

Regardless of limitations present to topographical and chemical switching mechanisms, it is still very important to be aware of other approaches to switching adhesion. Most likely contributions of topographical, chemical, and *mechanical* switches are what a gecko uses to traverse a tree for instance. As such, examples of other research revolving around chemical and topographical switching attempts are totally relevant and very helpful in developing a bio-inspired adhesive. The following subsections are broken into two groups: chemical switching and topographical switching; each approach containing supporting published literature.

2.1.1. Chemical Approaches to Switchable Adhesion

Chemical functionality can be used to switch adhesion by directing molecular interactions through hydrogen bonding, electrostatic or hydrophobic interactions [**11**]. Materials that are chemically switched usually have a transformation in material properties when triggered by external stimuli such as: solvents, pH, temperature, electric or biochemical signals [**11**]. The attempts at chemical approaches to switchable adhesion are numerous and several examples are provided below.

2.1.1.1. Thermal Switching

P. Fabre et al. demonstrated with fluorinated liquid crystal polymer adhesives the ability to switch adhesion by means of temperature change. The smectic fluorinated liquid crystal polymer adhesives were able to toggle between a crystalline structure and an amorphous state by undergoing a lamellar-to-isotropic first order phase transition. The first order phase transition change was triggered by a very narrow heating and cooling range of only 28°C compared to a 60-70°C window usually required for other PSAs using the glass transition temperature conversion as a switch. The fluorinated liquid crystal was a copolymer with 50 mol% acrylate

monomer with a perfluoroalkyl side chain (C_2H_4-C_8F_{17}) and 50 mol% methacrylate monomer with an alkyl chain ($C_{17}H_{35}$) as the adhesive. At room temperature the copolymer was partially crystalline, but at 35°C a transition occurred switching from an ordered structure to a mixed isotropic phase which made the polymer much tackier. The temperature change increased mobility in the liquid crystal polymer so that rearrangement of the polymer backbone was able to occur. Figure 13 is a schematic representation of the transition between the smectic and isotropic phase change [**31**].

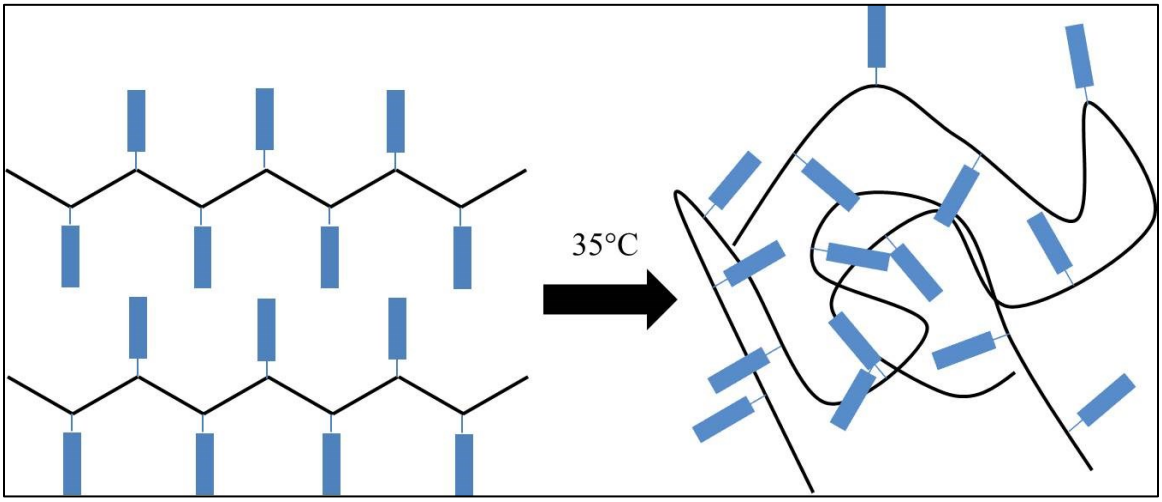

Figure 13: Transition between the smectic and isotropic phase

A probe tack adhesion test was utilized to measure tack and wettability. In the smectic phase, which was hard and non-wettable, no energy was required to separate the probe and adhesive. However, after a smectic-to-isotropic phase change, the adhesion energy decreased from 50 J/mm^2 at 37°C to 14 J/mm^2 at 50°C. The change allowed the probe to go from <10% contact area in the smectic phase to 100% contact in the isotropic phase. The transition temperature of the adhesive could be tailored by alternating the length of the pendant side chains on the polymer [**31**].

2.1.1.2. Light Switching

Research perfomred by I. Webster et al. showed that an acrylic PSA could be switched off and removed through photoinitated crosslinking caused by exposure to light. The acrylic adhesive copolymers used were itaconic anhydride, 2-ethylhexyl acrylate and *n*-butyl acrylate polymerized in ethyl acetate. The anhydride containing copolymer was modified with 2-hydroxyethyl methacrylate (HEMA) in toluene to create a methacrylate functional PSA. The PSA was further mixed with a visible light photoinitiator which ultimately produced a light sensitive adhesive. The adhesive solution was spread onto a thin elastic film so that peel strength adhesion could be tested.

Prior to testing, the methacrylate functionalized PSAs had an opaque backing shielding the adhesive interface from light until removal of the adhesive was desired. Upon irradiation to light, free radical cross-linking between vinyl groups occurred and an increase in hardness, and hence a reduction in adhesion, was measured. Peel strength tests showed that after irradiation of light, the adhesive peel strengths decreased by 90%. The light switchable PSAs were however non-reusable [**32**].

2.1.1.3. pH Switching

Adhesive changes with pH were studied by Keddie et al. in waterborne poly (butyl acrylate-co-acrylic acid) [P(BuA-*co*-AA)] latex films. The latex films consisted of a colloidal dispersion of core-shell particles that when dry, created a honeycomb structure. In some cases, the space between the dried latex honeycomb structures could be crosslinked covalently which tremendously impacts the macro-scale mechanical properties of the film. However, the adhesive waterborne [P(BuA-*co*-AA)] latex films had weaker bonding between particles allowing for

more variation, and therefore mechanical changes, during emulsion polymerization. Changes to the pH of the latex during polymerization had an effect on the drying kinetics of the adhesive films.

The acidic monomers during emulsion polymerization tended to concentrate on the shell surface because of monomers' hydrophilic carboxylic acid (COOH) groups. Conversely the hydrophobic monomers concentrated within the particle core and hence two distinct continuous phases were present within one particle. The particle shell surface, consisting of carboxylic acid groups, was pH responsive. While still wet, the monomers' carboxylic acid groups, located on the particle surface, were negatively charged. The negatively charged colloidal suspensions were stabilized through electrosteric interactions with a higher pH. As the pH increased from acidic to basic, the drying kinetics changed and in-turn altered the adhesive properties of the latex films.

When the pH was low, the carboxylic acid was not dissociated and, in the absence of water, contributed to hydrogen bonding to other colloidal particles. When the pH was high, the groups were deprotonated creating negatively charged ionized groups that were balanced with counterions which created neutral dipoles. Figure 14 shows the possible carboxylic acid interactions: (a) hydrogen bonds between COOH groups and water, (b) dimers between COOH groups, (c) lateral hydrogen bonding between COOH groups, and (d) ionic dipole created by COO^- and Na^+ counterions.

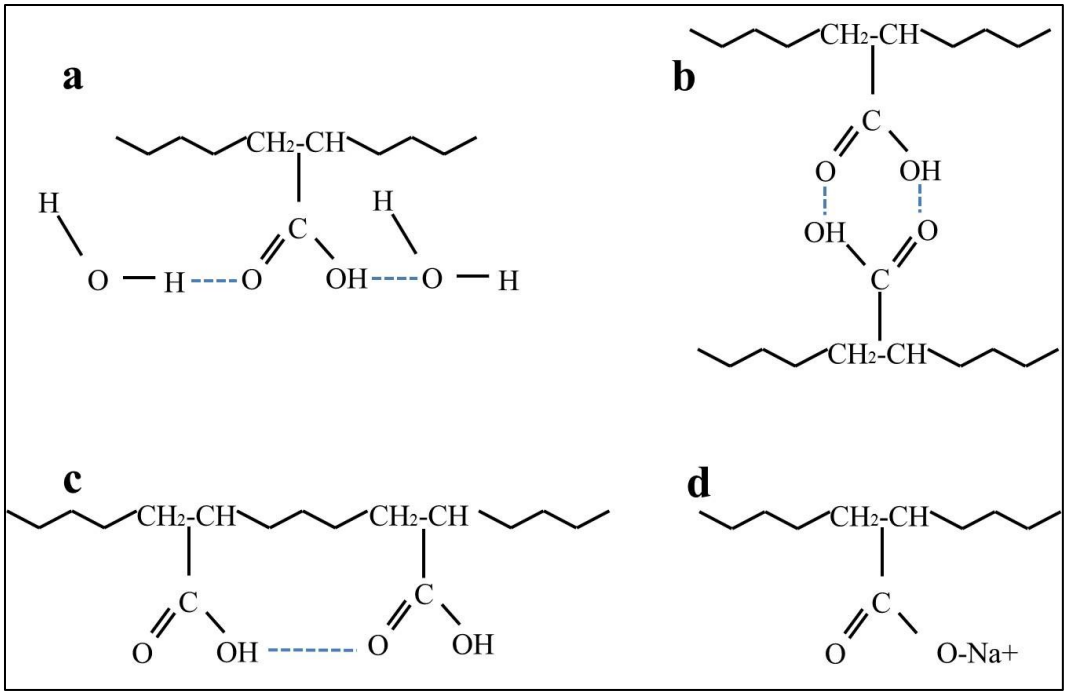

Figure 14: Carboxylic acid interactions of a pH responsive latex film

Probe tack measurements showed that latex films from low-pH dispersions were more deformable and had higher adhesion energy compared to high pH dispersions. Specifically films cast with a pH of 4 were more compliant and had higher viscoelasticity due to energy dissipation from hydrogen bond breakage. Films cast with a pH of 9 had a higher modulus because of stiffening attributed to the ionic dipolar interactions but intermediate viscoelasticity [**33**].

Another pH study performed by Stafford et al. investigated JKR adhesion measurements between a PDMS hemisphere lens coated with a polyelectrolyte multilayer (PEM) and a rigid substrate while varying exposure to aqueous solutions of controlled pH. The PDMS probe was coated with aqueous solutions of poly (allylamine hydrocholoride) (PAH) and poly (acrylic acid) (PAA). To coat the PDMS probe, the probe was dipped into each solution for a given amount of time creating bilayers which could be repeated until a desired layer-by-layer (LBL) coating thickness was attained. Glass slides and silicon wafers were treated with 3-

aminopropyltriethoxysilane (APTES) and used as substrates for JKR adhesion measurements between the coated PDMS-PEM hemisphere and the amine-functionalized substrates. Figure 15 summarizes the experiment [**34**].

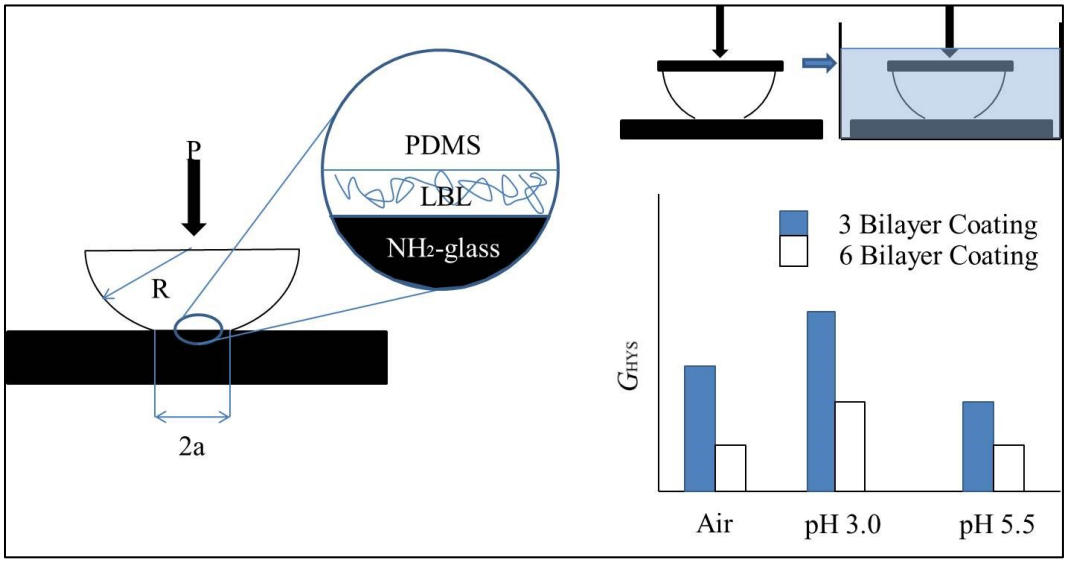

Figure 15: JKR measurement of a pH switchable adhesive

To isolate the effect of pH switching on adhesion, JKR contact mechanic adhesion measurements were performed in both air and pH solutions. The pH solutions consisted of either NaCl or HCl at a pH of 5.5 or 3.0. The PEM coating was chosen due to the abundance of ionizable carboxylic acid groups making the coating pH responsive. Previous studies by Stafford et al. showed that the coatings swelled substantially and were also plasticized when exposed to the aqueous solutions. The swelling and plasticization inhibited intimate contact because of increased surface roughness and an elevated coating modulus. The decrease in contact area decreased the overall adhesion between the coating and substrate and showed that pH could be used as a switch to turn off adhesion [**34**].

2.1.1.4. Solvent Switching

Minko et al. introduced a two-level structured switchable adhesives that changed surface morphology and surface properties when exposed to selective solvents. Adhesive samples were manufactured with a primary needle like structure on a micron length scale through plasma etching of poly(tetrafluoroethylene) (PTFE). Changes in plasma etching times governed the RMS surface roughness. Roughness was found to substantially amplify the range of switching.

A secondary structure was created on the needle like structures by utilizing an ammonia plasma treatment. The ammonia plasma treatment covalently introduced hydroxyl and amino end functional groups onto the roughed up PTFE. Spin-coating introduced carboxyl-terminated poly(styrene-*co*-2,3,4,5,6-pentafluorostyrene) (PSF-COOH) and carboxyl-terminated poly(2-vinylpyridine) (PVP-COOH) on the roughed up PTFE. Figure 16 shows a schematic representation of two-level structured adhesives along with the hydrophobic and hydrophilic functional groups [**35**].

Figure 16 (a) is a schematic of the needle like morphology, (b) is an SEM image after plasma etching, (c,d,e) show that each needle is grafted by a mixed polymer brush consisting of hydrophilic and hydrophobic layers, (f, g) are mock AFM images depicting morphology after treatment of selective solvents. The graphed on hydrophobic and hydrophilic polymer brushes of the nanometer length scale allowed the surface properties and morphology of the adhesives to be reversibly modified when exposed to certain solvents, namely: toluene, acidic water with a pH of 3, and 1,4 dioxane [**35**].

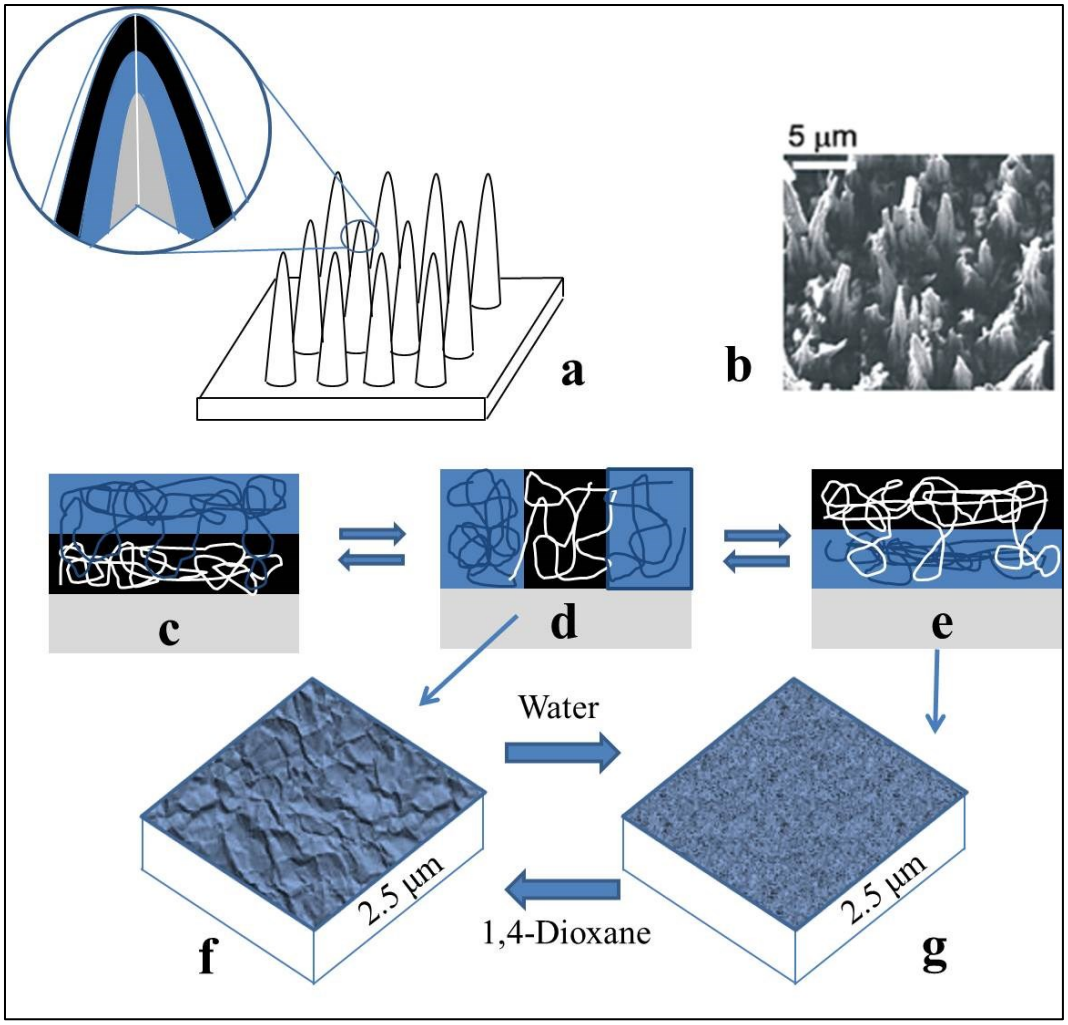

Figure 16: Solvent responsive switchable adhesive [35]

Creton et al. created a solvent switchable substrate for a hydrophilic PSA. When the substrate was exposed to selective solvents, the adhesion and wetting properties of the interface between the substrate and the hydrophilic PSA were altered. Tackiness and wettability changes of the PSA on the polymer brush substrate were verified by probe tack and contact angle measurements. The substrate was a silicon surface grafted with bicomponent polystyrene-poly(2-vinyl-pyridine) (PS-P2VP). The hydrophilic PSA consisted of a blend of poly(vinyl-pyrrolidone)-poly(ethylene glycol) (PVP-PEG).

The bicomponent silicon substrate was composed of moderately polar and apolar components which could switch from a hydrophilic to hydrophobic state depending on a solvent pretreatment. The switching states could toggle between non-adhesive, moderately adhesive, or extremely adhesive against the hydrophilic (PVP-PEG) soft adhesive. When the substrate was pretreated with toluene, the polystyrene brush swelled leaving a surface layer enriched with polystyrene. However, if the substrate was exposed to acidic water (pH 2), then poly(2-vinyl-pyridine) (P2VP) occupied the surface and the (P2VP) monomers were positively charged. Figure 17 illustrates solvent treatment events that toggled hydrophobic to hydrophilic behavior in both the wet and dry states [**36**].

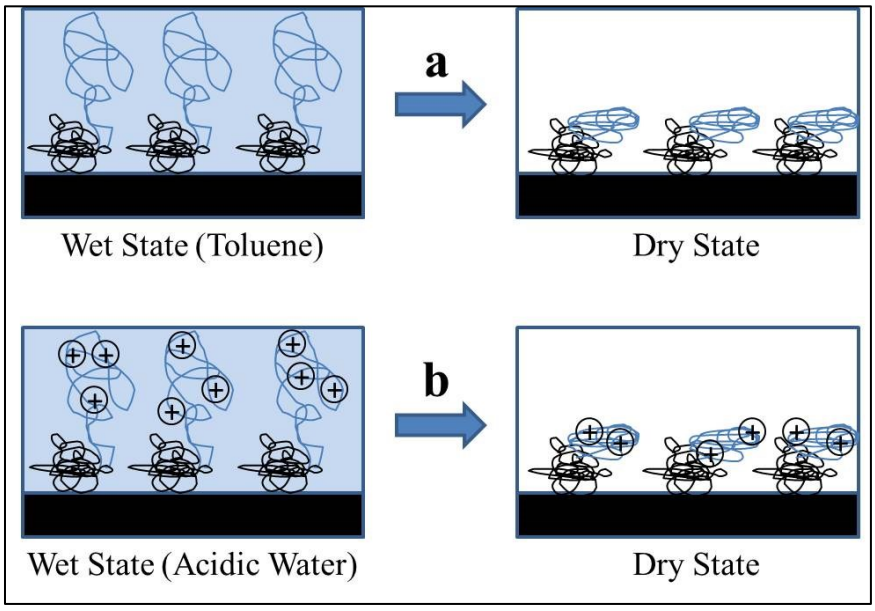

Figure 17: Solvent switching of hydrophilic to hydrophobic and vice versa

After exposure to acidic water, experiments showed that protons could be removed upon an ammonia solution treatment and the tackiness of the PVP–PEG could change reversibly depending on the neutrality of the P2VP. The extent of the reversible change in tack of the

PVP–PEG adhesive could be adjusted by the ratio between the two grafted polymers of the bicomponent brush layer allowing fine-tuning of the switchable adhesion [**36**].

2.1.2. Topography

The other design route for switchable adhesives historically has been to adjust topography. Again, topographical changes manipulate surface morphology so that contact area can be controlled. Topographical systems are triggered by external stimuli like temperature, magnetic and electric fields, stretching, pneumatic pressure and preload which ultimately change adhesive performance. These designs look to maximize and minimize contact area which results in reversible switchable adhesion [**11**]. Multiple examples of topographical switches are provided.

2.1.2.1. Thermal Switching

Del Campo et al. developed a thermosensitive switchable adhesive. Del Campo's bio-inspired switchable adhesives consisted of gecko like fibrillar patterns of shape memory thermoplastic elastomers. Shape memory polymers (SMP) can be deformed into temporary shapes and then recovered to a predefined original shape upon heating through a transition temperature. Through heating of the shape memory polymer posts, the posts became compliant and could be temporarily tilted away from the surface which effectively reduced the contact area and therefore decreased adhesion.

The adhesives were produced by a double molding process. Polydimethylsiloxane (PDMS) was cast into a lithographic master and then demolded. The demolded PDMS posts were then brought into contact and imprinted into a SMP (Tecoflex 72D-cycloaliphatic

polyertherurethane block copolymer) at elevated temperature. Once cooled, the PDMS imprint was removed leaving behind a shape memory micropatterned adhesive. The adhesive posts had micropillars with diameters between 0.5 and 50 μm and heights varying between 10 and 100 μm.

When the microstructured adhesive was heated above the transition temperature, the pillars became soft and deformable allowing them to be tilted so that the contact area was reduced. Figure 18 shows the molding process on the left and the thermosensitive tilting mechanism on the right (switching from adhesive to non-adhesive and vice versa) [**37**]. Adhesive characterization was made with an in-house built indenter system equipped with a sapphire sphere probe (similar to a JKR measurement) and a 200 fold increase in adhesion was measured [**37**].

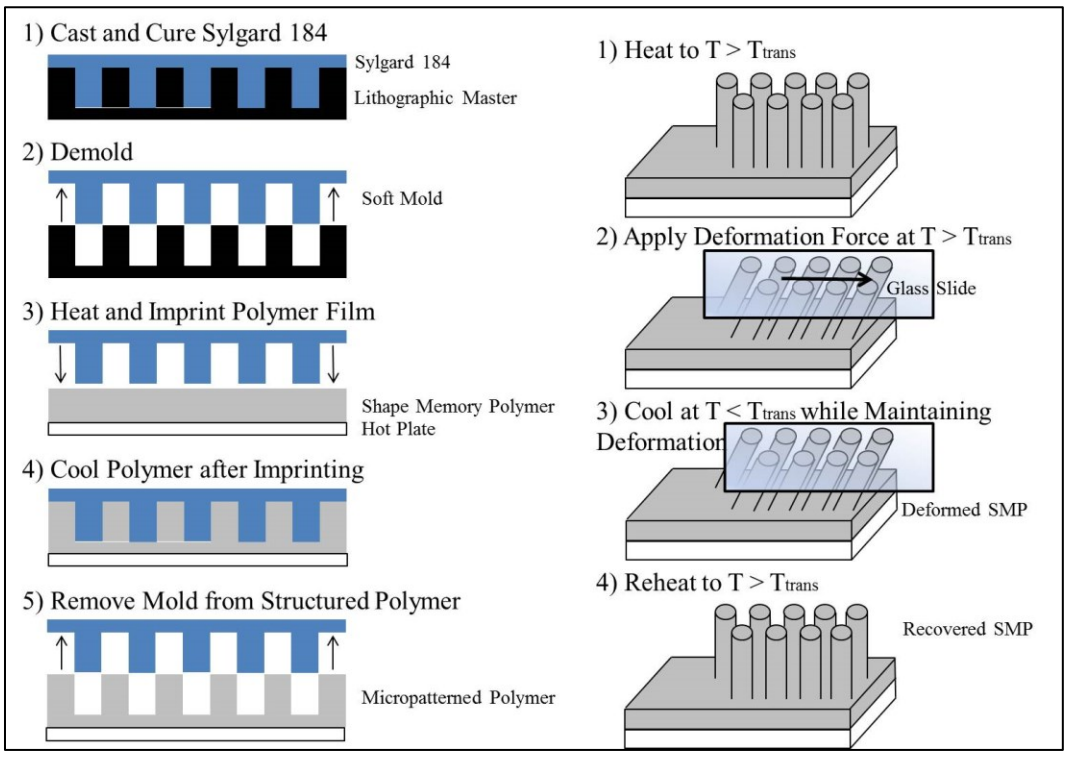

Figure 18: Molding process and pillar tilting

Xiao et al. produced a thermally controlled reversible adhesive that consisted of microfibrillar adhesive polymers on top of SMPs. The two part system cured a continuous elastomeric adhesive layer onto a SMP. Figure 19 illustrates the adhesive-SMP fabrication process [**38**]. Shape memory polymer microfibers were placed in contact with an uncured liquid adhesive polymer (a) until the polymer collected onto a microfiber post (b). Once the posts were dipped into adhesive polymer they were set onto a Mylar film and cured (c). After curing the Mylar film was removed (d) and the two part adhesive system remained.

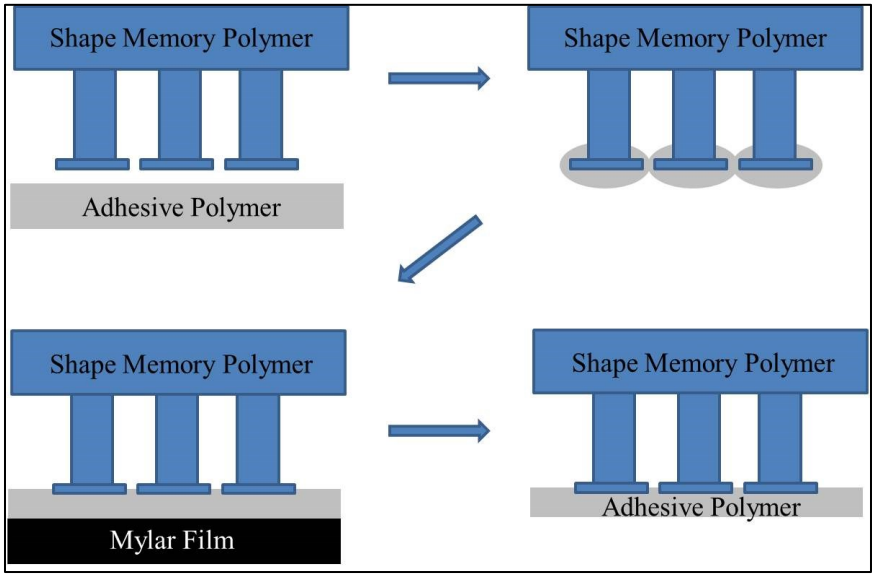

Figure 19: Fabrication of adhesive shape memory polymer array

The system had slight curvature due to the high stiffness from the SMP and as a result poor adhesion at room temperature. Using an infrared light as a heat source, the sample could be heated above the glass transition temperature so that the material was in a rubbery state. Adhesive characterization consisted of JKR spherical indentation pull off tests conducted in three conditions. The testing scenarios were: the sample was loaded and unloaded after it had been heated above the Tg (hot-hot), the sample was loaded and unloaded at room temperature (cold-

cold), and the sample was heated past the Tg loaded then cooled down and finally unloaded. Results indicated that both bulk and surface properties were thermally controllable. The overall performance of adhesion between a glass probe and adhesive-SMP increased from 0.6 J/m^2 to 3.1 J/m^2 by increasing the cooling rate. Other work studied alternate micro- structured adhesives however the complexity to produce the adhesives did not outweigh the adhesive performances [**38**].

2.1.2.2. Magnetic Switching

Northern et al. developed an adhesive that could be switched in the presence of a magnetic field. The adhesive relied on flexible nickel paddles which had hierarchical polymeric nano- rod cantilevers mounted on the surface. Figure 20 shows SEM images of the synthesized adhesives (left side) as well as a gecko's footpad (right side).

The nickel cantilevers and pads were fabricated by photolithography and etching. The polymeric nano- rods were created by random growth methods. The mechanism for switching adhesion depended on a magnetic field to actuate the nickel cantilevers. While under the influence of a magnetic field, the nickel paddles reoriented themselves away from an adhering surface drastically reducing the contact area and changing the adhesion by a factor of 40. All adhesive characterization was done with an in-house fabricated indentation system performing flat punch pull off adhesion analysis [**39**].

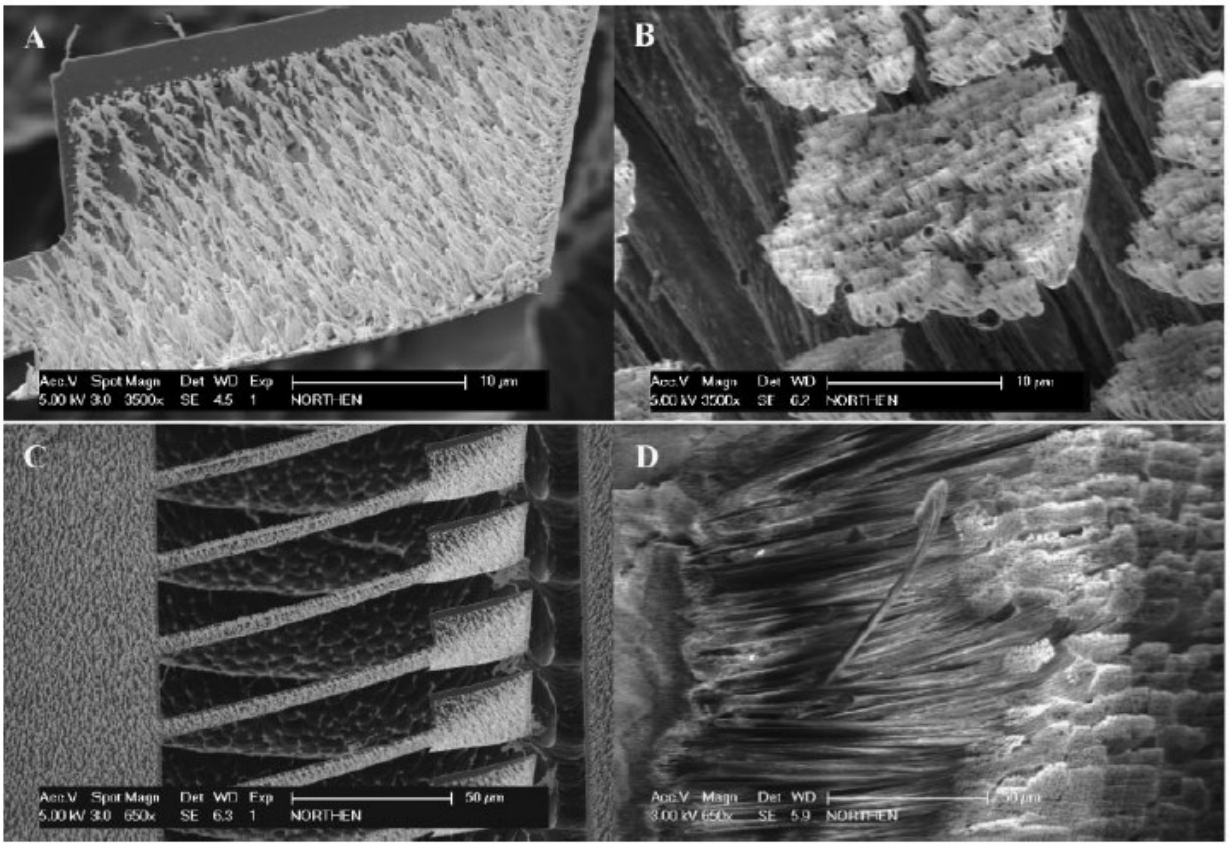

Figure 20: Magnetic pillars **[**39**]**

2.1.2.3. Electric Switching

Vogel et al. created a switchable electronically-controlled capillary adhesion device. Figure 21 is a schematic representation of the device [**40**]. The top portion of Figure 21 is defined as: (a) is a spacer, (b) holes in which droplets protrude, (c) wires to power supply, (d) electrodes, (e) epoxy seal, (f) fluid reservoir, (g) luer connector as reservoir continuation and filling port, (h) reservoir meniscus, and (i) is a support post.

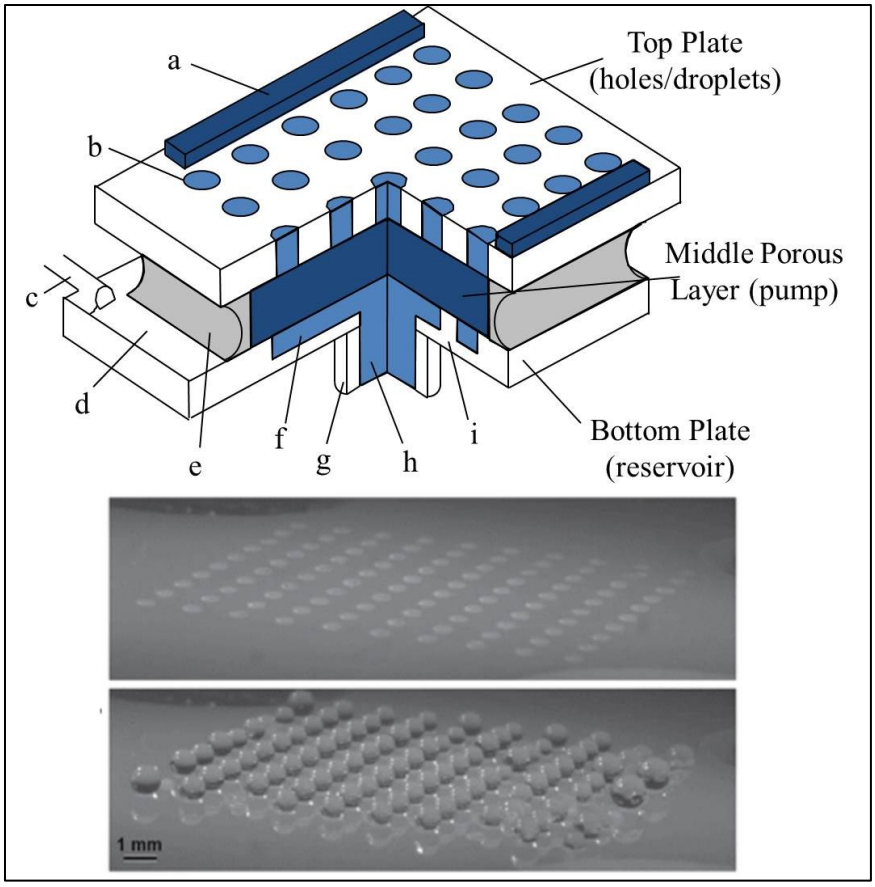

Figure 21: Switchable electronically controlled capillary adhesion device **[**40**]**

The surface tension of a large number of small liquid contacts created a strong adhesion that could be reversed quickly. Figure 22 shows the capillary mechanism by which adhesion was achieved [**40**]. Liquid was pumped through a hole with a low voltage pulse that facilitated electroosmotic flow. Pumping continued until contact was made with the device and substrate. Switching adhesion off occurred when the liquid was retracted. Only modest adhesive strengths (13 mN/cm^2) where measured through force-transducer experiments, however it was theorized that downsizing could rival permanent adhesive strengths since more/smaller droplets would be available to make contact [**40**].

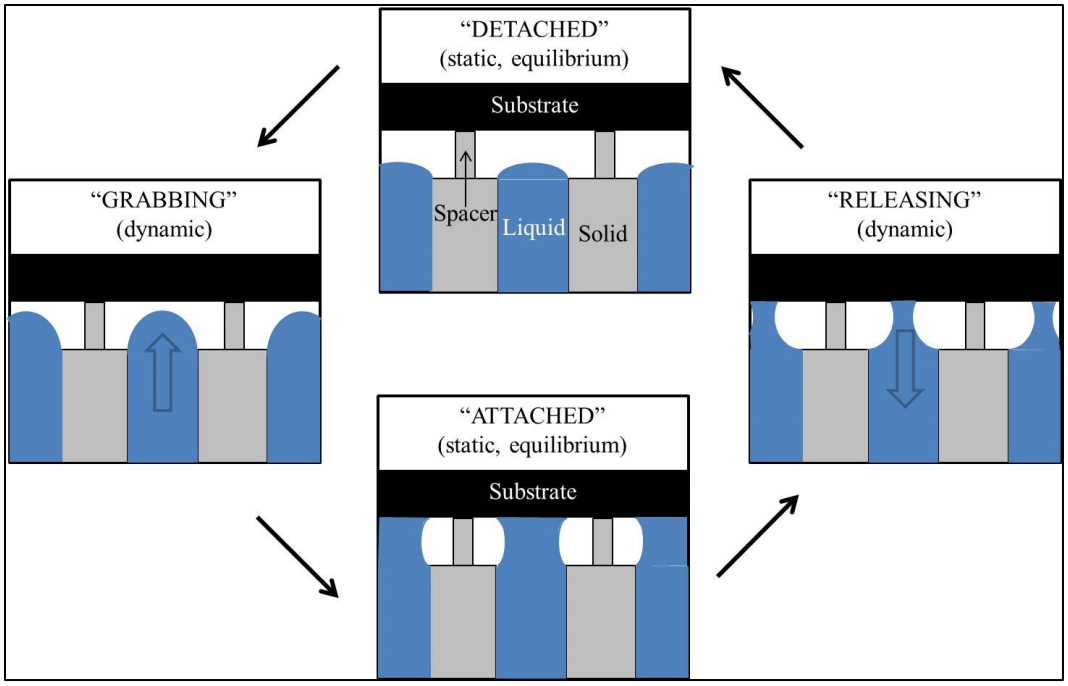

Figure 22: Capillary mechanism of adhesion

2.1.2.4. Additional Contact Area Examples

Suh et al. effectively switched a PDMS fibrillar array's contact area by stretching. The PDMS array was cured in a mold that was manufactured with photolithography and etching. To make the PDMS array wrinkle, the adhesive was stretched and then was placed in a UV-ozone exposure system for 20 minutes. Once the strain was removed a sinusoidal adhesive sample remained. An illustration of the switchable adhesive stretch mechanism and stretched adhesive array is shown in Figure 23 [**41**]. Upon stretching, the adhesion was turned on by orienting the fibrils normal to a substrate which aligned the contact patch so that contact area was increased. The film could recoil back into a wrinkled state and therefore decrease adhesion strength allowing the film to release. The stretchable adhesive worked well in both normal (10.8 N/cm^2) and shear modes (14.7 N/cm^2) [**41**].

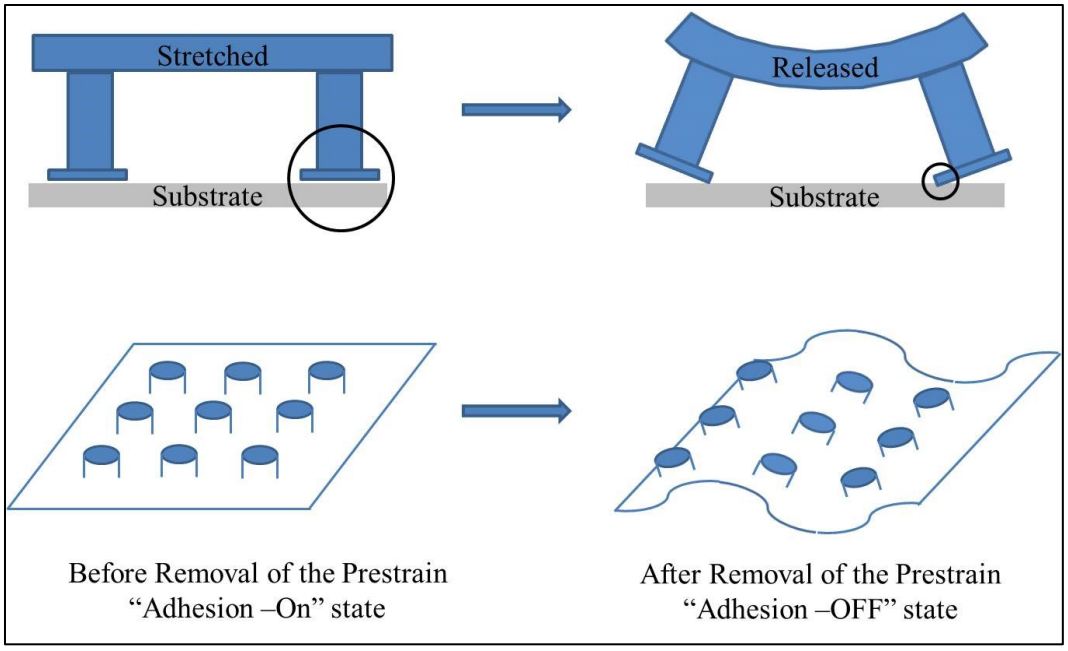

Figure 23: Switchable stretch adhesive

Crosby et al. used surface wrinkles of an elastomer film to control adhesion [**42**]. The samples were not able to be switched but showed that adhesive contact area could be controlled during synthesis. The adhesives were manufactured by curing a layer of poly (*n*-butyl acrylate) (PnBA) onto a substrate. Once cured, more (nBA) solution was poured onto the film which caused lateral swelling. The film was already cast onto a confined substrate therefore the addition of more (nBA) solution created surface wrinkles once a critical compressive stress surpassed an elastic stability. Finally the adhesives were UV cured to create a final adhesive sample. The thickness of the original (PnBA) film showed a direct correlation to the wavelength of the wrinkles. Adhesive characterization was carried out by an in-house compression probe adhesion tester. Adhesion was found to increase by a factor of 3 by decreasing the wavelength. Contact splitting was the mechanism by which the adhesion increased and was attributed to the increase in contact perimeter per area on the adhesive. An increase in contact perimeter per area increased the total contact area [**42**].

2.2. Gecko Research from the University of Massachusetts

The research that directly inspired this thesis was performed by the advisor to this work Dr. Croll, et al. at the University of Massachusetts. The preceding research studied fibrillar "feature-less" gecko like adhesion. The basic premise of the work attacked over design of fibrillar feature adhesive pads and argued for feature-less adhesives that instead aim to maximize contact area and loading in-plane stiffness. The adhesive pads designed showed high force capacities (29.5 N/cm^2 in shear), were scalable to macro-level sizes, and showed reversibility beyond 100 cycles.

The experiments performed consisted of adhering smooth compliant elastomeric pads, reinforced with fabric weaves for stiffness, to glass before lap-shear testing the pads for adhesive force capacity [**10**]. Experiments showed that high force capacities, or gecko-like adhesion, could be achieved without synthetic micro- and nano-scaled posts imitating "fake" setae normally found on the feet of geckos. Figure 24 highlights some important results from the fibrillar feature-less pad research.

Image (a) is a polyurethane carbon fiber reinforced pad supporting 135 kg (≈300 lbs) of weight under lap-shear loading, (b) are scanning electron microscope (SEM) images of a pad showing no fibrils present, (c) shows a force vs. extension plot for a polyurethane carbon fiber reinforced pad being sheared, (d) is data of force capacity over 100 cycles strongly suggesting reversibility, and (e) is a scaling plot showing multiple synthetic pads in agreement with Equation 4.

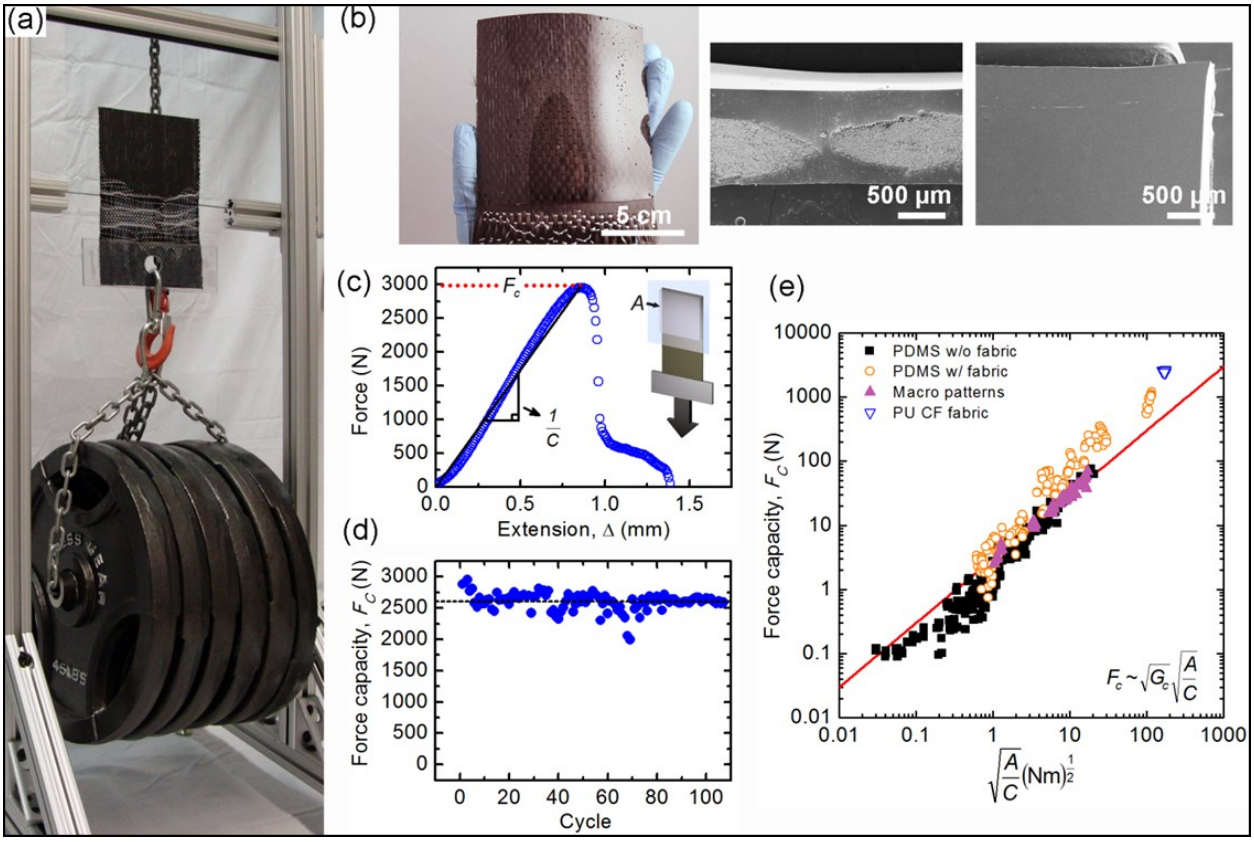

Figure 24: Summary of looking beyond fibrillar features-part I [10]

In addition to synthetic experimentation, live bio data was also collected. Lap shear testing of live geckos as well as a bevy of critters including beetles, flies, crickets and spiders allowed for a direct comparison between the performances of the synthetic adhesive pads with live bio data to be made. The comparisons were useful in evaluating the design and demonstrated that fibrillar features are not required for high force capacities. Figure 25 displays some of the bio data that was gathered.

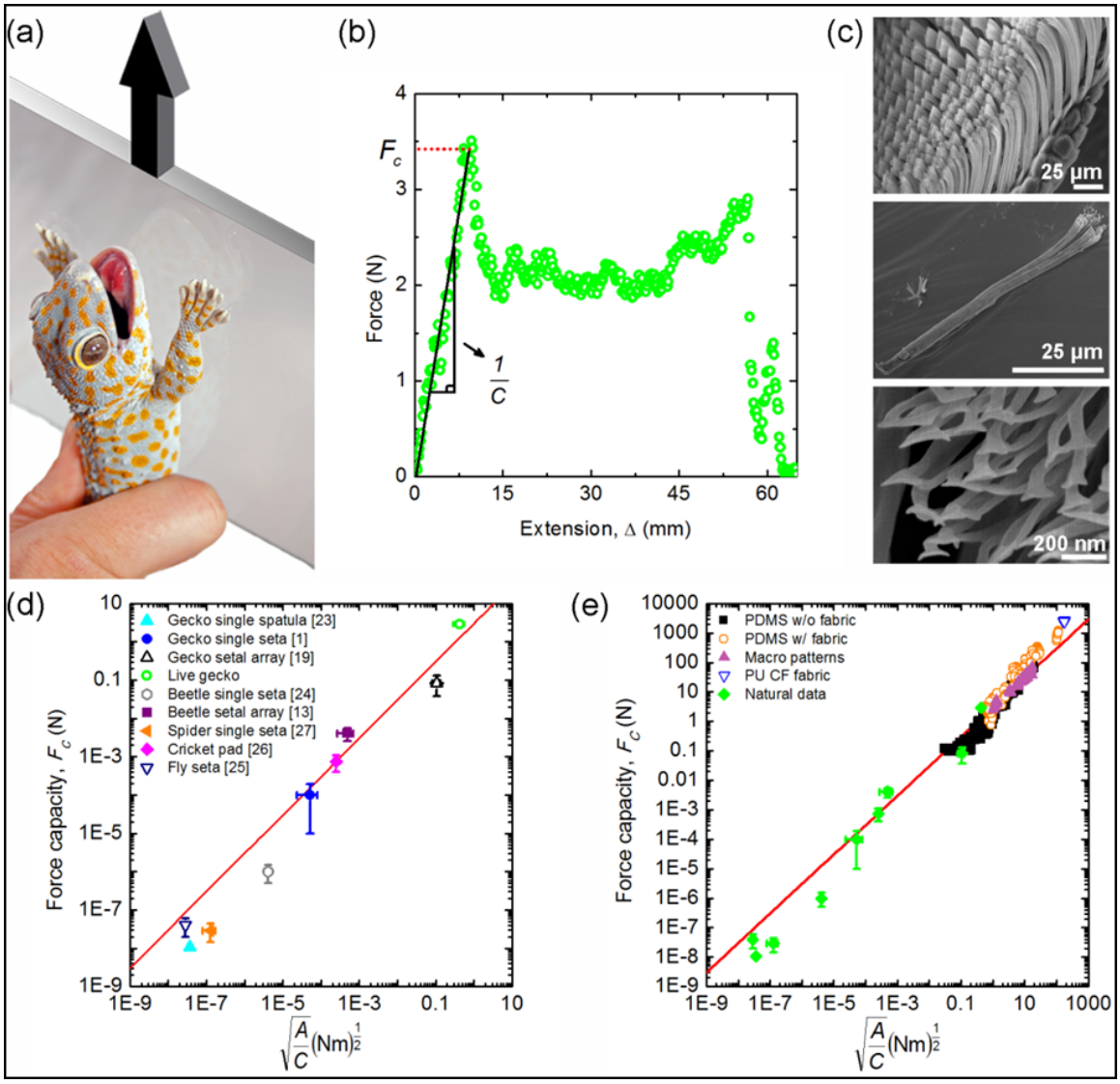

Figure 25: Summary of looking beyond fibrillar features-part II **[**10**]**

Image (a) illustrates a live gecko experiment where the front two paws of a gecko were adhered to glass and then tested for shear strength (b) is a force vs. extension plot for a live gecko (c) are SEM images showing rows of setae (top), a single seta (middle), and spatula tips on the end of a seta (bottom) (d) is a scaling plot of live data and (e) is an additional scaling plot super imposing live data with synthetic data illustrating that the synthetic pads obey the same scaling relationship [**10**].

The previous research concluded that gecko-like features on adhesive pads are likely helpful in promoting adhesion, but should not be solely relied upon in synthetic designs. Fibrillar features create highly compliant surfaces since synthetic posts split and allow for intimate contact between a pad and rough substrate, but features also need to be stiff in order to support any significant load. Commonly, as sizes of adhesive pads increase, the influence of post splitting decreases until no substantial gains of fibrillar features are even detectable. Instead the research showed only information regarding the contact area, A, and the compliance, C, is necessary to attain high force capacities (See Equation 4).

2.3. Research Objectives

The introduction and literature review adequately demonstrated the importance of switchable adhesives. In the introduction, much background information was supplied so that the reader could gain a comfortable understanding of the terms and concepts presented within the scope of adhesive research. The literature review examined research performed at other research institutions illustrating that by-and-large research on switchable adhesion has fallen into two distinct categories: chemical switching and topographical switching. The goal of this thesis is to prove that pursuit of *mechanical* switching is worthwhile in the development of a practical releasable adhesive.

While past research has focused on chemical and topographical reversibility, this research examines mechanical reversibility through switching compliance. Therefore the objectives of this research are to:

- Develop a releasable adhesive system that can be switched using compliance
    - Synthesize adhesive samples sensitive to compliance changes

    - Investigate adding value enhancing magnetic particles to control compliance
- Demonstrate that compliance can be switched by using a mechanical clamp
- Explore magnetic switching as an alternate switching method
    - Work to understand influential magnetic switching variables such as:
        - Role of particle sizes
        - Modifications to amounts of cross-linker
- Verify that work performed is repeatable and consistent with published data

CHAPTER 3: EXPERIMENTAL SETUP

As stated, the main goal of this thesis is to prove that an adhesive can be switched by manipulating compliance alone. This chapter outlines the materials used in the fabrication of a compliantly controlled switchable adhesive while giving justification for the materials selected. In addition, sample synthesis methods are discussed which cover both, attempts at micro-emulsion created adhesive pastes as well as fabrication of continuum thin adhesive films, in an effort to showcase that an investigation into more than one synthesis method can be beneficial in developing a platform for a compliantly controlled switchable adhesive. Finally, details and schematics are provided for a lap-shear adhesive testing apparatus. Familiarity with the mechanical characterization technique, lap-shear testing, aids in assessing the success or failure of the switchable adhesives developed for this research.

3.1. Sample Synthesis

A soft elastomeric material must be used in order to synthesize an adhesive that has tack. In addition, the use of a low modulus, soft material is helpful when modifying the material's compliance since a hard material with a high modulus would be initially too rigid and exhibit very non-adhesive behavior. Thus, the use of a highly compliant two part polymer system was selected for a "proof-of-concept" demonstration that by mechanical clamping, compliance could be effectively decreased and the adhesive force to failure could be controlled. A subclass of magnetically active switchable adhesives, polymer composites containing magnetic particles, was fabricated to explore magnetic clamping as an alternate clamping method to control compliance.

In order to perform this research, two main synthesis procedures were explored. The first synthesis method attempted to develop adhesive pastes through micro-emulsion so that magnetic particles could be combined to make a magnetically active and extremely tacky substance. The second synthesis method cured polymer into thin continuum adhesive films creating a material that was also magnetically responsive however much more workable than a tacky paste. In either case, both synthesis methods used the same materials and so it is logical to first introduce the materials used in the fabrication of the switchable compliant adhesive samples. In addition, discussing material properties provides a rationale for the materials chosen prior to further explaining the finer details of the synthesis methods.

3.1.1. Material Properties

Polydimethysiloxane (PDMS), iron powder, and nickel powder were selected as the constituent materials used in the fabrication of the switchable adhesives characterized within this thesis. Figure 26 shows all the synthesis materials used in this study. This section provides an account of the materials chosen as well as lists the material properties for each substance. Listing the influential material properties rationalizes the selection of PDMS, iron powder, and nickel powder as constituent materials used for composite adhesives.

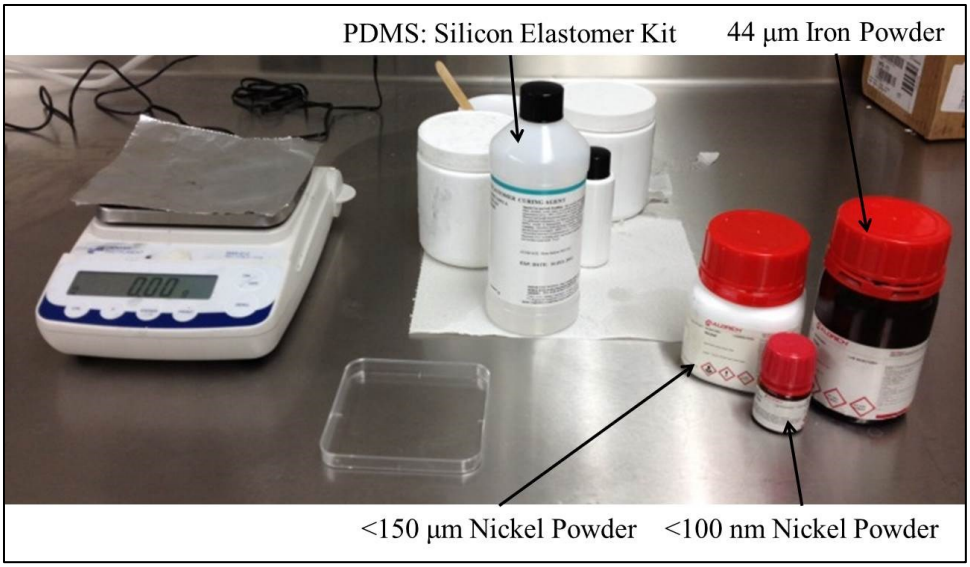

Figure 26: Materials in the lab

3.1.1.1. Polydimethylsiloxane (PDMS)

PDMS is an optically clear, commercially available, two part thermosetting elastomeric rubber that is inexpensive, non-toxic, and can be used as an adhesive. PDMS is compatible with several material classes and is resistant to harsh environmental conditions such as oxidation, ozone, UV, water, and temperature. Conveniently, PDMS has a shelf life of over 2 years and only takes 48 hours to fully cure at room temperature [**43**]. There are several reasons for selecting PDMS as a material used for sample synthesis: PDMS is safe, easily available, inexpensive, and highly compliant. However that PDMS is a *poor* adhesive may be the most compelling. The logic behind selecting a poor adhesive, such as PDMS, is to demonstrate that despite limitations to adhesive properties, observing that mechanics, and not material chemistry, is the relevant factor in the development of a reversible adhesive device that can strongly adhere to multiple surfaces.

The PDMS used in this research was Sylgard 184, a silicone elastomer kit manufactured by Dow Corning Corporation, USA. Through a combination of one part silicone elastomeric crosslinker with ten parts uncured liquid PDMS, a 10:1 ratio, PDMS rubber can be made by addition polymerization. Adjusting the crosslinker ratio gives latitude to tune the modulus and hardness for a specific application and in this case, adhesion. For example, increasing the PDMS to crosslinker ratio to 40:1 yields an extremely tacky low modulus substance. The mechanical properties can be further controlled by adjusting the curing times and temperatures. For instance, increasing the curing temperature to 150°C decreases the cure time to only 10 minutes producing a much more rigid rubber compared to a room temperature cure for 2 days. Table 2 lists properties of PDMS used in this research:

Table 2: Properties of PDMS [43]

Property	Value
Density	1.03 g/cm^3
Young's Modulus	1.5 MPa*
Cost /Gram	≈ $0.09

*value measured in Dolve Hall, room 127

3.1.1.2. Iron

Iron is a commercially available ferromagnetic (i.e. permanently magnetic) metal that is non-toxic, inexpensive and has much better mechanical properties than PDMS. Combining iron powder reinforcement with a PDMS matrix yields a magnetic rubber-metal composite. The inclusion of iron to PDMS is twofold: enhancement of the overall mechanical properties of the elastomeric rubber, and production of a magnetically active adhesive that can be used to explore magnetism as an alternate clamping method to switch compliance.

Iron powder by Sigma-Aldrich, USA, was used in this study. The powder was sifted with a 325 mesh filter corresponding to an approximate particle size of 44 μm, as labeled by the manufacturer. Table 3 lists important physical and mechanical properties of iron powder:

Table 3: Properties of iron powder [44]

Property	Value
Density	7.86 g/cm^3
Particle Size	44 μm
Magnetic Affiliation	Ferromagnetic
Young's Modulus	200 GPa
Cost/Gram	≈ $0.04

3.1.1.3. Nickel

Similar to iron, nickel is also a commercially available ferromagnetic (i.e. permanently magnetic) metal that is non-toxic and has much better mechanical properties than PDMS. The same reasons for including iron as reinforcement to PDMS equally applies to nickel as well. Investigations of alternate reinforcement materials, as well as investigations of a range of particle sizes, were made possible by including nickel powders. Two types of nickel powders with different particle sizes by Sigma-Aldrich, USA were used in this study. Particle size and other important properties for nickel powders used in this research are listed in Table 4:

Table 4: Properties of nickel powder [44]

Property	Value
Density	8.88 g/cm^3
Particle Sizes	<100 nm or <150 μm
Magnetic Affiliation	Ferromagnetic
Young's Modulus	207 GPa
Cost/Gram (both particles)	≈ $5.28 or ≈ $3.09

3.1.2. Micro-Emulsion

Micro-emulsion, or the mixture of phase separated liquids (e.g. oil and water), was first considered as a synthesis method for developing compliantly controlled switchable adhesives. Conceptually, the agitation of an uncured polymer in a solvent, and utilizing a surfactant, would allow the polymer to cure in the shape of microspheres while still submerged within a solvent. Simply evaporating the remaining solvent would leave behind a sticky paste of polymer microspheres which could be combined with magnetic powder. The combination of magnetic powder and polymer microspheres would create a magnetically sensitive and tacky paste that could be actuated by a magnetic field. The influence of a magnetic field on the magnetically sensitive adhesive paste could alter its compliance.

To produce a sample, uncured PDMS was first mixed with solvents (e.g. toluene, chloroform) to decrease the viscosity of PDMS while allowing easier agitation of the polymer mixture. Separately, a surfactant (i.e. ***surf***ace ***act***ive ag***ent***-e.g. detergent) was added to water so that subsequent blending of PDMS with the water would inhibit polymer coagulation. Next, the PDMS mixture was poured into the water, water that was saturated with surfactants, creating an uncured PDMS-water emulsion. Successive sonication further stirred up the mixture. The emulsion was then vacuumed to evaporate and remove solvents prior to curing the PDMS. While the emulsion was agitated on a hot plate with a stir stick, the PDMS slowly cured as time and temperature were monitored. Time and temperature proved to be extremely important parameters in controlling the curing kinetics. After curing, the PDMS paste could be combined with magnetic powder to create a magnetically sensitive and tacky adhesive.

Unfortunately a staggering number of combinations of independent variables (amounts of PDMS, solvents, surfactants, water/durations of sonication, hand mixing, exposure times to temperature/hot plate mixing speeds/temperature settings, etc.) proved to be extremely challenging for the scope and short timeframe of this study. While failure to create a tacky magnetically active PDMS paste was certainly a discouraging result, future efforts at micro-emulsion pastes would surely be worthwhile as a promising synthesis procedure to continue this research. Alternatively, simply casting continuum thin films proved to be a much easier method to make adhesive samples.

3.1.3. Continuum Thin Films

Continuum thin adhesive films were prepared using PDMS and magnetic powder. To prepare a sample, uncured liquid PDMS was hand mixed in a vial with a liquid silicone elastomeric crosslinker at a 10:1 ratio. Once mixed, magnetic powder was added and stirred into the mixture. The liquid polymer-metal mixture was then poured into a plastic tray and set aside to cure. The uncured polymer-metal mixture had many air bubbles from mixing; therefore samples were placed inside a vacuum-furnace and degassed at 25 inHg pressures to remove voids. It was found that leveling the samples was paramount in achieving consistent thicknesses during the curing process. To accelerate the curing process, samples were heated to 85°C for 1 ½ hours. Figure 27 illustrates the curing process of an adhesive sample inside a vacuum-furnace.

Figure 27: Adhesive sample curing in a vacuum-furnace

After samples were cured, they were pulled from the vacuum–furnace and cut into square adhesive pads before characterization as seen in Figure 28. Samples were subjected to some modifications such as varying amounts of reinforcement, changing reinforcement types/particle sizes, and modulus adjustments by changing the crosslinking ratios.

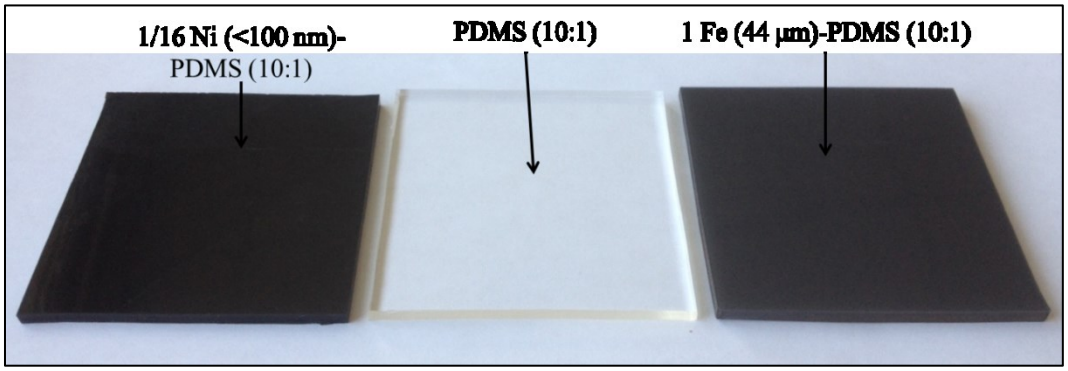

Figure 28: Examples of continuum thin film adhesive samples

3.1.3.1. Scanning Electron Microscopy

Scanning electron microscopy (SEM) characterization can provide information regarding the effect of particle sizes on the uniformity of the reinforcement within a composite. SEM was performed on the cross sections of adhesive samples to observe magnetic particle distributions and/or layering of the reinforcement inside the polymer matrix. The polymeric-metal adhesive samples were sectioned with a razor blade and gold coated before being mounted on a sample chuck. A JEOL JSM-6490LV high-performance variable pressure SEM was used in this study. Figure 29 is a generic SEM micrograph of a sample being analyzed at 3,000 X magnification while using a 2 kV accelerating voltage, a working distance of 4.6 mm, and imaging with a secondary electron detector. From the figure, it is easy to identify distinct polymer and metal phases within the composite rendering SEM a tremendously useful characterization tool to evaluate particle distributions.

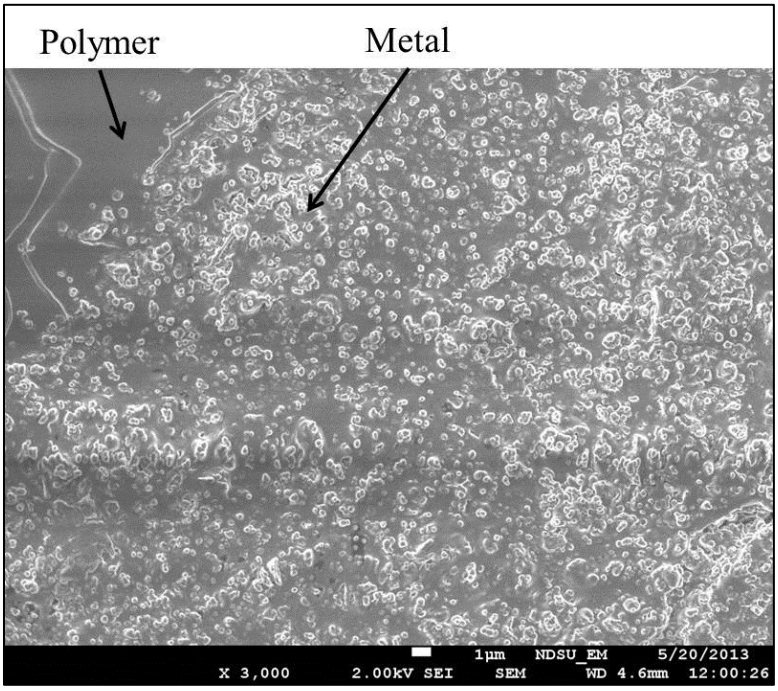

Figure 29: SEM characterization of a polymer-metal composite

3.2. Lap-Shear Testing Apparatus

A lap-shear test was utilized in the characterization of the adhesive films due to the simplicity of the method, which can relate material properties back to a measurement, and because of the availability of the required equipment at the Mechanical Engineering Department of North Dakota State University. An image of a typical lap shear test setup with the schematic used in this study is depicted in Figure 30:

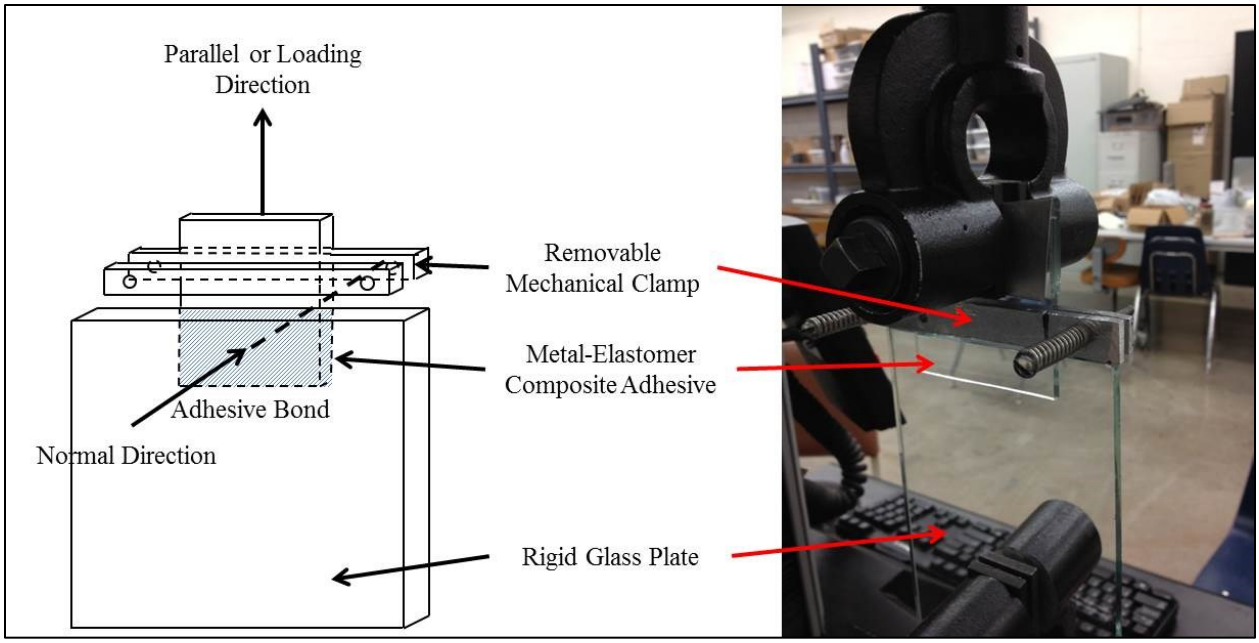

Figure 30: Schematic of a lap-shear testing apparatus with actual test

Before performing a measurement, an adhesive sample is cleaned with masking tape to remove dust and the substrate is washed with acetone so that oils are also removed. During the setup portion of a lap-shear test, an adhesive sample is placed in an upper grip and then bonded at zero degrees to a substrate that is fixed to a lower grip. Ensuring sample-substrate parallelism is absolutely vital during this step in eliminating unwanted moments and forces that might have been wrongly introduced due to misalignment. An account of the contact area of the bond region

(see the blue section of Figure 30) must be recorded along with a record of the un-gripped gage length. A constant displacement in the parallel direction to the upper grip crosshead produces a force within the sample that can be measured with a transducer.

An Instron, model 5567 screw-driven tester was used along with a ±2 kN load cell. The tests were performed at a rate of 5 mm/min and samples were deemed to have failed once a complete reduction in the glass/sample contact area occurred. Alternatively a 1 mm/min testing rate was experimented with however initially no significant differences were noticed between the two rates therefore the 5 mm/min rate was chosen since it reduced testing time. A general force-displacement curve for a lap-shear adhesive test is shown in Figure 31.

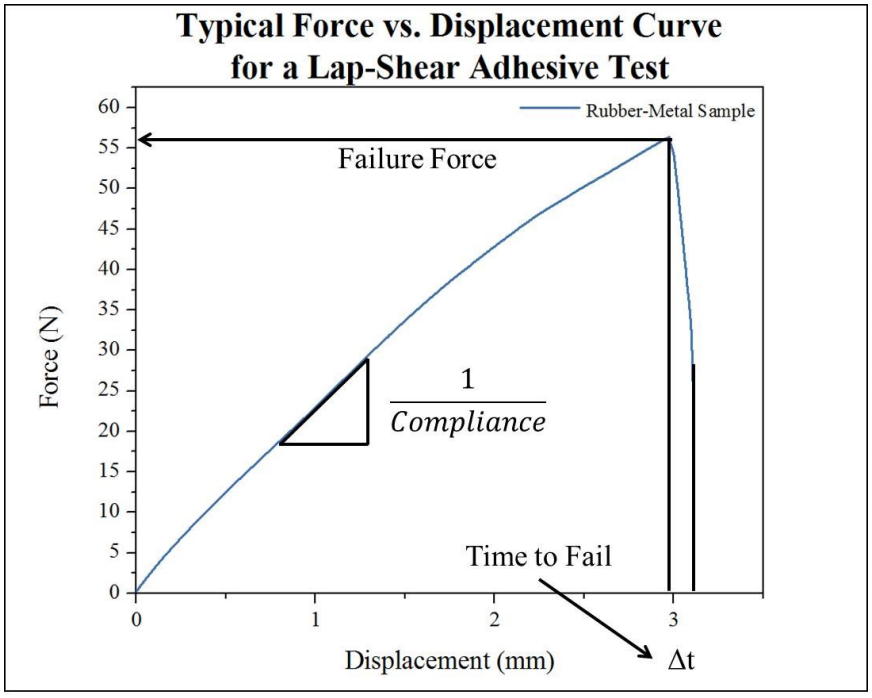

Figure 31: Representative force vs. displacement curve for a lap-shear test

The slope of the force displacement curve is given by Hooke's law of elasticity and the inverse of the slope is the total compliance. The total compliance measured contains the normal

and shear compliance of the sample as well as the instrument compliance. It is interesting to note that sample compliance dwarfs the instrument compliance, and within the sample compliance, the normal component is significantly larger than the shearing component along the bonded plane to the point where the shearing compliance and instrument compliance is only 10%. In addition to the compliance, the failure force and the time of failure of an adhesive sample is provided by such a test. The time to fail can be calculated since the displacement of the crosshead is occurring at a constant rate. An approximate crack velocity can be calculated from the time to fail for a bonded area.

3.2.1. Nanoindentation

Nanoindentation is a characterization technique in which a sample is probed, measurements of the forces and displacements are recorded and mechanical properties such as hardness and reduced modulus can be calculated. A TI-900 Hysitron Triboscope NanoIndenter was attempted to independently verify compliance by measuring the elastic modulus. The compliance can be subsequently calculated from the modulus if information is known regarding the probe geometry. Two very large probes, a 400 μm spherical and a flat punch, were used to indent PDMS. An accurate and reliable force could not be maintained due to the sample being too soft for even the most sensitive transducer equipped on the instrument and after indenting to a large depth of 2.5 μm. The obtained results showed that nanoindentation was unable to successfully characterize the compliance in this study. A JKR adhesion test, similar to nanoindentation, would probably be a valuable avenue to pursue for characterizing switchable adhesives, as would nanoindentation with a more sensitive force transducer.

3.3. Testing Method

As stated in the introduction, one of the goals of this work is to switch compliance. Through controlling compliance, the adhesive force capacity can be adjusted. One obvious method to switch compliance is to use a mechanical clamp. However, for a more controllable method of clamping, synthesis of adhesive samples included ferro-magnetic particles in order to utilize and explore magnetic clamping.

The characterization performed herein is not intended to provide mechanical property feedback and optimize adhesive sample synthesis in order to develop a product that will be available to purchase on the market tomorrow, but is intended as a first step towards a fundamental understanding. Therefore different clamping methods such as mechanical, magnetic, and non-contact magnetic (e.g. implementing Helmholtz Coils and the manufacturing a hands free jig) were examined in order to provide a broad understanding of compliance switching within the class of magnetically active adhesives.

3.3.1. Mechanical Clamping

A simple mechanical clamp was fabricated and implemented to control compliance. When a sample is clamped, the rubber is restricted from deforming and results in an increase in compliance. Applying a clamp or removing it is a mechanical method to switch compliance. Figure 32 shows the clamp by itself as well as the clamp during testing.

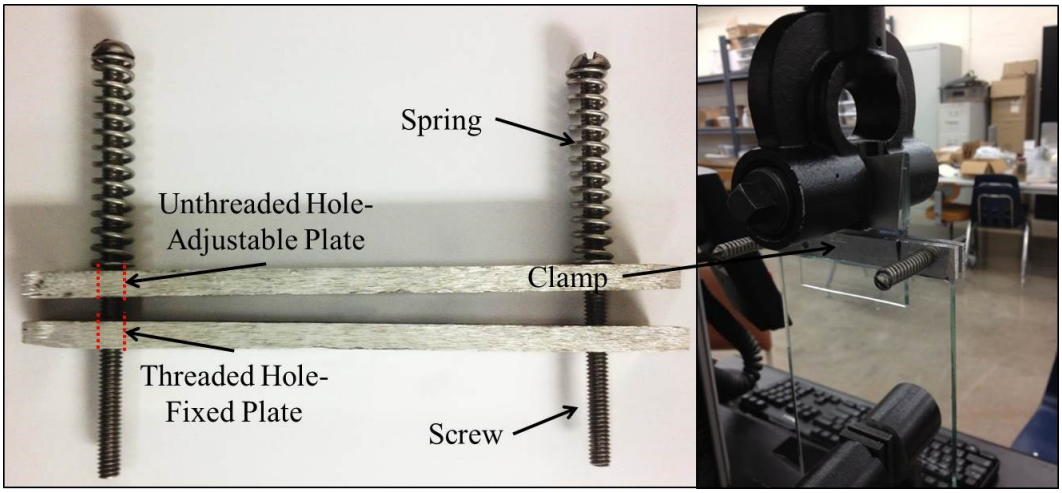

Figure 32: Mechanical clamp

The mechanical clamp consists of two screws, two springs (k=2 N/mm), and two clamp faceplates. The clamp faceplate touching the spring had holes bored out larger than the radius of the screws so that the plate was adjustable allowing it to slide along the screws. The clamp faceplate opposite of the screws had holes that were threaded so that by turning the screws the distance between the threaded plate and screw head could be controlled. Deceasing the distance between the screw head and threaded faceplate put a compressive force on the spring and on the adjustable plate, clamping a sample located between the plates. By measuring the number of turns applied to the screws, the springs could be accurately compressed within a hundredth of a millimeter maintaining remarkable control of the clamping pressure.

3.3.2. Magnetic Clamping

Magnetic clamping was explored as a second, more easily controlled method to switch compliance. The attraction of rare earth magnets on each side of a magnetically sensitive adhesive rubber film held the magnets in place and squeezed the adhesive similar to a mechanical clamp as depicted in Figure 33.

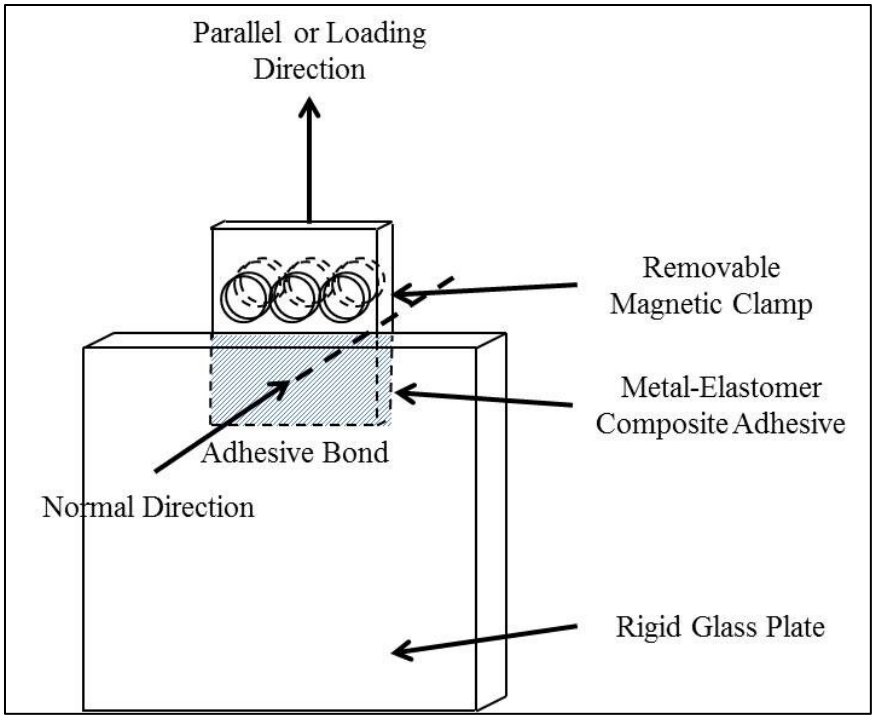

Figure 33: Magnetic clamping schematic

In order to directly compare pressures between the mechanical and magnetic experiments, force-displacement curves were measured for the magnets used in the experiments. Figure 34 shows a magnetic clamp setup and a resulting plot of the attractive force between two magnets as a function of the extension. Assuming that the magnetic separation corresponds to sample "thickness" then the applied force over the magnetic disc area can be determined. For example, magnetic experiments used 3 columns of magnets for an area of ≈ 3.5 cm^2. Each column had magnets stacked 3 deep, and for the particular magnetic separation used, corresponded to a force of ≈ 23 N therefore applying 64 KPa of pressure to the sample. Further magnetic clamping studies were undertaken which varied the area (i.e. number of columns of magnets used) as well as explored clamping with magnets on only one side so comparisons between magnetic and mechanical clamping could be drawn.

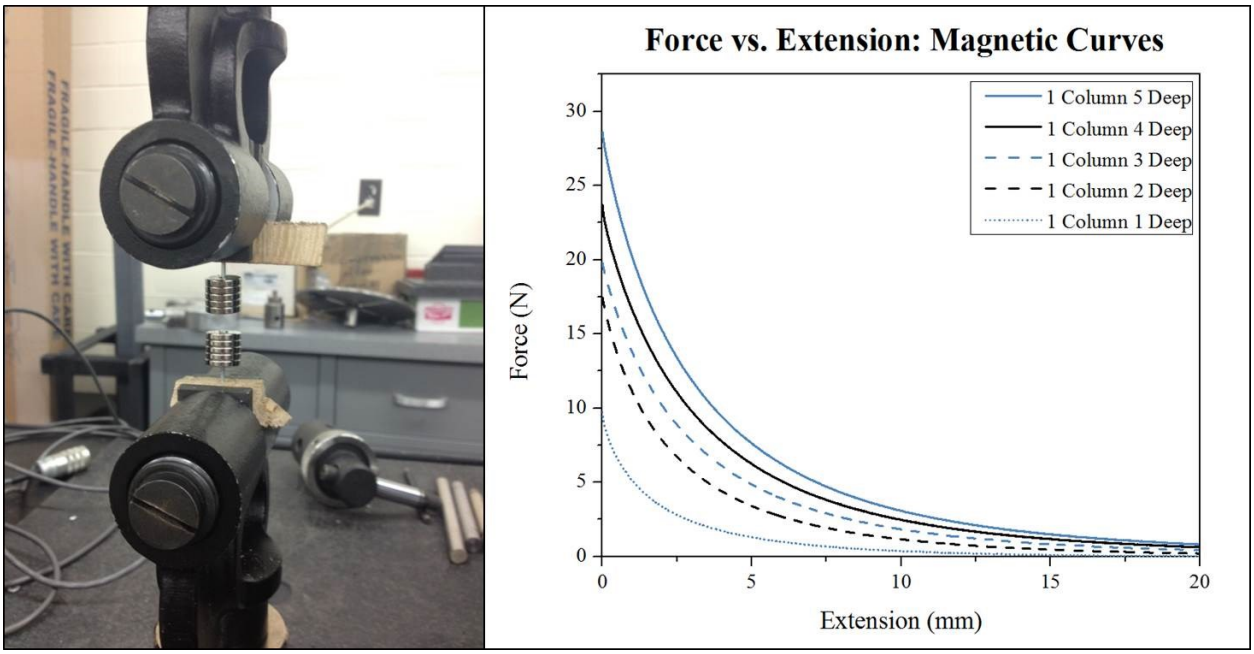

Figure 34: Force extension plot for magnetic attraction

3.3.3. Non-Contact Clamping

Non-contact clamping separates magnetic interactions from frictional components of force since touching of a clamp and sample is completely nonexistent. The forces associated with "contact full" magnetic clamping (i.e. magnets placed directly on a sample) can be either attributed to magnetism or friction. It was the intent to show that magnetism could be isolated as an independent variable and therefore directly analyzed for its effect on sample material characteristics. Therefore, non-contact magnetic clamping was used to distinguish differences between magnetic and mechanical clamping. Two methods of non-contact clamping were attempted: application of Helmholtz coils and an in-house built hands free magnetic jig.

3.3.3.1. Helmholtz Coils

Helmholtz coils are a pair of aligned, parallel coils with the same radius which, when placed close enough to each other, produce a uniform magnetic field while an electric current runs through the wrapped wire. Helmholtz coils were introduced in this study so a controllable and sophisticated method of applying non-contact magnetic clamping could be accomplished. Figure 35 is a picture of Helmholtz coils during testing.

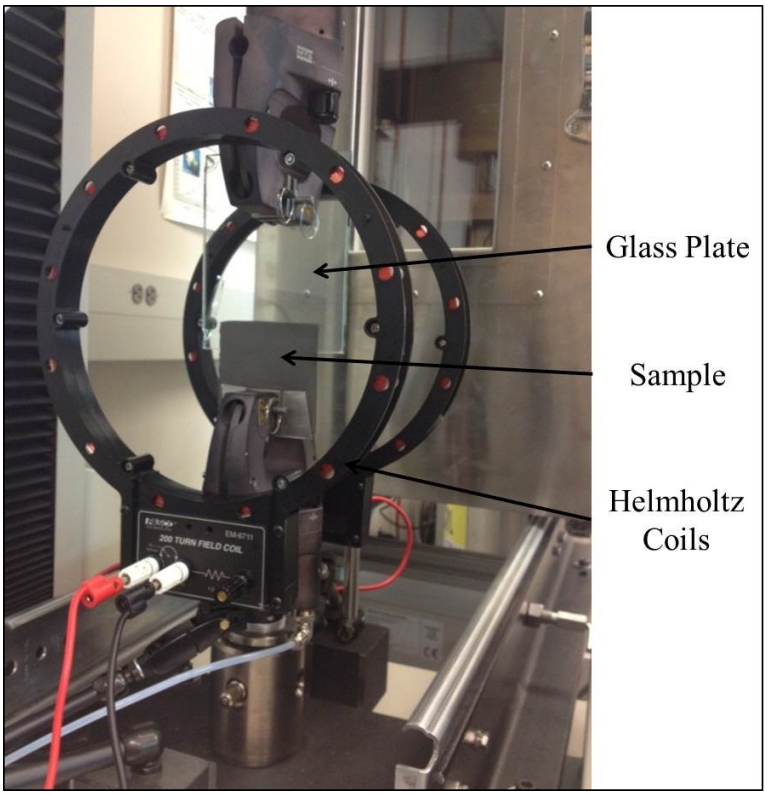

Figure 35: Magnetic non-contact clamp: Helmholtz coils

A power source is used to control the current and voltage supplied to the coils. If the coils are placed exactly the distance of the radius apart from each other, then Equation 31 can be used to find the value of the magnetic field at the center point.

$$B = \left(\frac{4}{5}\right)^{\frac{3}{2}} \frac{\mu_0 nI}{R} \quad \text{(Equation 31)}$$

B is the magnetic flux density, u_0 is the permeability constant, n is the number of wire loops in a coil, I is the coil current, and R is the coil radius [**45**]. The application of a magnetic field while testing a magnetically sensitive adhesive sample determines whether magnetism affects the mechanical properties.

3.3.3.2. Hands-Free Clamp

A customized hands free clamp capable of holding rare-earth magnets was designed and manufactured in this study. Rare-earth magnets have much stronger field strengths than the Helmholtz coils used in this research. Figure 36 shows clamping schematics and pictures of the hands free clamp. Figure 36 (d) indicates the separation of the clamp to the sample was a mere few millimeters. The hands-free jig was designed and fabricated from polyethylene plastic to avoid using ferromagnetic metal which make handling of magnets inconvenient.

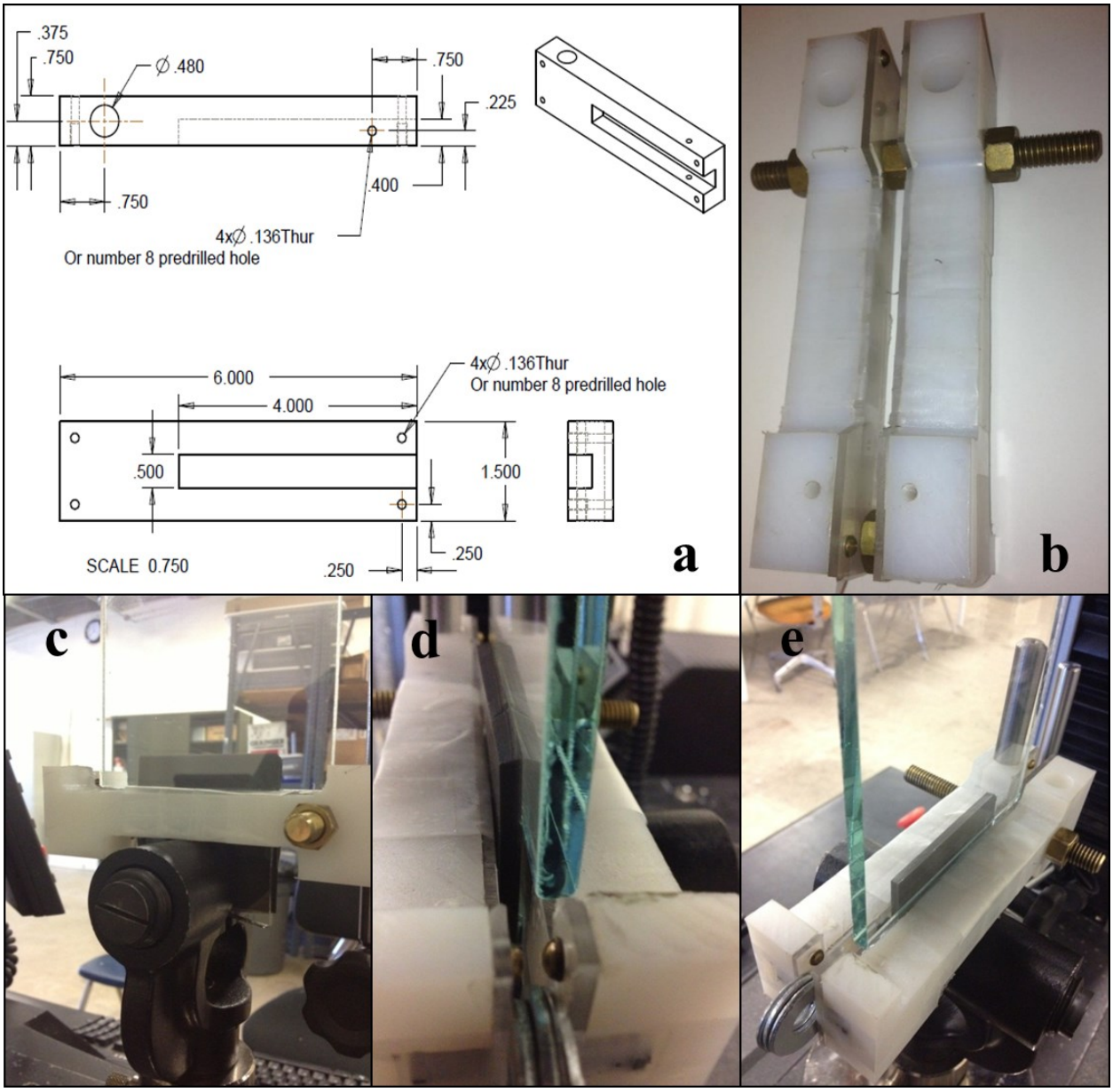

Figure 36: Magnetic non-contact clamp: hands free jig

CHAPTER 4: RESULTS AND DISCUSSION

In this research, the effect of mechanical, magnetic and non-contact magnetic clamping on compliance was studied. By changing compliance the adhesive force to failure of an elastic film under shear could be controlled. Magnetic nanoparticles were introduced to adhesive rubber films so magnetic clamping could be examined as an alternate clamping method. To potentially enhance magnetic clamping, different sizes, concentrations, and types of magnetic particle reinforcements were added to the adhesive rubber films. The value of nanoparticle reinforcement was investigated by using rare-earth magnets and Helmholtz coils.

Sample preparation consisted of mixing paramagnetic powder or nanopowder reinforcement with PDMS rubber. The composite adhesive samples produced were PDMS/Fe (45 μm particle size), PDMS/ Ni (150 μm particle size), and PDMS/Ni (<100 nm particle size). The concentration of particle reinforcement was adjusted for each type of adhesive composite prepared in this study. The sample concentration ratios were 0:1, 1/16:1, 1/8:1, 1/6:1, ¼:1, ½:1, 1:1, 2:1 reinforcement by weight to polymer by weight. Table 5 summarizes all the sample variations for 24 different samples that were synthesized in this study.

Each measurement of a sample consisted of lap-shear testing with a clamp, both on and off, three times (n=3). Prior to a test, the samples were cut into square pads and the widths, length, and thickness of the pads were recorded. Each sample was then adhesively bonded with the exposed curing side (e.g. non tray side) to a fixed glass plate at a given overlap and a predefined gage length. The overlaps chosen in this study were 15 mm, 10 mm, and 5 mm, with gage lengths being 20 mm, 25 mm, and 30 mm respectively.

Table 5: Sample reinforcement matrix

		Particle Type and Size		
		Fe (45 μm)	Ni (150 μm)	Ni (<100 nm)
Concentration by Weight	0	Sample 1	Sample 9	Sample 17
	1/16	Sample 2	Sample 10	Sample 18
	1/8	Sample 3	Sample 11	Sample 19
	1/6	Sample 4	Sample 12	Sample 20
	1/4	Sample 5	Sample 13	Sample 21
	1/2	Sample 6	Sample 14	Sample 22
	1	Sample 7	Sample 15	Sample 23
	2	Sample 8	Sample 16	Sample 24

Adjusting the overlap and gage length permits a comprehensive critical energy release rate, G_c, for a particular sample set to be extracted from the data due to changes in both compliance and contact area. Specifically, both measured compliance and force from a lap shear experiment can be matched with a sample's contact area allowing G_c to be approximated through the rearrangement of Equation 4. A force against square root (A/C) plot can be produced and the slope of the trend line for each contact area data point represents an average G_c by testing multiple contact areas within a given sample set. Figure 37 shows a sample plot of a force against square root (A/C) curve for 5 overlaps. The markers represent lap shear testing for 5 unique overlaps and each marker is an average of several measurements as shown in Figure 37.

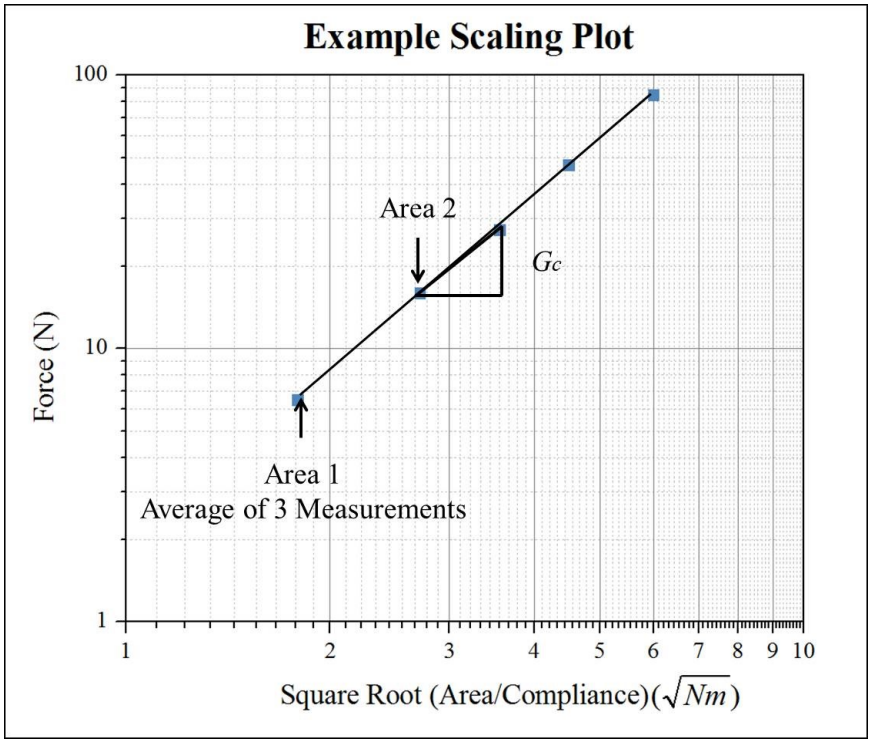

Figure 37: Generalized scaling plot

4.1. SEM Characterization

All samples were bonded with the non-tray side to glass due to visual differences observed between sides. Visual differences between sides suggested non-uniform particle reinforcement, and therefore SEM characterization was performed on the cross section of each sample type for confirmation. Figure 38, Figure 39, and Figure 40 are 1/8 reinforcement by weight SEM images of PDMS/Fe (45 μm particle size), PDMS/ Ni (<100 nm particle size), and PDMS/Ni (150 μm particle size) respectively. In each figure, a low magnification cross-sectional image is presented on top as well as 350 X and 2,500 X magnification images revealing particle size, aspect ratio, and particle matrix interaction.

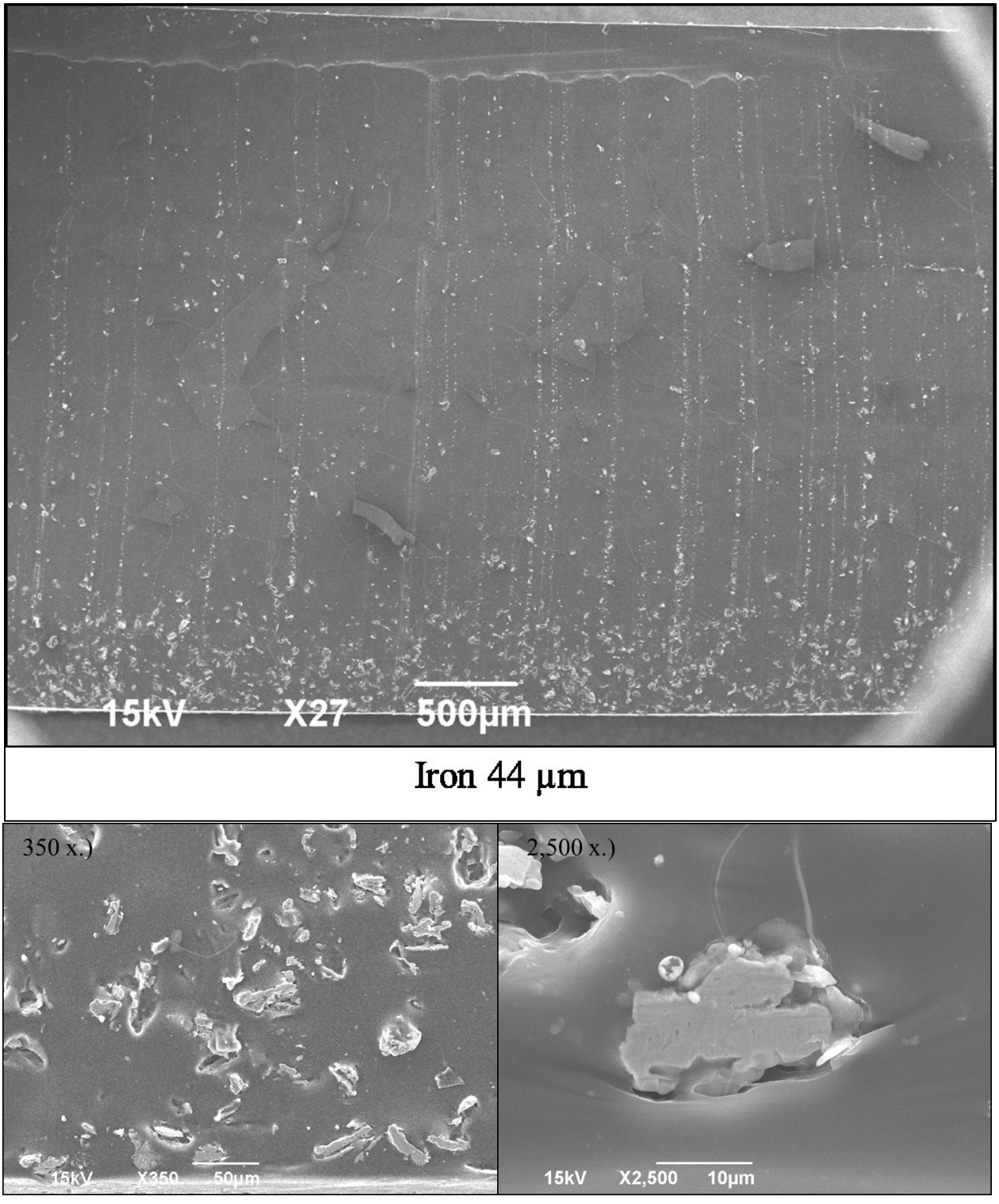

Figure 38: SEM of iron particles

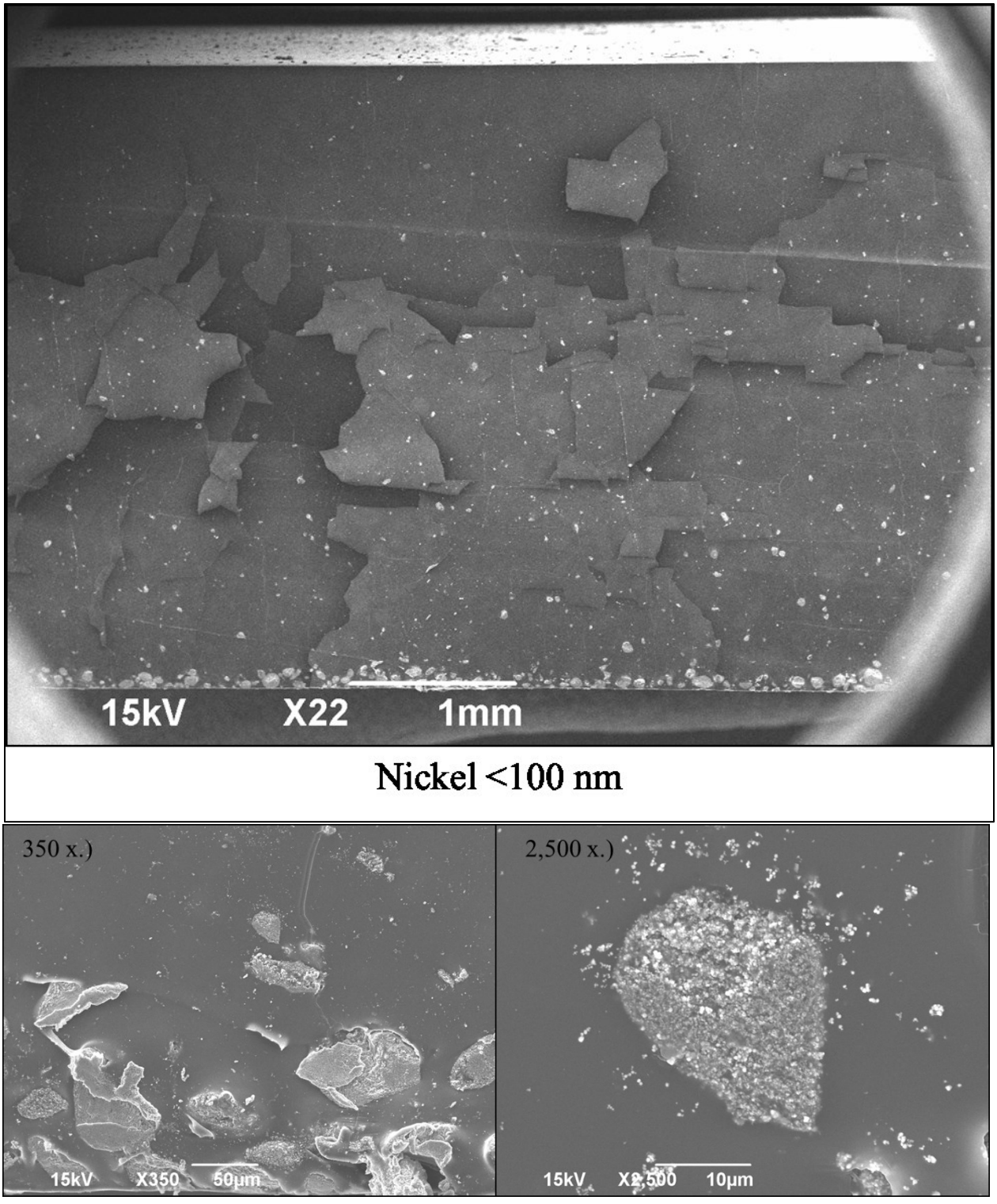

Figure 39: SEM of small nickel particles

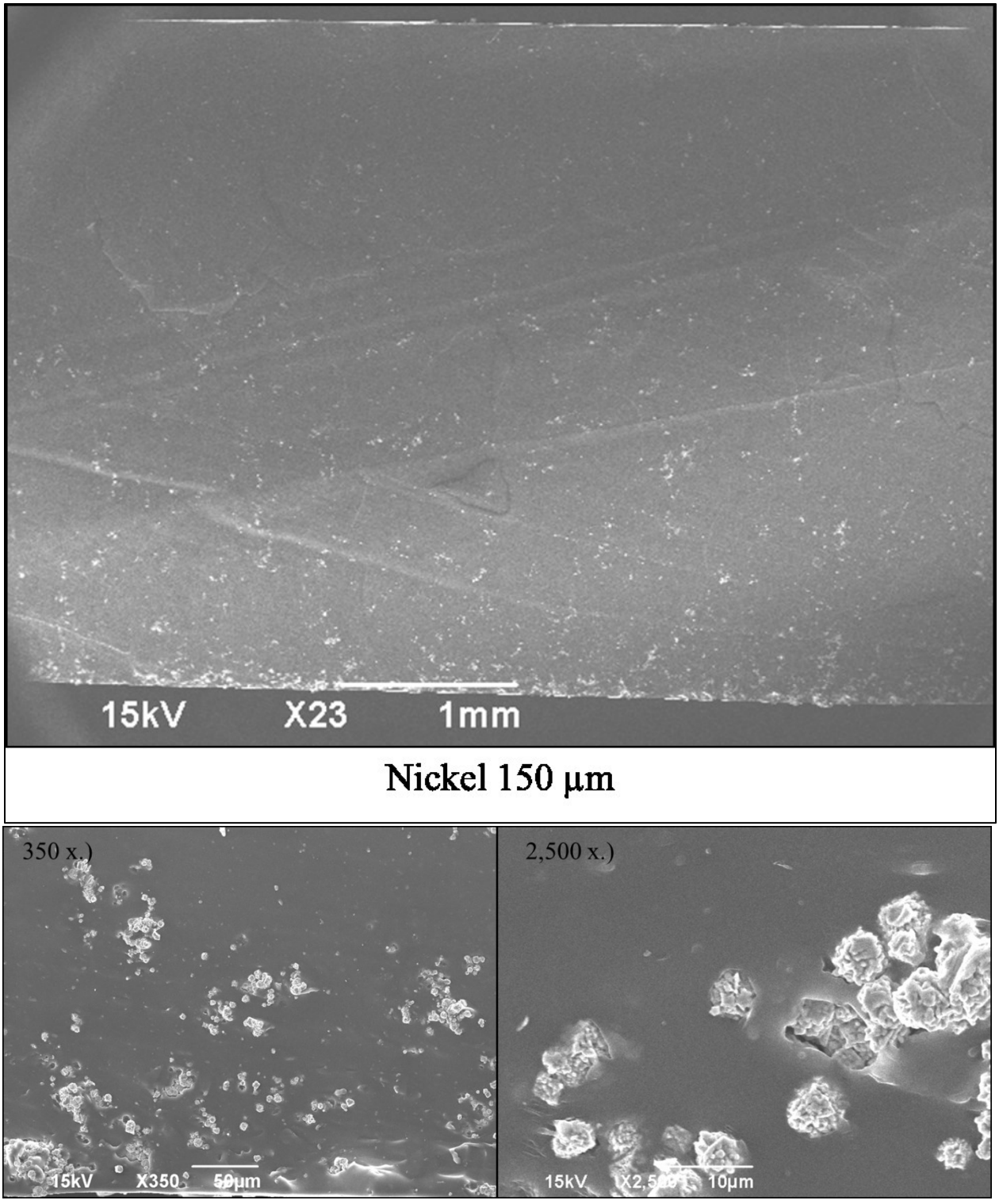

Figure 40: SEM of large nickel particles

In all samples, the top cross sectional micrograph shows a gradient of particle reinforcement through the depth of the matrix confirming particle settling. The images suggest that the higher density metallic particles sank to the bottom of the liquid PDMS during cure creating non-uniform, layered composites. All samples were tested with the top (i.e. particle deficient side) surface touching the glass plate ensuring potential particle induced roughness on the bottom side would not affect the contact area during adhesive measurements.

High magnification 2,500 X images show the high surface energy metallic particles were coated by the low surface energy PDMS matrix. The coating of particles implies particle matrix "compatibility" which might not occur if alternate particle material classes were selected for reinforcement. The high magnification images also indicate the <100 nm nickel particles, originally selected to prevent settling due to Brownian motion, agglomerated and sank similar to large particles. Further mixing would break up the agglomerations, as particles are observed diffusing from rather than diffusing to particle rich locations.

In addition to particle matrix interactions and layering, high magnification micrographs revealed inconsistencies with the labelled particle sizes from the manufacturer and the true particle sizes. The largest difference occurred within the 150 μm nickel particle size sample set which was actually confirmed to be in the 5-10 μm range. Despite the differences in particle sizes, the SEM images showed relatively low aspect ratios consistent with the assumption of particulate reinforcement as opposed to metallic fiber reinforcement.

The effect of location of particles (i.e. layering) within the matrix can be understood with a rule of mixtures plot (further discussed in Section 4.2.2-see Figure 44). If there is experimental consistency with a rule of mixtures, then particle layering has no effect on the mechanical

properties of the adhesives since the model of any rule of mixtures does not rely upon specific particle location.

4.2. Mechanically Clamped Data

The clamp described in Section 3.3.1 was used to perform the mechanical clamping experiments. Data of mechanically clamped pure PDMS as well as iron reinforced samples is presented below. Measurement of pure PDMS acts as a baseline datum from which to compare all magnetically reinforced samples. The mechanical value of adding reinforcement to the clamped magnetic iron composite samples is discussed. In addition, the influence of clamping on the force capacity for all the reinforced samples is reported. Finally a simple mechanical clamping model is proposed to support the experimental results.

4.2.1. Pure PDMS

A baseline measurement was first made with pure PDMS to demonstrate, using the simplest method possible, that changes in compliance can control adhesive force capacities. Measuring non-reinforced PDMS provided a reference from which to evaluate the mechanical differences that occurred within the composite samples. A mechanical clamp was applied to PDMS and a typical measurement for a 5 mm overlap is plotted in Figure 41.

Figure 41 indicates that the clamp decreased sample compliance (i.e. the sample stiffened) and the adhesive force to failure was increased. The increase in sample stiffness is evident in that the slope of the clamped data is much steeper than the unclamped data. Also the adhesive force to failure increased from approximately 6.5 N to 9 N which is roughly a 40% increase for this particular sample before it failed.

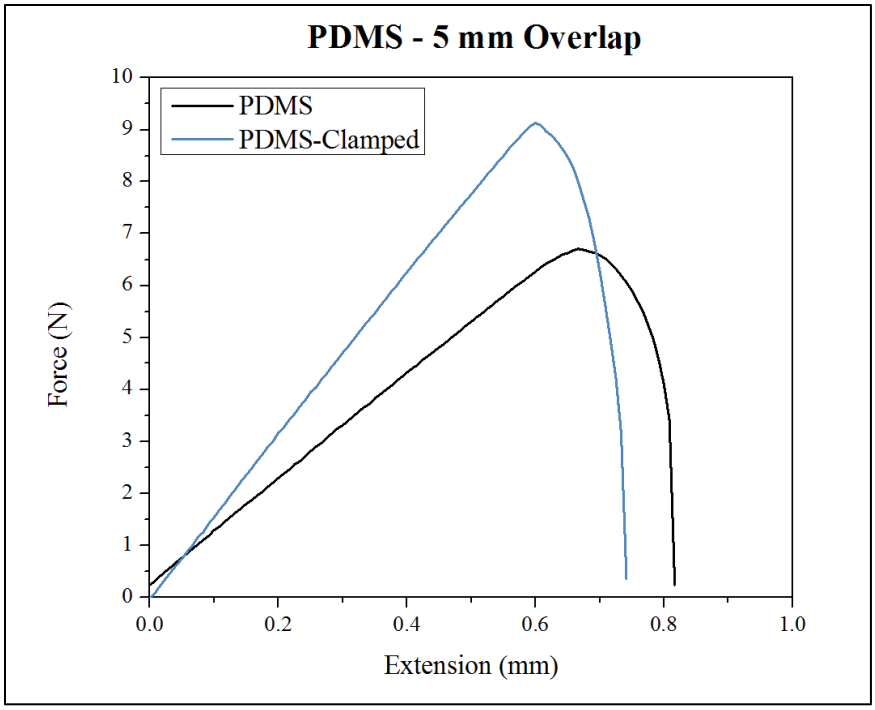

Figure 41: Mechanical clamp: effects on PDMS for a 5 mm overlap

The scaling relationship of Equation 4 should predict adhesive force capacities expected from lap shear testing. Assuming the scaling relationship holds, then a straight line is expected when sample compliance and contact areas are varied. Figure 42 is a comprehensive scaling plot of all the mechanically clamped data collected for PDMS.

Figure 42 indicates that the force capacity is increased when the ratio of contact area to compliance is increased. When a sample is clamped, the adhesive force to failure is increased as the clamped (black) markers are largely shifted along the slope predicted from the unclamped (blue) data. However, the slope of the marker lines has changed slightly indicating a small change in the critical energy release rate between clamped and unclamped states may also occur. The small change in G_c could be accounted for by a change in the crack velocity during sample failure when a clamp is present (i.e. the failure is quicker) as outlined in Section 1.4.3.2.

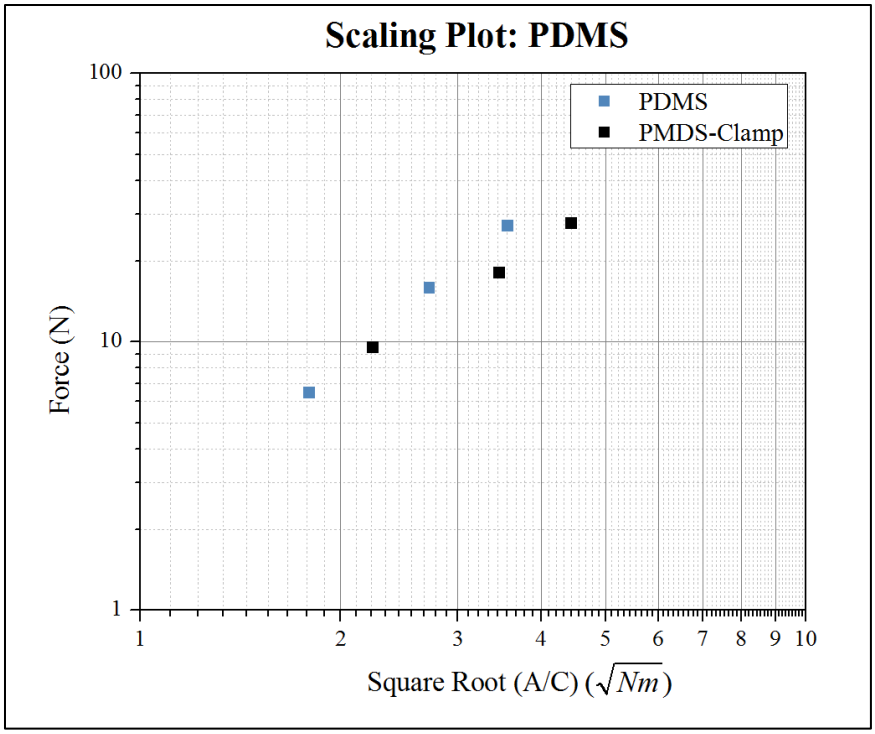

Figure 42: Mechanical clamp: scaling plot of PDMS

4.2.2. Magnetic Composites-Iron

The cost of iron is quite inexpensive relative to nickel magnetic reinforcement, only $0.04 per gram compared to $3.09 per gram, therefore it was chosen as the standard reinforcement material to study differences between mechanical and magnetic clamping. It is assumed that the inclusion of iron hardly influences mechanical clamping. Nevertheless, and counterintuitive to our assumptions, we collected iron reinforced mechanically clamped data regardless so that the magnetic impact of iron reinforcement could be comparatively evaluated against equal baseline mechanically clamped data. Therefore out of necessity, magnetic adhesive composites were mechanically clamped to compare the effect of different clamping mechanisms.

The mechanical value of adding reinforcement is shown in Figure 43. Force displacement curves for several samples from the 15 mm overlap classification, ranging from pure PDMS to a composite heavily loaded with iron reinforcement, is plotted. Adding metal to rubber increases the stiffness and sample failures are more abrupt (i.e. steeper failure after peak force). The increase in stiffness from our measured data is consistent with the modified Mooney rule of mixtures equation for particulate-polymer composites.

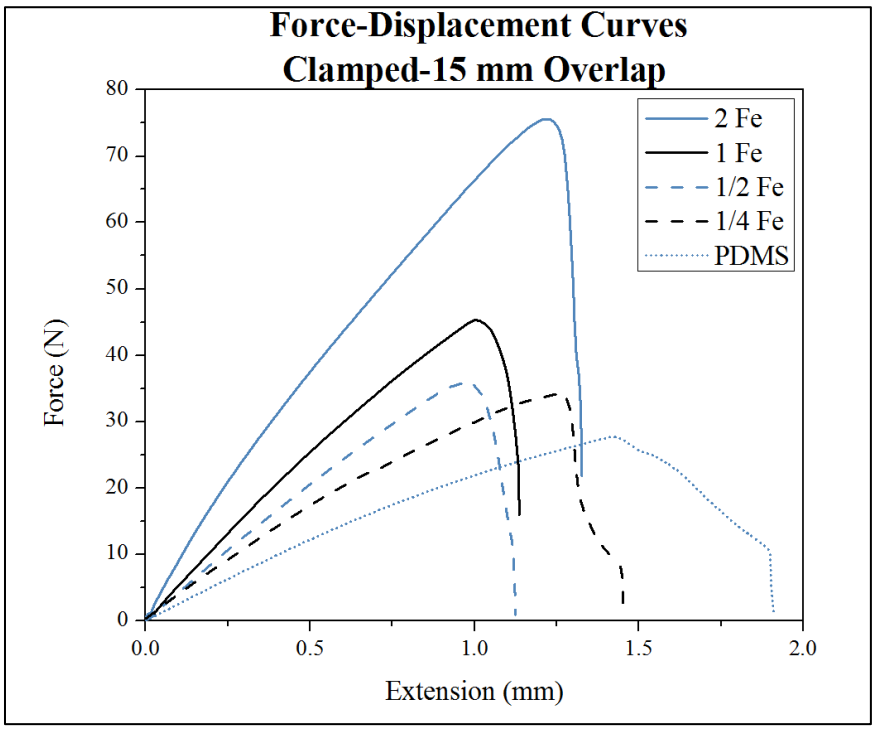

Figure 43: Mechanical clamp: force disp. curves for Fe concentrations (clamped)

A plot of the composite elastic modulus against a sample's corresponding volume fraction is commonly used as graphic confirmation supporting a rule of mixtures. To generate a plot, the measured stiffness must be converted to a modulus and the prepared weight fraction can be rewritten as a volume fraction. The reason for converting stiffness into a modulus as well as rewriting weight fraction as a volume fraction is presented below.

Stiffness is dependent on the geometry and structure of a material. A steel paper clip can easily be bent, but a steel I-beam is difficult to deform. Even though the paperclip and I-beam are made from the same material, *steel*, differences arise in their deformability because of the geometry. When geometry is taken into consideration, stiffness can be reduced to a modulus which is an inherent material property.

The weight of reinforcement is dependent on the density of material. It is convenient to measure amounts of a sample by weight when preparing samples. However, two parts by weight of material A could have a different volume compared to two parts by weight of material B because materials A and B might have different densities. Therefore it is much more reasonable to compare different types of reinforcement, since they have differing densities, as a volume fraction instead of a weight fraction.

A more impartial approach to view the mechanical influence of including magnetic particle reinforcement, independent of the type of reinforcement used, on rubber is to prepare a rule of mixtures plot. Figure 44 plots the increase of the modulus with respect to the volume of iron added into the rubber samples.

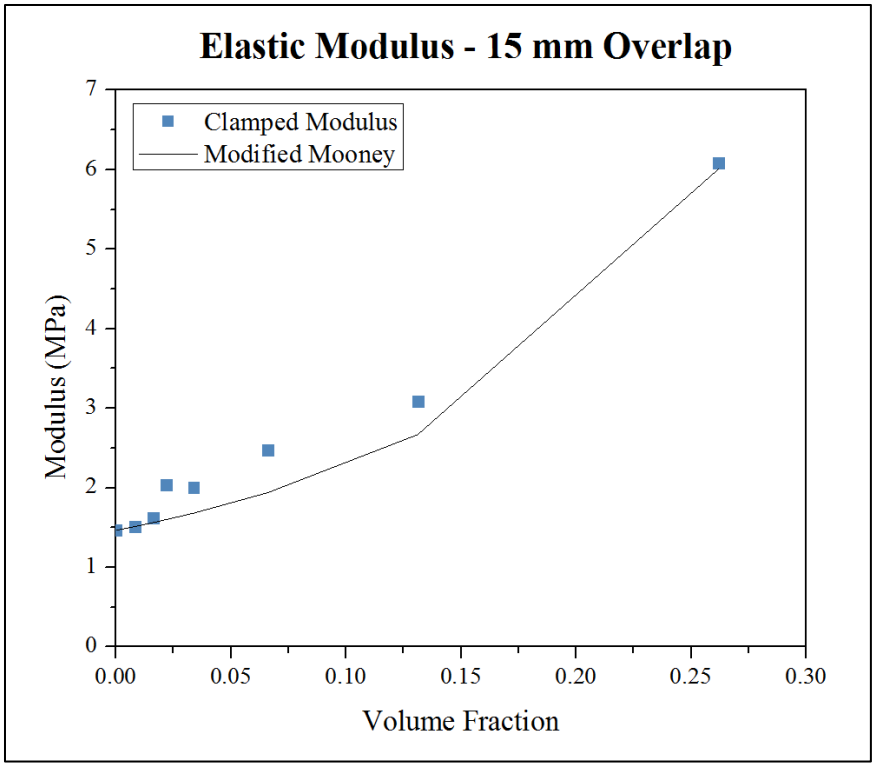

Figure 44: Mechanical clamp: modulus vs. volume fraction-iron

For all sample concentrations the modulus increases as metal particle reinforcement is added, which also implies that compliance decreases when more iron is present since sample geometries are approximately the same. The measured increase in sample modulus is consistent with the modified Mooney rule of mixtures equation for rigid particulate-polymer composites which is presented as Equation 32.

$$\frac{E_c}{E_m} = exp\left(\frac{2.5V_p + 0.407(P-1)^{1.508}V_p}{1 - sV_p}\right) \qquad \text{(Equation 32)}$$

Where E_c is the composite modulus, E_m is the modulus of the matrix (PDMS), V_p is the volume fraction of the particle reinforcement, P is the aspect ratio of the particle reinforcement with $1 \leq P \leq 15$, and s is a crowding factor for the ratio of the apparent volume occupied by the particle to its own true volume with $1 \leq s \leq 2$ [**46**]. Importantly, experimental consistency with a rule of

mixtures implies particle layering has no effect on the mechanical properties of the adhesives since the model of any rule of mixtures does not rely upon specific particle location.

The influence mechanical clamping on the adhesive force capacity for 15 mm overlapped samples is portrayed in Figure 45. The clamped force capacity has been normalized by the unclamped force capacity and is plotted against the volume fraction of iron reinforcement. Normalization provides a true representation of the influence that mechanical clamping has on force capacity. A value of 1 indicates no effect, while a value of 1.3 indicates a 30% increase in adhesive force before failure. In almost every case, the clamp increases the force capacity, except for one sample which shows no effect. Figure 45 also clearly shows that no clamping benefit is obtained by adding iron reinforcement. There is no trend between adding particles and the increase of adhesive force which means that mechanical clamping is independent of particle reinforcement.

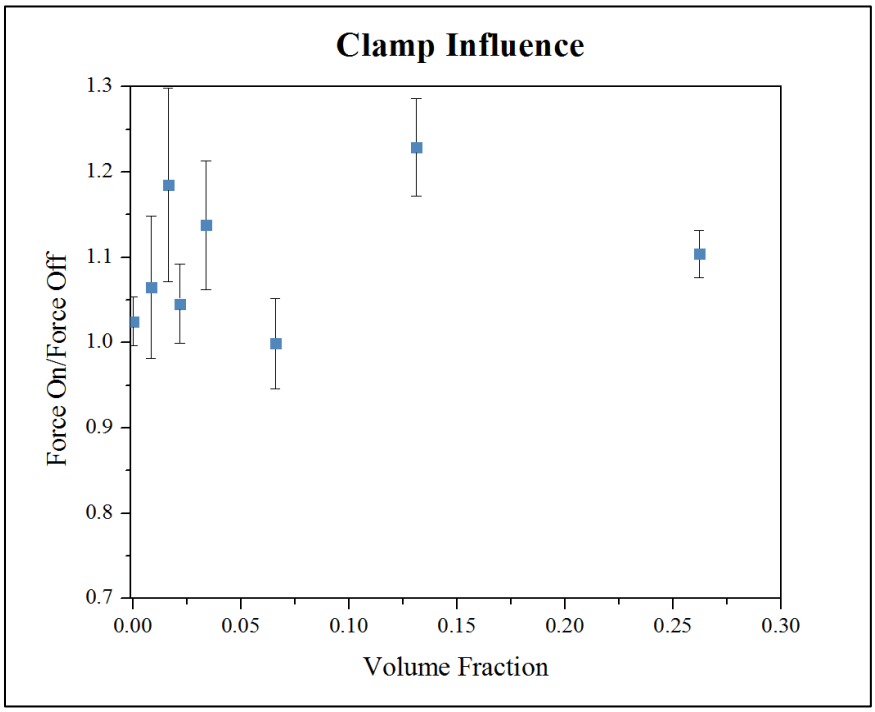

Figure 45: Mechanical clamp: clamping influences vs. volume fraction-iron

All the mechanically clamped measurements are summarized on the scaling plot in Figure 46. The data is entirely consistent with the trends of Equation 4 and falls within the range of the previously published data that is presented in Figure 24 (e). Note that each clamped marker for all samples has shifted to the upper right relative to the unclamped counterparts indicating an increase in force capacity and A/C ratio.

Each marker is an average of three measurements. To move up on the plot requires an increase in force; to move to the right on the plot requires a change in area, change in compliance, change in G_c, or a combination of change in area, compliance, and G_c. Each sample has three points corresponding to the three overlaps tested (e.g. unclamped PDMS has 3 blue circle markers corresponding to the 5 mm, 10 mm, and 15 mm overlaps). All the samples were tested with the same overlaps implying that the shift can be attributed to change in compliance or a change in G_c. For example, the shift of the top blue pentagon marker to the top open pentagon marker (2 Fe) is a direct comparison between the clamped and unclamped 15 mm overlap 2 Fe samples suggesting sample compliance and/or G_c has changed.

A better understanding of changes in G_c and compliance would allow for a more definitive cause and effect statement to be made regarding the measured increase in force capacity. It is intuitive that clamping changes the compliance, therefore a translation of each marker might suggest that mechanical clamping does indeed switch the adhesive force capacity. Although to be certain, a closer look at G_c, and adhesive failure times would give a clearer indication as to the effect that G_c has on the observed switch. In conjunction with a study of G_c, an investigative look at a mechanical clamping model would help give quantitative insight into compliance change.

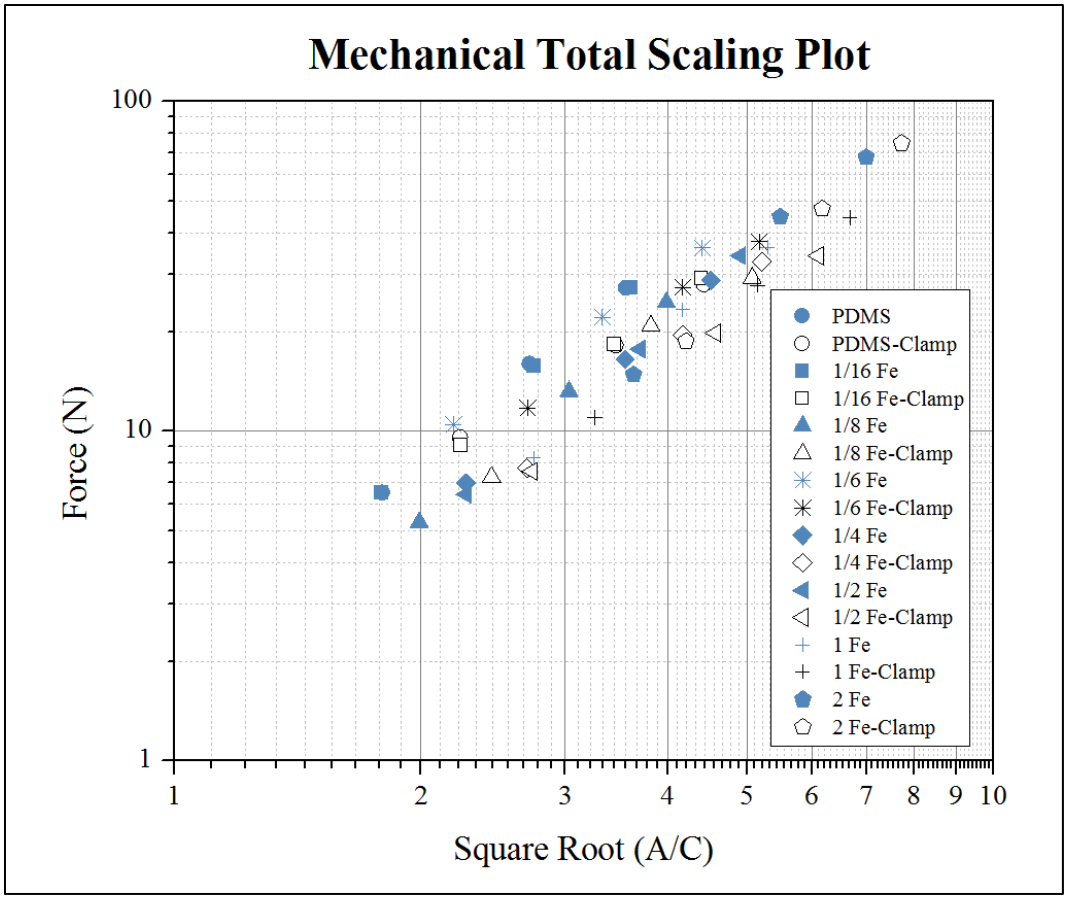

Figure 46: Mechanical clamp: total scaling plot-iron

4.2.3. Mechanical Clamping Model

The changes in compliance can be accounted for in a simple mechanical clamping model. Figure 47 illustrates the basic details of the model. In a lap-shear test, total compliance is equal to the sheared compliance experienced at the bonded interface in addition to the compliance due to stretching the gage length of a sample. Sheared compliance is small relative to the normal compliance, meaning that most of deformation is in the gage length section, and in fact sheared compliance only accounts for approximately 10% of the total compliance.

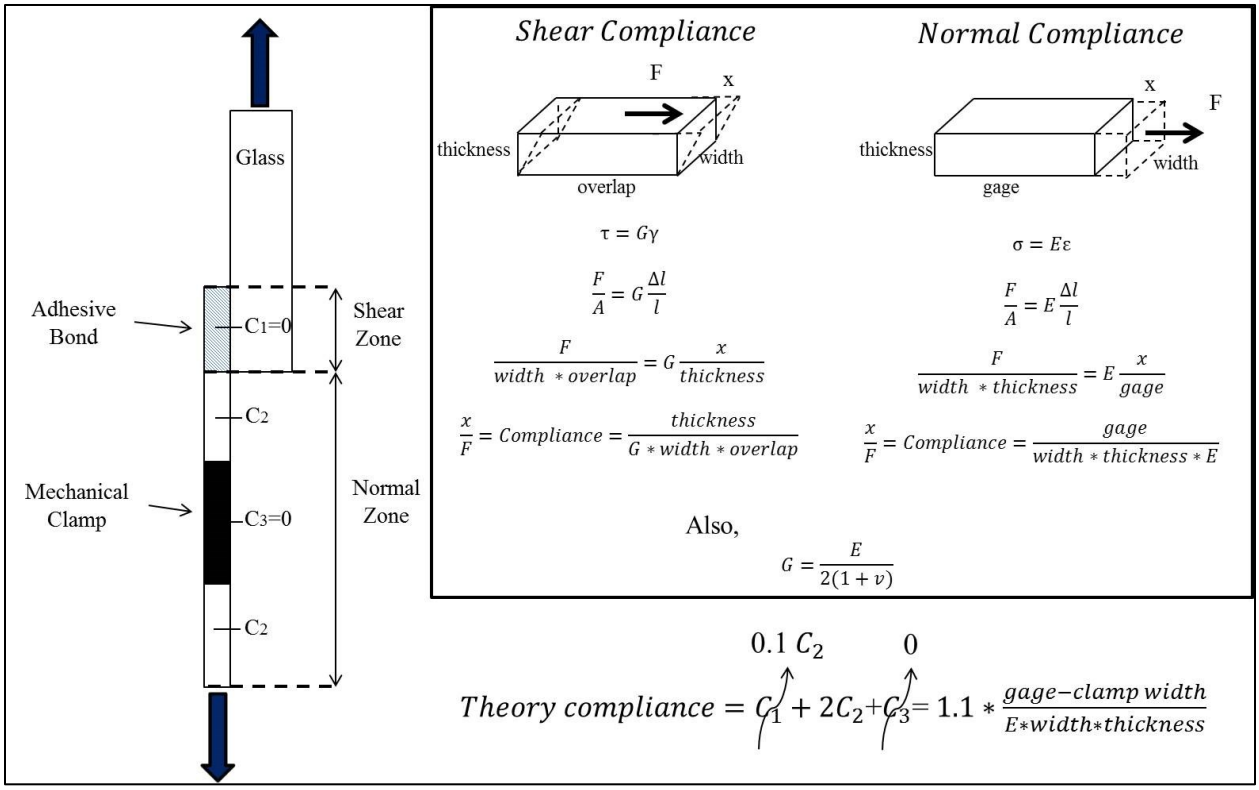

Figure 47: Clamping model illustration

It is assumed when a mechanical clamp is present, the volume of material held within the clamped zone (C_3 in Figure 47) is unable to deform. In other words, the mechanical compliance of zone C_3 goes to zero. In essence the model can be summarized as: mechanical clamping "removes" a chunk of rubber from the sample resulting in diminished compliance.

Figure 48 plots total measured compliance against theoretical (i.e. clamp *completely* removes a chunk of rubber) compliance. The theoretical data is not a "smooth" curve since compliance is dependent on sample geometry and each data point in Figure 48 is a theoretical value for a specific sample. The discrepancy between the measured values and the theoretical model could be due to slip between the sample and the clamp. In this study the clamped width used was 13.5 mm however if a clamp width is "assumed" to be 6 mm, then the percent error between the theoretical model and measured data is less than 1%. Essentially the discrepancy is

asserting that a 13.5 mm clamp only *completely* clamps 6 mm of rubber sample since a finite amount of clamping pressure is applied.

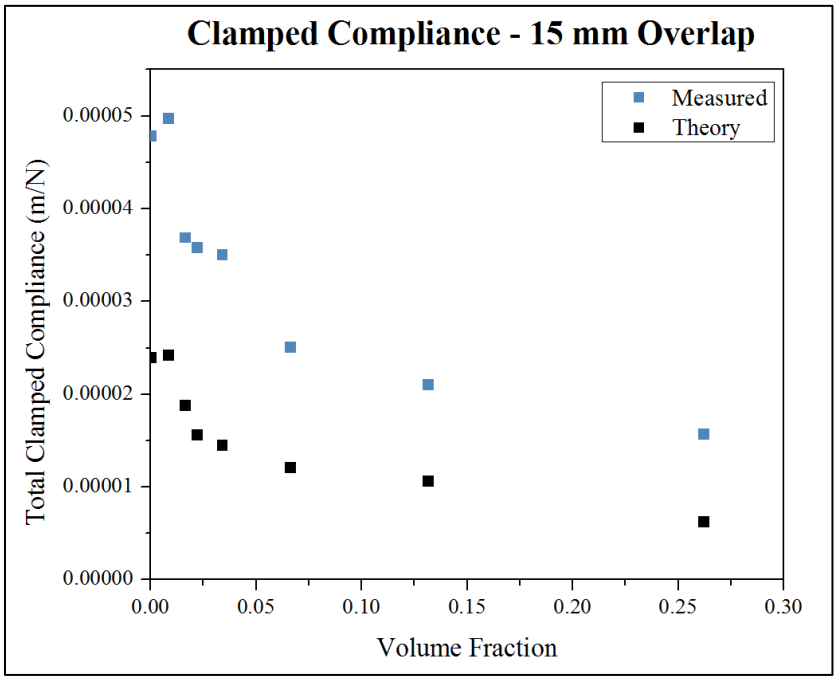

Figure 48: Theoretical compliance-I

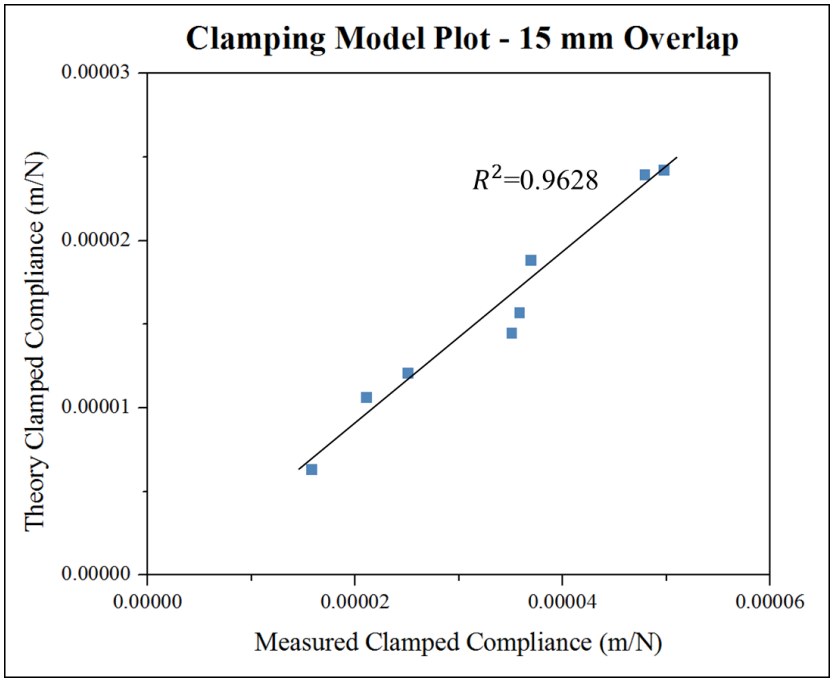

Figure 49: Theoretical compliance-II

Figure 49 plots theoretical compliance against measured compliance. A perfect model should have a one-to-one correlation (R^2 value of 1), however the theoretical calculations are based on measured dimensions, therefore Figure 49 has an R^2 value of 0.9628. The theoretical compliance is calculated based on of measured widths, thicknesses, gage lengths, etc. whereas the measured compliance is obtained directly from a lap-shear test. Changes in compliance for the mechanically clamped data are supported by this simple mechanical clamping model.

4.3. Magnetically Clamped Data

The addition of ferromagnetic nanopowder reinforcement permitted magnetic clamping to be explored as an alternate clamping method. Three stacks of three deep rare-earth magnets were placed on each side of a magnetically sensitive adhesive rubber film. The attraction of the magnets to each other squeezed the sample together allowing the magnets to act as a magnetic clamp. The amount of rare earth magnets used was equivalent in pressure (64 KPa) to the mechanical clamp. The same testing procedures for mechanical clamping were applied to magnetic clamping.

4.3.1. Magnetic Composites-Iron

Iron was chosen as reinforcement due to its ferromagnetic properties since an adhesive rubber containing iron would be magnetically active and would respond to a magnetic field. In addition, iron was selected for magnetic testing because it is inexpensive and iron mechanically clamped data had been previously collected. Furthermore, testing with the same reinforcement eliminated an unnecessary increase an independent variable which would occur if an alternate particle type or size had been chosen.

The data plotted in Figure 50 is a clear demonstration that placing a magnet on an adhesive sample influenced the force capacity. The adhesive force capacity was increased under magnetic clamping as all values are greater than 1. The positive results are favorable however the impact that particle volume fraction has on the switching effect is not clear from these experiments. A local maximum is located at a volume fraction of approximately 0.035 which suggests that particle reinforcement might influence the switching effect, however due to large error bars the data is inconclusive. A further examination into other particle sizes or types of particles might help confirm the effect particle reinforcement has on the switching ability of the adhesives.

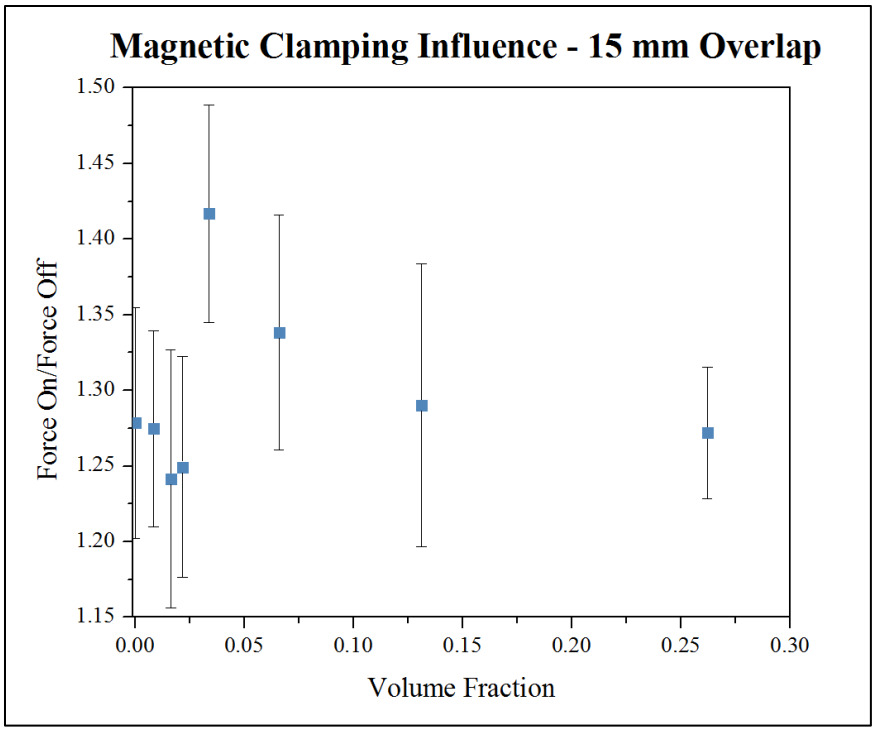

Figure 50: Magnetic clamp: clamping influence vs. volume fraction-iron

A summary of all the magnetically clamped data for iron is presented in Figure 51. Similar to the mechanically clamped experiments, each clamped marker for all samples has

shifted to the upper right relative to its unclamped pair. In these experiments area is constant which implies that compliance or G_c has changed. The data forms a straight line in both clamped and unclamped states strongly suggesting a fixed G_c throughout the experiments, and indicates G_c is consistent with chemical specificity. Assuming G_c is undoubtedly constant, then the shift in data is fully explained by a change in compliance alone.

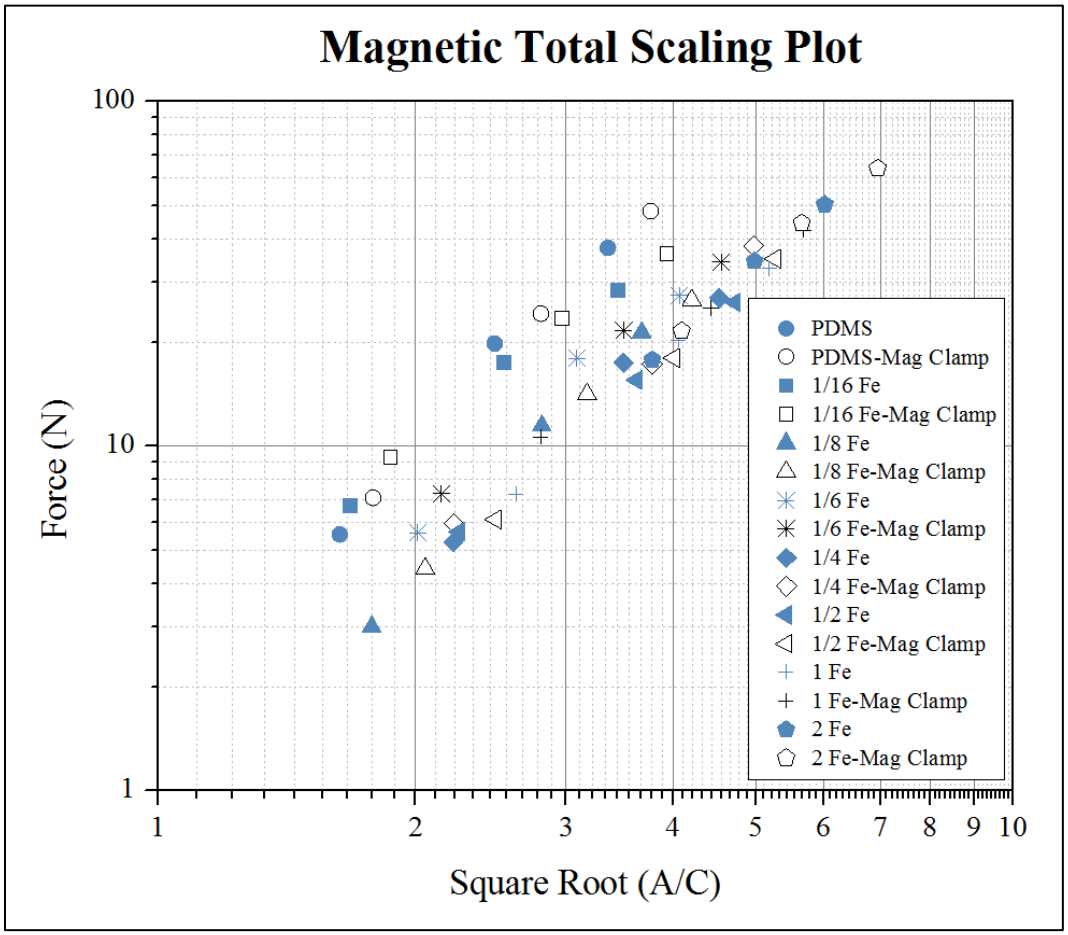

Figure 51: Magnetic clamp: total scaling plot

However, changes in compliance routinely change sample failure times. An approximate time to fail can be lifted from a force displacement plot. Figure 52 plots the time to fail for each sample in a magnetically clamped and unclamped state. For each sample, magnetic clamping caused more abrupt failure (i.e. sample failure times were smaller) and the stiffer, less compliant

samples failed more quickly compared to unclamped samples. The speed of failure likely causes a change in crack velocity, since contact area is constant, which in turn changes G_c as it has already been discussed in Section 1.4.3.2. Possible changes in G_c, due to changes in sample crack velocity, leave the exact reason for the shift in Figure 51 unanswered and give reason to examine adhesive failure times more thoroughly.

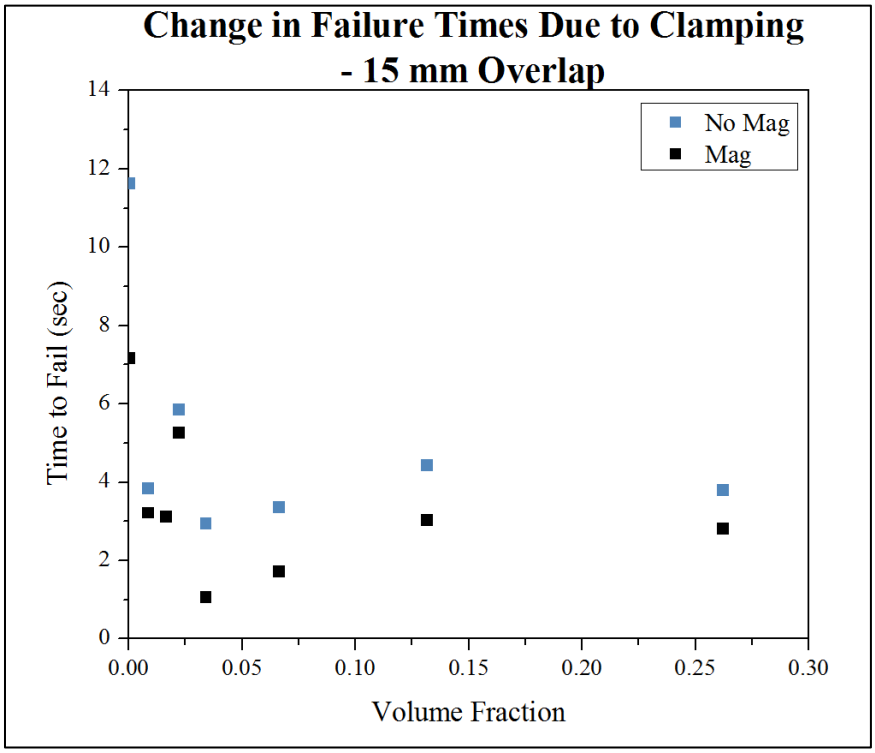

Figure 52: Change in failure times due to magnetic clamping

4.3.2. Adhesive Time of Failure: A Commentary on G_c

To be certain compliance is the only changing factor, it is useful to examine G_c more closely. In the derivation of Equation 4, it is assumed that once a critical force is reached the failure of an adhesive bond occurs in a single step. The implication of this assumption is that a crack during failure is instantaneous proving G_c to be a constant parameter. The assumption of uncontrolled rupture has been outlined in 1.5.3 and is as follows:

$$\frac{\partial^2 U_T}{\partial A^2} = \frac{\partial G_c}{\partial A} = \frac{\partial^2 U_E}{\partial A^2} + \frac{\partial^2 U_P}{\partial A^2} < 0 \qquad \text{(Equation 33)}$$

Solving for *x* in Equation 21 and substituting into Equation 24 yields an explicit expression for U_p which can be subsequently substituted into the expression above. Equation 26 can also be used as an explicit expression for U_E and also substituted into Equation 33 which gives:

$$\frac{\partial^2 U_T}{\partial A^2} = \frac{\partial G_c}{\partial A} = \frac{\partial^2 \left(\frac{1}{2}\frac{\Delta c}{bdE}\right) F^2}{\partial A^2} + \frac{\partial^2 \left(-\frac{\Delta c}{bdE}\right) F^2}{\partial A^2} < 0 \qquad \text{(Equation 34)}$$

Simplification yields:

$$\frac{\partial^2 U_T}{\partial A^2} = \frac{\partial G_c}{\partial A} = -\frac{\Delta c F^2}{A^3 E} < 0 \qquad \text{(Equation 35)}$$

Since F, A, E, and Δc are all positive quantities, Equation 35 is always negative, implying uncontrolled rupture. From a design standpoint, sudden uncontrolled fracture is preferred for a switchable adhesive due to the ease in the release and separation of adhesive and substrate.

4.3.2.1. Magnetic Data - G_c

Experimentally it was found that sample failure times are not instantaneous and therefore the assumption of the constant nature of G_c may be inaccurate. During a lap shear test, force, compliance, and area are measured which allows a G_c to be calculated through the rearrangement of Equation 4. Data collected on the critical energy release rate is plotted Figure 53. The plot indicates G_c is not constant between sample concentrations or between clamped and unclamped data. If G_c was constant, then all the data would be overlaid on a straight horizontal line

indicating that G_c would be unaffected by clamping or amount of reinforcement. Instead, all of the clamped data shows a higher G_c suggesting that changes are attributed to the difference in failure times due to clamping.

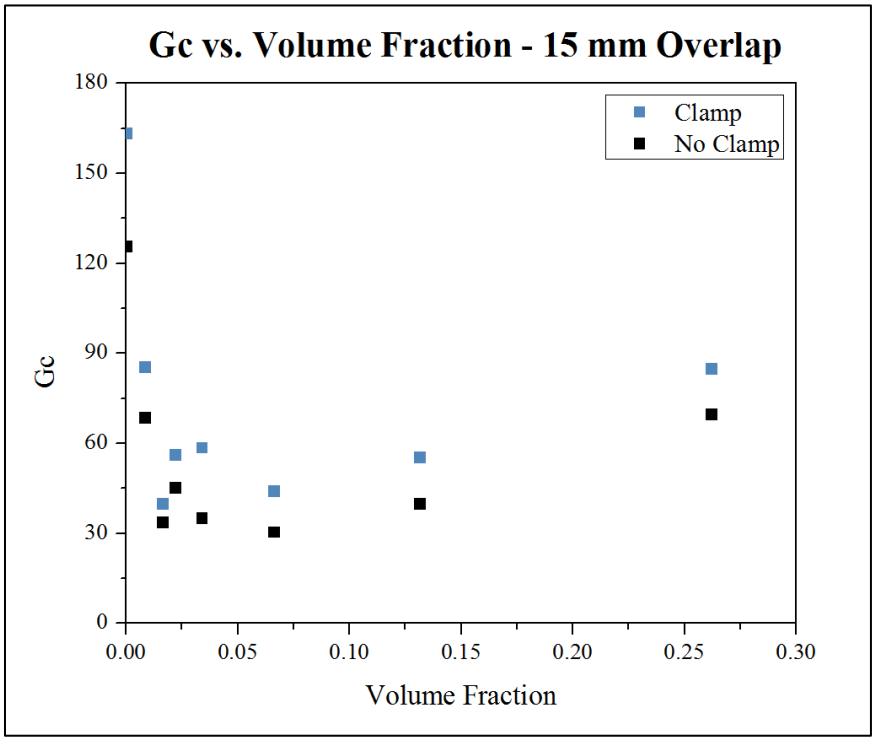

Figure 53: Magnetic clamp: G_c vs. volume fraction

The classic explanation for a higher G_c is that viscoelastic losses, inherently associated with rubber adhesives, resist movement of the crack front during fracture. A plot of the percentage amount of drop in G_c against a percentage increase time to failure is presented by Figure 54.

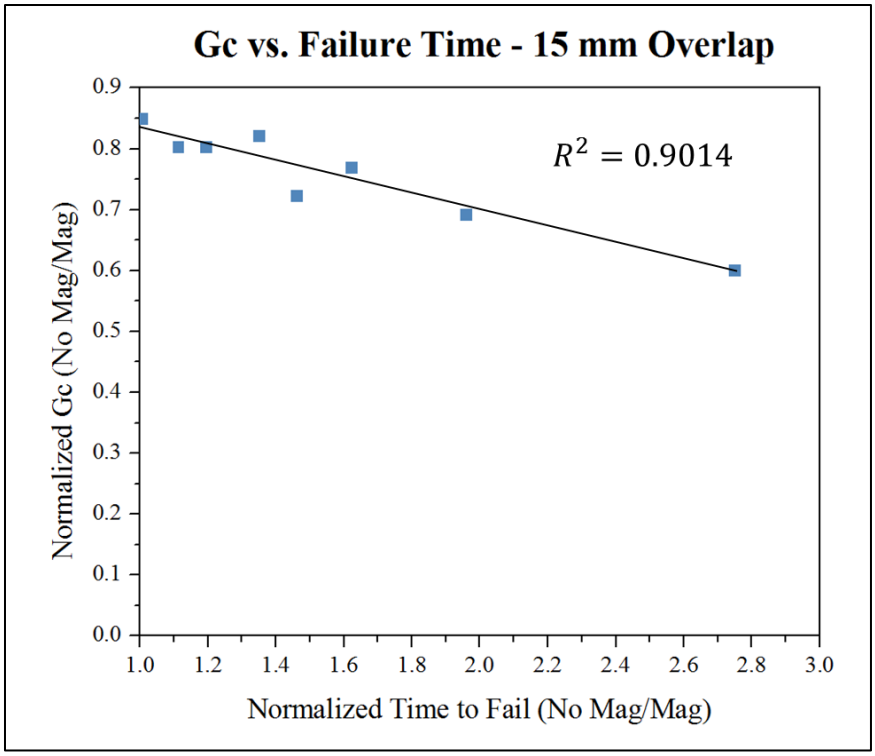

Figure 54: Magnetic clamp: G_c vs. failure time

To read the plot, consider the data point corresponding to 1.95 on the normalized time to fail axis from Figure 54. The point states that without a magnet, the failure is two times longer than with a magnet (i.e. no magnet/slower failure) and that the unclamped G_c is only 70% of its clamped value. Theoretical data should pass through the point (1,1) meaning that G_c would be the exact same if the time to fail was the same. The general trend of this plot is showing that the percentage drop of G_c due to the removal of a magnet is correlated with failure speeds, independent of sample clamping and modulus.

Section 1.4.3.2 discussed G_c dependence on crack velocity. This work has shown that sample failure times change G_c, however it was originally assumed that sample fracture was instantaneous. Single step failure is a useful assumption since it simplifies influential parameters that control adhesive force capacity. The data, however, presented within this work shows

deviation from this assumption. To remedy the inconsistency, future work might look to examine faster rates such that failure times match theoretical assumptions more closely, or rates might be adjusted so G_c is unchanged during both clamped and unclamped tests. Alternatively, it was assumed G_c is equivalent to $(F^2C)/A$ which may be inexact. In addition to G_c changing, sample failure times could alter the measured failure force since a sample might be loaded faster than a crack front can propagate, inaccurately increasing the measured force.

4.4. Non-Contact Clamped Data

During magnetic clamping, uncertainty as to the exact cause for compliance change arose. The change in compliance could either be caused by simple clamping or by particles being trapped within a magnetic field. In other words, the friction from the squeezing magnets, and not magnetic interaction between the field and particles, could be the reason for an increase in force. Experimentation with non-contact magnetic clamping was used to isolate whether friction or magnetism caused compliance change. Both Helmholtz coils and a hands-free jig were used on nickel and iron reinforced samples to study non-contact magnetic clamping. Originally, Helmholtz coils were used as a magnetic field source but no additional adhesive force capacity or change in compliance was measured. It was theorized that the field strength generated by a Helmholtz source was simply too low to measure any change. Instead, a hands-free jig was built which incorporated very strong rare-earth magnets that could apply a much stronger magnetic field. Yet, even when the hands-free jig was placed within a few millimeters of a sample, no enhanced affect was measured. The lack of "magnetic" results proved that friction caused compliance change when samples were magnetically clamped.

4.5. Comparison between Mechanical and Magnetic Clamping

Non-contact experiments gave a clear indication that compliance change observed by magnetic clamping was caused by friction. To further strengthen this observation, a more detailed magnetic clamping study was undertaken. The study varied magnetic contact area but maintained a fixed applied pressure so that comparisons between magnetic and mechanical clamping could be drawn. Also magnets were place on one side which showed no observable effect, consistent with the results from non-contact clamping experiments. The complete study is presented in Figure 55.

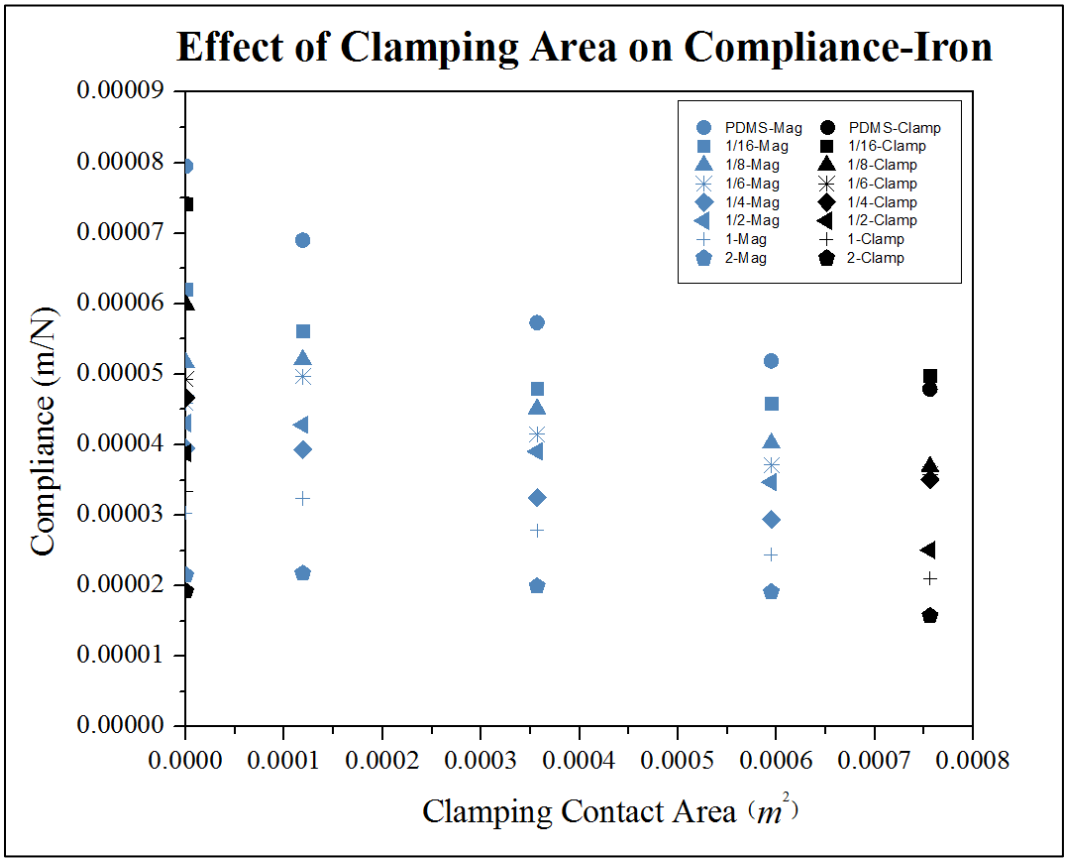

Figure 55: Effect of clamping area on compliance-a comparison

Data on the left side is unclamped and an increase in magnetic clamping contact area (i.e. more stacks of magnets were placed on a sample indicated by blue markers) is plotted before

finally the mechanical clamped area (far right black markers) is presented on the right side of the plot. The symbol shows the various particle concentrations. The results suggest that the amount of contact area within the clamp controls compliance which implies that the volume of material restricted within a clamp, mechanical/magnetic, is the only influential parameter. The results verify that friction by clamping is responsible for the changes in compliance. Discrepancies between black and blue markers which fall away from the trend can be attributed to different clamping mechanisms and testing occurring on different days.

4.6. Reproducibility

Generating repeatable data is important for any meaningful scientific work. In the previous section it was noted that discrepancies existed between data sets. This section showcases measurement to measurement consistency of a single sample being measured, as well as demonstrates sample to sample reliability.

4.6.1. Measurement to Measurement Consistency

Inter measurement results showed remarkable reproducibility. For the 1/8 weight fraction of iron sample with a 10 mm overlap, three consecutive tests are plotted in Figure 56 showing typical repeatability between measurements. For all the data presented thus far, an average compliance and force to failure has been reported. Figure 56 shows that sample compliances and failure forces were highly repeatable.

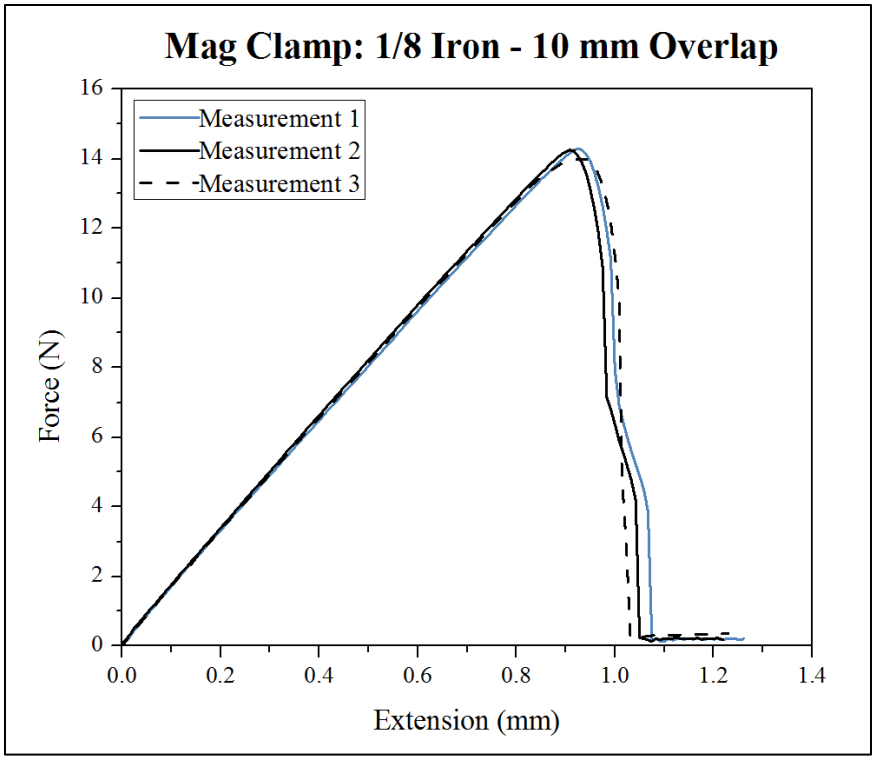

Figure 56: Typical reproducibility between measurements

4.6.2. Sample Reliability

While measurement to measurement repeatability is critical, whether data is reproducible on separate days or can be repeated by another instrument might be even more significant. Comparative results of PDMS measured on separate days (6-6-2013 and 6-7-2013) using different instruments (located at Dolve Hall and The Center for Nanoscale Science and Engineering-CNSE) are displayed in Figure 57. Dolve Hall measured PDMS samples show a slightly stiffer force displacement curve with somewhat less peak force. Slight differences in the data sets might be explained by sample aging since the measurements were a day later. However, both sets of data show the compliance and peak force all fall within the same magnitude which implies that measurements performed on different instruments and separate

days are reasonably accurate. Moreover, the clamp influence (i.e. force On/force Off) ratio for both samples (i.e. Dolve: 37 N/25 N=1.48 and CNSE 39 N/27 N=1.44) is nearly identical.

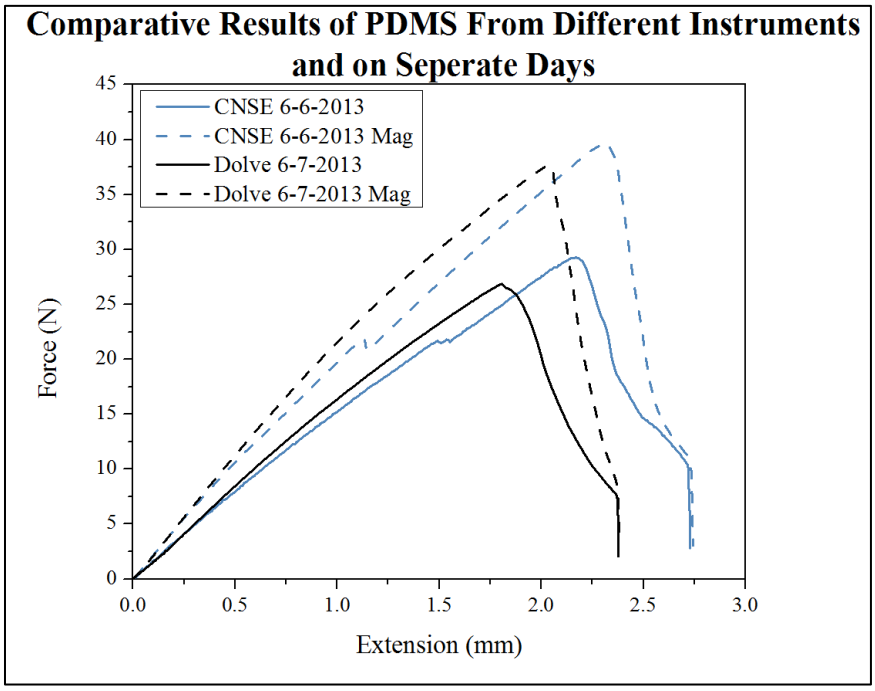

Figure 57: Comparative results of PDMS: different instruments and separate days

CHAPTER 5: SUMMARY AND RECOMMENDATIONS

Gecko-like adhesion is a broad research topic that is currently being studied. Attempts to synthetically emulate gecko-like adhesion are motivated by a gecko's capacity for switching between strong attachment and ease of release. Furthermore, geckos have the repeated ability to adhere to multiple surfaces throughout the entire lifetime of a gecko. A synthetic adhesive which could exhibit the characteristics of gecko-like adhesion (i.e. unlimited use, adhesion to any surface, switching between strong attachment and ease of release) will find its place in a broad range of industries, let alone is scientifically interesting on a very fundamental level.

To date, contemporary gecko-like adhesive research has primarily been studied by utilizing two approaches: chemical switching and topographical switching. Chemical switching requires a reaction to occur which often takes time, depends on a specific surface, and/or can only be used once. Topographical switching relies upon changes to surface area when triggered by external stimuli. Commonly topographical systems are composed of tiny arrays of posts which can be manipulated to maximize contact area. Tiny arrays of posts, however, are not only complex but are also expensive to manufacture since they rely upon lithographic etching fabrication techniques which are found only inside costly cleanroom laboratories. In addition to complexity and cost, topographical systems often have size limitations. Adhesives which possess micro- scaled posts have been shown to exhibit no additional adhesive benefit when scaled larger than micron length scales.

Recently it has been shown that adhesion is largly controlled by the mechanical properties of adhesive materials. This research demonstrated *mechanical* switching by providing a very general method for controlling compliance. Mechanically switched adhesion would

essentially open new research avenue for gecko-like adhesion which is not limited by slow switching, a specific surface chemistry, repeatability issues, expense, or size limitations often found in chemcial and topographical approaches.

As previously stated, mechanical switching aims to control compliance. If compliance is low (i.e. high stiffness/rigid), high adhesive force capacities are attainable but samples have limited tackiness. Conversely, if a material is highly compliant, the loading capacity is lower, but the material is much more sticky. Therefore controlling compliance leads to changes in adhesive force capacity. The research already presented herein outlined a novel method for compliance controlled adhesive switching as well as developed magnetically active switchable adhesives.

Changes in material compliance was demonstrated using two different mechansims. First, mechanically clamped PDMS prevented deformation during lap-shear testing. The clamp decreased the compliance resulting in a higher adhesive force before failure. The removal of the clamp signaled a lower force capacity before the adhesive released. Applying and removing the clamp changed the compliance of PDMS and experimental results could be explained by a simple mechanical clamping model.

The second explored mechansim alternatively created a magnetically senstive adhesive system. The magnetically sensitive adhesive was fabricated with mirco- and nano- sized magnetic particles embeaded within a PDMS matrix. To switch the nanocomposite compliance, magnets were arranged and attracted to both sides of the adhesive. Magnetic clamping effectively stiffened the material by applying pressure similar to the mechanical clamp.

The amount of reinforcement added was consistent with a modified Mooney rule of mixtures for determining the elastic modulus for rigid particulate-polymer composites. As more reinforcement was added, the compliance of the adhesives diminished. The increase in adhesive force due to clamping was shown to be independent of the type or amount of particles present. Compliance changes in the presence of a magnetic clamp were attributed soley to friction and not magnetism as results were verified by non-contact magnetic clamping.

Unexpectedly, observations showed that magnetic and mechanical clamping changed the failure time during a lap shear test. Failure speed likely changed the critical energy release rate, G_c which was originially assumed to be constant when the scaling relationship was formulated. Plots of G_c in both adhesion "on" and "off" states showed a deviation from the constant G_c assumption creating uncertainty as to the exact reason for the measured increase in adhesive force due to clamping.

Future work should either aim to lap shear test such that the speed of failure is consistent for both clamped and unclamped states (i.e. slow down the crosshead during clamping) so that a constant G_c might be maintained. While it is extremely likely that an increase in adhesive force is primarily attributed to change in compliance, a constant G_c would certainly remove any alternate explainations. In addition, the force at failure was theorized to be dependent on fracture speeds since a sample might be loaded faster than the crack propegation. Constant failure speeds between clamped and unclamped states would also alleviate suspicions of any inaccurate force measurements.

The second continuation of this research should aim to completely control compliance entirely by magnetism instead of relying upon magnetic clamping friction. One such study

might use an extremely tacky polymer (40:1 PDMS) and magnetic particle reinforcement so that the presence of a magnetic field might restrict the movement of the magnetic particles resulting in higher compliance. Adhesive characterization would be better suited with a JKR experimental setup so that delicate changes in compliance as well as G_c could be easily monitored. A JKR experiment would allow for easier characterization of a tacky substance since lap shear testing with magnets would likely be problematic.

In closing, this thesis demonstrated that mechanical switching by changing compliance can control the adhesive force capacity. In addition, a magnetic adhesive was successfully developed as an alternate, more easily controlled method to switch compliance and therefore adhesion. Ultimately though, magnetic switching was consistent with mechanical switching, and both could be explained with a simple clamping model. Finally the work performed was repeatable and consistent with published data.

CHAPTER 6:REFERENCES

[1] D. Packham, *Handbook of Adhesion*. New York: John Wiley and Sons, 1992.

[2] I. Skeist, *Handbook of Adhesives* , 3rd ed. New York: Van Nostrand Reinhold, 1990.

[3] G. Salomon, *Adhesion and Adhesives*. New York: Elsevier Publishing Company, 1965.

[4] B. Strong, *Plastics: Materials and Processing*. Upper Saddle River: Peason Prentice Hall, 2006.

[5] W. D. Calister, *Materials Science and Engineering: An Introduction*. Hoboken, NJ: Jon Wiley & Sons, Inc, 2010.

[6] M. J. Cima. (2012, December) Surface Energy and Surfactants. MIT Chemistry Lecture. [Online]. http://www.youtube.com/watch?v=oVzvF6swZA4

[7] L.- H. Lee, *Fundamentals of Adhesion*. New York, NY: Plenum Press, 1991.

[8] H. Zeng, *Polymer Adhesion, Friction, and Lubrication*. Hoboken, New Jersey: Jon Wiley & Sons, Inc., 2013.

[9] K. Mittal A. Pizzi, *Handbook of Adhesive Technology*. New York: Marcel Dekker, Inc., 1994.

[10] A. Croll, D. King, B. Paret, D. Irschick, A. Crosby M. Bartlett, "Looking Beyond Fibrillar Features to Scale Gecko-Like Adhesion," *Advanced Materials*, vol. 24, no. 8, pp. 1078-1083, January 2012.

[11] A. Synytska, M. Kamperman, "Switchable Adhesion by Chemical Functionality and Topography," *Journal of Materials Chemistry*, pp. 19390-19401, 2012.

[12] C. Greiner, E. Artz, A. del Campo L. Boesel, "Gecko-Inspired Surfaces: A Path to Strong and Reversible Dry Adhesives," *Advanced Materials*, vol. 22, no. 19, pp. 2125-2137, 2010.

[13] S. Gorb, R. Spolenak E. Artz, "From Micro to Nano Contacts in Biological Attachment Devices," in *Proceedings of the National Academy of Sciences of the United States of America*, 2003, pp. 10603-10606.

[14] C. Hui A. Jagota, "Adhesion, Friction, and Compliance of Bio-Mimetic and Bio-Inspired Structured Interfaces," *Materials Science & Engineering R-Reports*, vol. 72, no. 12, pp.

253-292, 2011.

[15] L. Ge, L. Ci, P. Ajayan, A. Dhinojwala S. Sethi, "Gecko-Inspired Carbon Nanotube-Based Self-Cleaning Adhesives," *Nano Letters*, vol. 8, no. 3, pp. 822-825, 2008.

[16] S. Sethi, L. Ci, P. Ajayan, A. Dhinojwala L. Ge, "Carbon Nanotube-Based Synthetic Gecko Tapes," in *Proceedings of the National Academy of Sciences of the United States of America*, 2007, pp. 10792-10795.

[17] K. Chawla and M. Meyers, *Mechanical Behavior of Materials: Second Edition*. New York: Cambridge, 2009.

[18] A. Griffith, "The Phenomena of Ruptrue and Flow in Solids," *Philosophical Transactions of the Royal Society of London. Series A, Containing Papers of a Mathematical or Physical Character, Vol 221*, pp. 163-198, 1921.

[19] G. Irwin, "Analysis of Stresses and Strains Near the End of a Crack Traversing a Plate," *Journal of Applied Mechanics*, pp. 361-364, 1957.

[20] A. Fatemi, R. Stephens, H. Fuchs R. Stephens, *Metal Fatigue in Engineering*, 2nd ed. New York: John Wiley and Sons, Inc., 2001.

[21] M. Barquins D. Maugis, "Fracture Mechancis and the Adherence of Viscoelastic Bodies," *Journal of Applied Physics*, vol. 11, pp. 1989-2023, 1978.

[22] H. Hertz, "On the Contact of Elastic Solids," *Journal for Pure and Applied Mathematics*, pp. 156-171, 1881.

[23] A. Fischer-Cripps, *Nanoindentation*, 2nd ed. New York: Springer, 2004.

[24] K. Shull, "Contact Mechanics and the Adhesion of Soft Solids," *Materials Science and Engineering Research*, pp. 1-45, 2002.

[25] K. Kendall, A. Roberts K. Johnson, "Surface Energy and the Contact of Elastic Solids," *Proceedings of the Royal Society of London*, pp. 301-313, 1971.

[26] ASTM Standard D-1002, *Test Method for Strength Properties of Adhesives in Shear by Tension Loading (Metal-to-Metal)*. West Conshohocken, PA: ASTM International, 2010.

[27] ASTM Standard D-0903, *Test Method for Peel or Stripping Strength of Adhesive Bonds*. West Conshohocken, PA: ASTM International, 2010.

[28] ASTM Standard D-1781, *Method for Climbing Drum Peel Test for Adhesives*. West Conshohocken, PA: ASTM International, 2012.

[29] ASTM Standard E-229, *Test Method for Shear Strength and Shear Modulus of Structural Adhesives*. West Conshohocken, PA: ASTM International, 2003.

[30] K. Kendall, "Thin-Film Peeling - The Elastic Term," *Journal of Applied Physics*, vol. 8, pp. 1449-1452, 1975.

[31] P. Fabre, J. Corpart, L. Leibler G. Crevoisier, "Switchable Tackiness and Wettability of a Liquid Crystalline Polymer," *Science*, vol. 285, no. 5431, pp. 1246-1249, August 1999.

[32] E. Millan, I. Webster J. Boyne, "Peeling Performance of a Novel Light Switchable Pressure-Sensitive Adhesive," *International Journal of Adhesion and Adhesives*, vol. 21, no. 1, pp. 49-53, July 2001.

[33] E. Canetaa, T. Weerakkody, J. Keddie, U. Rivas T. Wang, "pH Dependence of the Properties of Waterborne Pressure-Sensitive Adhesives Containing Acrylic Acid," *ACS Applied Materials and Interfaces*, vol. 1, no. 3, pp. 631-639, 2009.

[34] J. Chung, M. Walker, C. Stafford A. Nolte, "In Situ Adhesion Measurements Utilizing Layer-By-Layer Functionalized Surfaces," *ACS: Applications of Material Interfaces*, vol. 1, no. 2, pp. 373-380, February 2009.

[35] M. Muller, M. Motornov, M. Nitschke, K. Grundke, M. Stamm S. Minko, "Two-Level Structured Self-Adaptive Surfaces with Reversibly Tunable Properties," *Journal of the American Chemcial Society*, vol. 125, no. 13, pp. 3896-3900, March 2003.

[36] A. Kiriy, V. Senkovskyy, M. Stamm, M. Feldstein, C. Crenton H. Retsos, "Controlling Tack with Bicomponent Polymer Brushes," *Advanced Materials*, vol. 18, pp. 2624-2628, 2006.

[37] E. Artz, A. del Campo S. Reddy, "Bioinspired Surfaces with Switchable Adhesion," *Advanced Materials*, vol. 19, no. 22, pp. 3833-3837, October 2007.

[38] M. Sitti, T. Xie, X. Xiao S. Kim, "Reversible Dry Micro-Fibrillar Adhesives with Thermally Controllable Adhesion," *Soft Matter*, vol. 5, no. 19, pp. 3689-2693, May 2009.

[39] C. Greiner, E. Artz, K. Turner M. Northern, "A Gecko-Inspired Reversible Adhesive," *Advanced Materials*, vol. 20, no. 20, pp. 3905-3909, 2008.

[40] P. Steen M. Vogel, "Capillarity-Based Switchable Adhesion," *Proceedings of the National Academy of Sciences of the United States of America*, vol. 107, no. 8, pp. 3377-3381,

August 2009.

[41] M. Kwak, K. Suh H. Jeong, "Stretchable, Adhesion-Tunable Dry Adhesives by Surface Wrinkling," *Lagmuir Letter*, vol. 26, no. 4, pp. 2223-2226, February 2010.

[42] E. Smith, R. Hayward, A. Crosby E. Chan, "Surface Wrinkles for Smart Adhesion," *Advanced Materials*, vol. 20, no. 4, pp. 711-716, February 2008.

[43] Dow Corning Corporation. (2013, September) Sylgard 184 Silicone Elastomer Kit Product Data Sheet. [Online]. http://www.dowcorning.com/

[44] MatWeb. (2013, Septmeber) Material Property Data. [Online]. www.matweb.com

[45] R. Resnick, J. Walker D. Halliday, *Fundamentals of Physics*, 7th ed. United States: John Wiley and Sons, Inc., 2005.

[46] X.-Q. Feng, B. Lauke, Y.-W. Mai S.-Y. Fu, "Effects of Particle Size, Particle/Matrix Interface Adhesion and Particle Loading on Mechanical Properties of Particulate-Polymer Composites," *Journal of Composites, Part B: Engineering*, vol. 39, pp. 933-961, January 2008.